

Appendix I, Old and Middle River Flow Management

Attachment I.3 Delta Export Zone of Influence Analysis

I.3.1 Introduction and Background

The Sacramento–San Joaquin River Delta (Delta) provides habitat for migrating anadromous fish while also serving as critical infrastructure for California water supply. In the winter and spring months, Old and Middle River (OMR) flows are managed to protect emigrating Delta smelt, Longfin smelt, juvenile winter-run Chinook salmon, yearling spring-run Chinook salmon, and Central Valley steelhead from entrainment into the export facilities in the south Delta. During these months, changes to velocity distributions in channels, due to south Delta exports, may affect the fate of fish. This document describes techniques to evaluate the spatial extent of hydrologic alteration considering changes to velocity (hereinafter described as “Delta export zone of influence”) and changes to the probability distributions of hourly average velocity as a result of pumping under varying OMR flow conditions.

I.3.1.1 Methods

An analysis using DSM2-Hydro was conducted to analyze the spatial extent of influence of exports under CVP and SWP diversions. The DSM2-Hydro velocity results were used to generate Delta export zone of influence contour maps in the Delta.

The subsections below describe the exploration of drivers of hydrologic alteration, the subsequent use of inflow categories to standardize across combinations of San Joaquin and Sacramento River inflows, and DSM2 modeling and post-processing steps to quantify the influence of the export facilities in the south Delta (DSM2 Modeling and Post-Processing). Probability density curves of hourly average velocity at specific locations were created for pumping (export) and no pumping conditions (described in Gaussian Kernel Density Estimation) and the proportion overlap of the curves was used as a comparative metric to capture the effects of exports. Then, based on proportion overlap, two methods for evaluating Delta export zone of influence are presented for differing inflow groups and OMRs: (1) maps that illustrate the spatial extent of changes to velocity throughout the Delta (described in Gaussian KDE Proportional Overlap Contour Maps), and (2) figures that illustrate the proportion of channel lengths influenced by exports (described in Channel length associated with Delta export ZOI).

I.3.1.1.1 Drivers of hydrologic alteration

To quantify the extent of pumping influence, proportion overlap data were filtered to DSM2 nodes with values <70% (less than 70% of the velocity distribution overlapping). Channel lengths were calculated between each remaining node and its neighbor and summed across month (Dec-June) and OMR flow bins (-2000, -3500, -5000, and -6500 cfs). Results were initially viewed by month, based on analyses similar to those in the 2019 Biological Assessment on the Long-term operation of the CVP and SWP. It was expected that increasingly negative OMR flows (associated with increased exports) would result in increasing sum of channel lengths experiencing hydrologic alteration. While this pattern is demonstrated in March-June, several months contradicted this expectation (Figure I.3-1). In December, fewer meters of channel length were influenced by OMR flows of -5000 than by OMR flows of -3500. In January, OMR flows of -5000 and -2000 influenced similar lengths of channels, while a shorter length of channels was influenced by an OMR flow of -3500. In February, OMR flow of -5000 influenced a shorter length of channels than did OMR flows of -3500 or -2000. This suggested that month was not an appropriate way to look at hydrologic alteration and to consider other drivers to understand what may be influencing hydrodynamic alteration and OMRs. Next, results were aggregated across combinations of San Joaquin and Sacramento River inflows, which are modeled to vary by month, and are hypothesized to be the main driver of variable OMR flows.

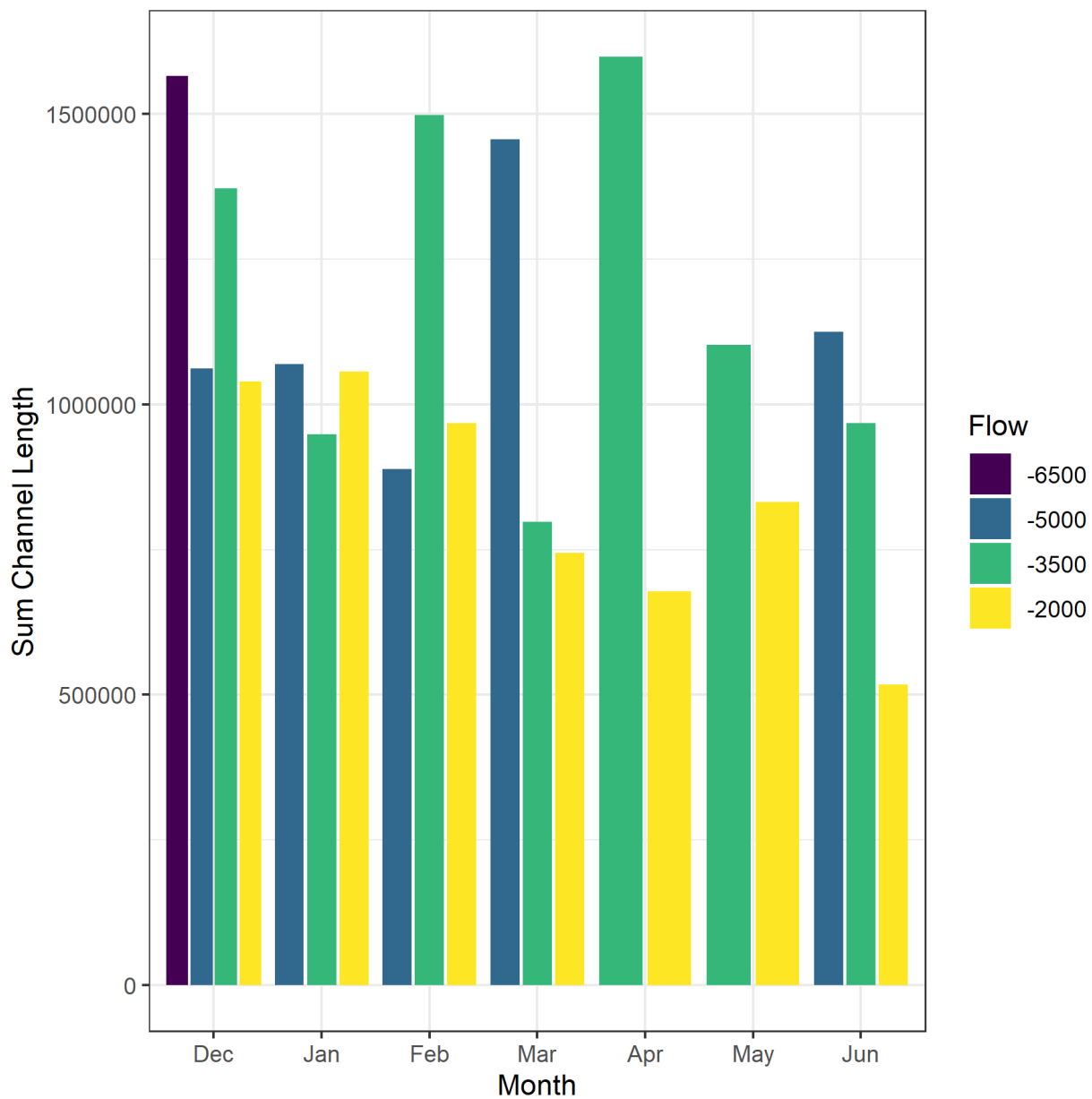


Figure I.3-1. Sum of channel lengths connecting DSM2 nodes with 70% overlap binned by month and different OMR flows.

I.3.1.1.2 Inflow Categories

To standardize across San Joaquin (SJR, Vernalis) and Sacramento (SR, Freeport) inflows, representative combinations of average monthly SJR and SR inflow were identified. Inflow ranges are based on the Calsim 3-modeled No Action Alternative (NAA) results, which cover December 1921-May 2021. Data from December to June are used to represent the OMR management season. Flows are categorized into low (minimum value to less than 0.333 quantile), medium (0.333 to less than 0.666 quantile), and high (0.666 to maximum value) inflow groupings for SJR and SR. Data are then assigned one of the nine inflow categories representing different combinations of low/medium/high SJR inflows and low/medium/high SR inflows (Table I.3-1). For certain alternatives, data fell outside of the inflow categories. These instances were rare in all alternatives (Table I.3-2).

Table I.3-1. December – June ZOI flow groups based on Calsim 3 Sacramento (Freeport) and San Joaquin (Vernalis) River inflows under the No Action Alternative (NAA). Values have been rounded to the nearest integer.

Inflow Group	Description	SR Inflow Range (cfs)	SJR Inflow Range (cfs)	Mean OMR (cfs)	Mean Exports (cfs)
lolo	Low SR Low SJR	5117 - 13415	890 - 1983	-3049	3745
medmed	Med SR Med SJR	13416 - 24725	1984 - 4096	-3758	5328
hihi	High SR High SJR	24726 - 87222	4097 - 61005	-2005	9227
himed	High SR Med SJR	24726 - 87222	1984 - 4096	-4242	6548
medhi	Med SR High SJR	13416 - 24725	4097 - 61005	-2506	6271
lomed	Low SR Med SJR	5117 - 13415	1984 - 4096	-2805	3864
medlo	Med SR Low SJR	13416 - 24725	890 - 1983	-5070	6069
lohi	Low SR High SJR	5117 - 13415	4097 - 61005	-2916	5713
hilo	High SR Low SJR	24726 - 87222	890 - 1983	-4562	6158

Table I.3-2. Sample sizes (months) of alternatives in each inflow group based on Calsim 3 and DSM2 results. Values have not been filtered for OMR group.

Inflow group	NAA	Alt1	Alt2 woTUCP woVA	Alt2 woTUCP DeltaVA	Alt2 woTUCP AlIVA	Alt2 wTUCP woVA	Alt3	Alt4
lolo	132	108	137	138	138	135	170	143
lomed	70	84	75	82	73	75	70	75
lohi	31	30	30	30	23	29	20	29
medlo	81	76	72	64	64	72	62	66
medmed	101	105	96	97	106	97	62	96
medhi	51	54	50	50	55	51	41	52
hilo	20	21	20	19	18	20	29	20
himed	62	68	68	68	68	68	78	66
hihi	152	153	152	152	155	152	164	153
NA	0	1	0	0	0	1	4	0

I.3.1.1.3 OMR Bins

For zone of influence analysis, data are also assigned OMR bins based on average monthly OMR, with data falling within +/-500 cfs of -2000 cfs, -3500 cfs, and -5000 cfs assigned to the respective -2000, -3500, and -5000 OMR bin categories, and data with OMR less than -5500 cfs assigned to the less than -5500 bin (Table I.3-3). These values (-2000, -3500, -5000) were selected to reflect values used for real-time management during OMR season. We chose to keep the bins somewhat discrete for greater relevance to management values and to distinguish bins from each other in analyses, although this led to the exclusion of certain values from the analysis (Table I.3-4, Table I.3-5; see points without colored outlines in Figure I.3-3 for data excluded in NAA).

Table I.3-3. Summary Statistics for Inflow Groups and OMR Bins used in Analyses. Cells populated with "NA" indicate a lack of data falling within the specific inflow-OMR grouping. Mean OMR and Mean Exports are associated with the No Action Alternative (NAA).

Inflow Group	OMR Bin	OMR Range	Mean OMR (cfs)	Mean Exports (cfs)
lolo	-2000	-2500 to -1500 cfs	-1933	2281
lolo	-3500	-4000 to -3000 cfs	-3526	4294
lolo	-5000	-5500 to -4500 cfs	-4941	6046
lolo	<-5500	less than -5500	-6991	8341
lomed	-2000	-2500 to -1500 cfs	-2084	3041
lomed	-3500	-4000 to -3000 cfs	-3474	4911
lomed	-5000	-5500 to -4500 cfs	-4841	6008
lomed	<-5500	less than -5500	NA	NA
lohi	-2000	-2500 to -1500 cfs	-2051	4273
lohi	-3500	-4000 to -3000 cfs	-3409	7673
lohi	-5000	-5500 to -4500 cfs	-4915	6721
lohi	<-5500	less than -5500	NA	NA
medlo	-2000	-2500 to -1500 cfs	-1512	2963
medlo	-3500	-4000 to -3000 cfs	-3633	5038
medlo	-5000	-5500 to -4500 cfs	-4990	5761
medlo	<-5500	less than -5500	-8137	9678
medmed	-2000	-2500 to -1500 cfs	-2124	3253
medmed	-3500	-4000 to -3000 cfs	-3591	5371
medmed	-5000	-5500 to -4500 cfs	-4908	6464
medmed	<-5500	less than -5500	-8530	10782
medhi	-2000	-2500 to -1500 cfs	-2081	4385
medhi	-3500	-4000 to -3000 cfs	-3517	6907
medhi	-5000	-5500 to -4500 cfs	-5015	8577
medhi	<-5500	less than -5500	NA	NA
hilo	-2000	-2500 to -1500 cfs	NA	NA
hilo	-3500	-4000 to -3000 cfs	-3645	5344
hilo	-5000	-5500 to -4500 cfs	-4882	6455
hilo	<-5500	less than -5500	NA	NA
himed	-2000	-2500 to -1500 cfs	-2285	3100
himed	-3500	-4000 to -3000 cfs	-3567	5811

Inflow Group	OMR Bin	OMR Range	Mean OMR (cfs)	Mean Exports (cfs)
himed	-5000	-5500 to -4500 cfs	-4958	7483
himed	<-5500	less than -5500	NA	NA
hihi	-2000	-2500 to -1500 cfs	-1979	7624
hihi	-3500	-4000 to -3000 cfs	-3566	8617
hihi	-5000	-5500 to -4500 cfs	-4735	9849
hihi	<-5500	less than -5500	NA	NA

Table I.3-4. Sample sizes (months) of alternatives in each inflow group and OMR bin based on Calsim 3 and DSM2 results.

Inflow Group	OMR Bin	NAA	Alt1	Alt2 woTUCP woVA	Alt2 woTUCP DeltaVA	Alt2 woTUCP AllVA	Alt2 wTUCP woVA	Alt3	Alt4
lolo	-2000	27	29	31	29	24	29	27	31
lolo	-3500	18	17	21	25	25	22	9	19
lolo	-5000	22	10	14	11	10	13	3	19
lolo	<-5500	10	12	6	9	7	6	0	9
lolo	NA	55	40	65	64	72	65	131	65
lomed	-2000	25	38	35	23	20	33	11	32
lomed	-3500	9	8	8	5	6	9	2	10
lomed	-5000	12	5	4	3	3	4	1	4
lomed	<-5500	0	6	0	0	0	0	1	1
lomed	NA	24	27	28	51	44	29	55	28
lohi	-2000	10	7	7	2	1	7	5	7
lohi	-3500	3	11	12	9	6	12	3	13
lohi	-5000	3	3	1	2	1	1	0	1
lohi	<-5500	0	0	0	0	0	0	0	0
lohi	NA	15	9	10	17	15	9	12	8
medlo	-2000	1	4	3	2	3	3	14	2
medlo	-3500	11	0	22	17	19	21	2	13
medlo	-5000	45	18	16	15	16	16	11	19
medlo	<-5500	10	49	12	11	12	12	1	8
medlo	NA	14	5	19	19	14	20	34	24
medmed	-2000	26	10	16	13	17	16	4	15
medmed	-3500	25	12	40	25	24	43	4	33

Inflow Group	OMR Bin	NAA	Alt1	Alt2 woTUCP woVA	Alt2 woTUCP DeltaVA	Alt2 woTUCP AlIVA	Alt2 wTUCP woVA	Alt3	Alt4
medmed	-5000	20	8	6	6	6	6	7	17
medmed	<-5500	5	65	5	5	5	5	0	4
medmed	NA	25	10	29	48	54	27	47	27
medhi	-2000	11	7	11	7	8	11	0	11
medhi	-3500	8	13	24	19	21	25	1	25
medhi	-5000	1	5	2	2	2	2	3	4
medhi	<-5500	1	11	0	0	0	0	0	1
medhi	NA	30	18	13	22	24	13	37	11
hilo	-2000	0	0	0	0	0	0	4	0
hilo	-3500	2	1	6	6	5	6	1	3
hilo	-5000	10	0	8	8	7	8	13	8
hilo	<-5500	1	20	1	1	2	1	1	0
hilo	NA	7	0	5	4	4	5	10	9
himed	-2000	4	0	3	5	5	3	7	2
himed	-3500	12	1	21	14	14	21	5	13
himed	-5000	24	0	20	19	19	20	29	32
himed	<-5500	3	65	3	3	3	3	4	1
himed	NA	19	2	21	27	27	21	33	18
hihi	-2000	16	12	13	17	17	13	5	14
hihi	-3500	26	10	33	15	17	33	6	20
hihi	-5000	34	9	35	35	35	35	39	40
hihi	<-5500	5	65	7	7	7	7	8	6
hihi	NA	71	57	64	78	79	64	106	73
NA	-2000	0	0	0	0	0	1	0	0
NA	-3500	0	0	0	0	0	0	0	0
NA	-5000	0	0	0	0	0	0	0	0
NA	<-5500	0	0	0	0	0	0	0	0
NA	NA	0	1	0	0	0	0	4	0

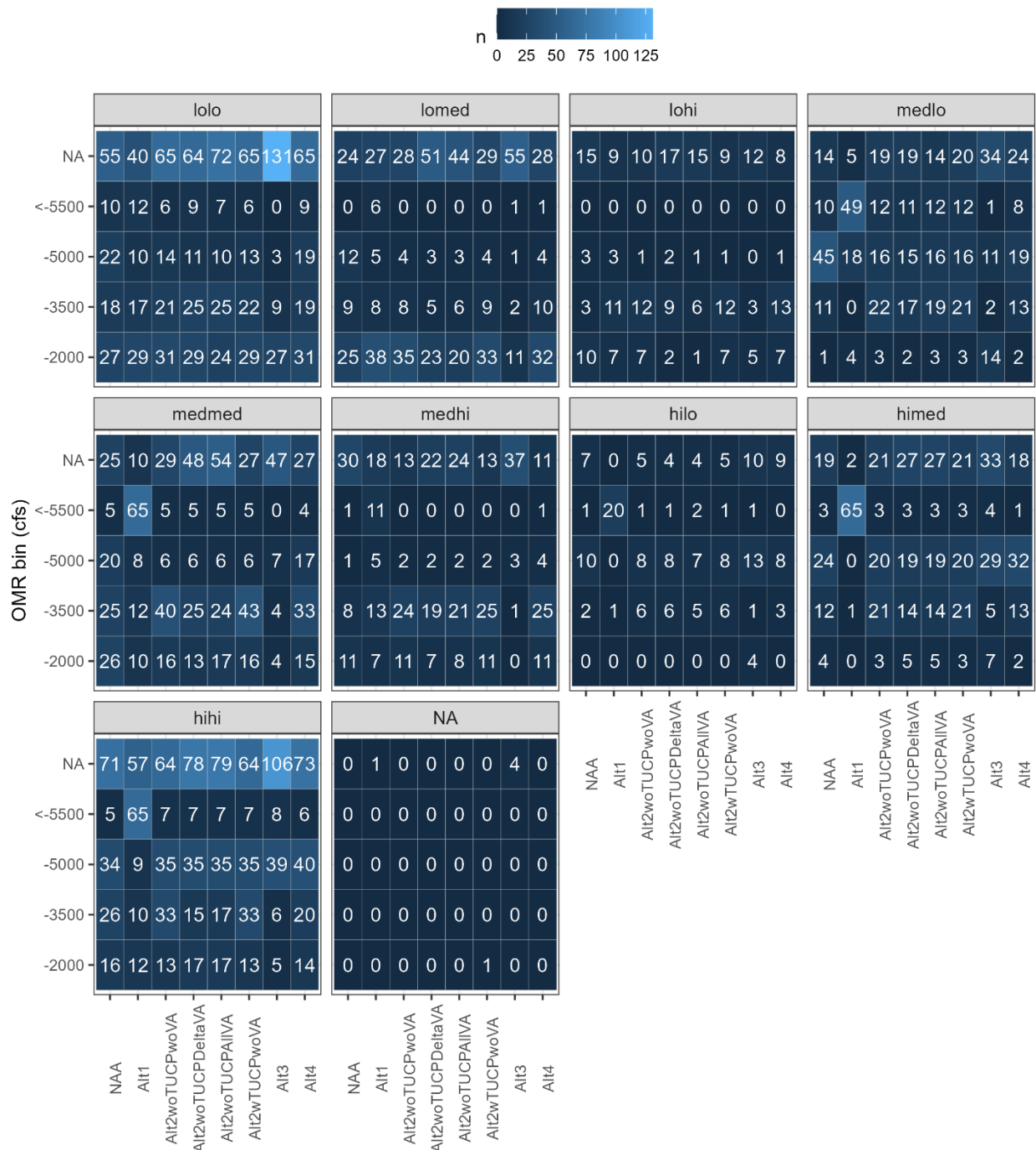


Figure I.3-2. Sample sizes (months) of alternatives in each inflow group and OMR bin based on Calsim 3 and DSM2 results. Text denotes sample size in each group. NA indicates values do not fall into pre-designated OMR bin or inflow group.

Table I.3-5. Proportion of dataset excluded from analysis based on Calsim 3 output under the No Action Alternative (NAA). OMR values in the "Other" bin fall between -2500 to -3000 and -4000 to -4500 cfs.

OMR	NAA	Alt1	Alt2 wTUCP woVA	Alt2 woTUCP woVA	Alt2 woTUCP DeltaVA	Alt2 woTUCP AIIVA	Alt4
Greater than -1500	0.13	0.08	0.09	0.09	0.15	0.18	0.09
Other	0.2	0.14	0.3	0.3	0.27	0.27	0.3

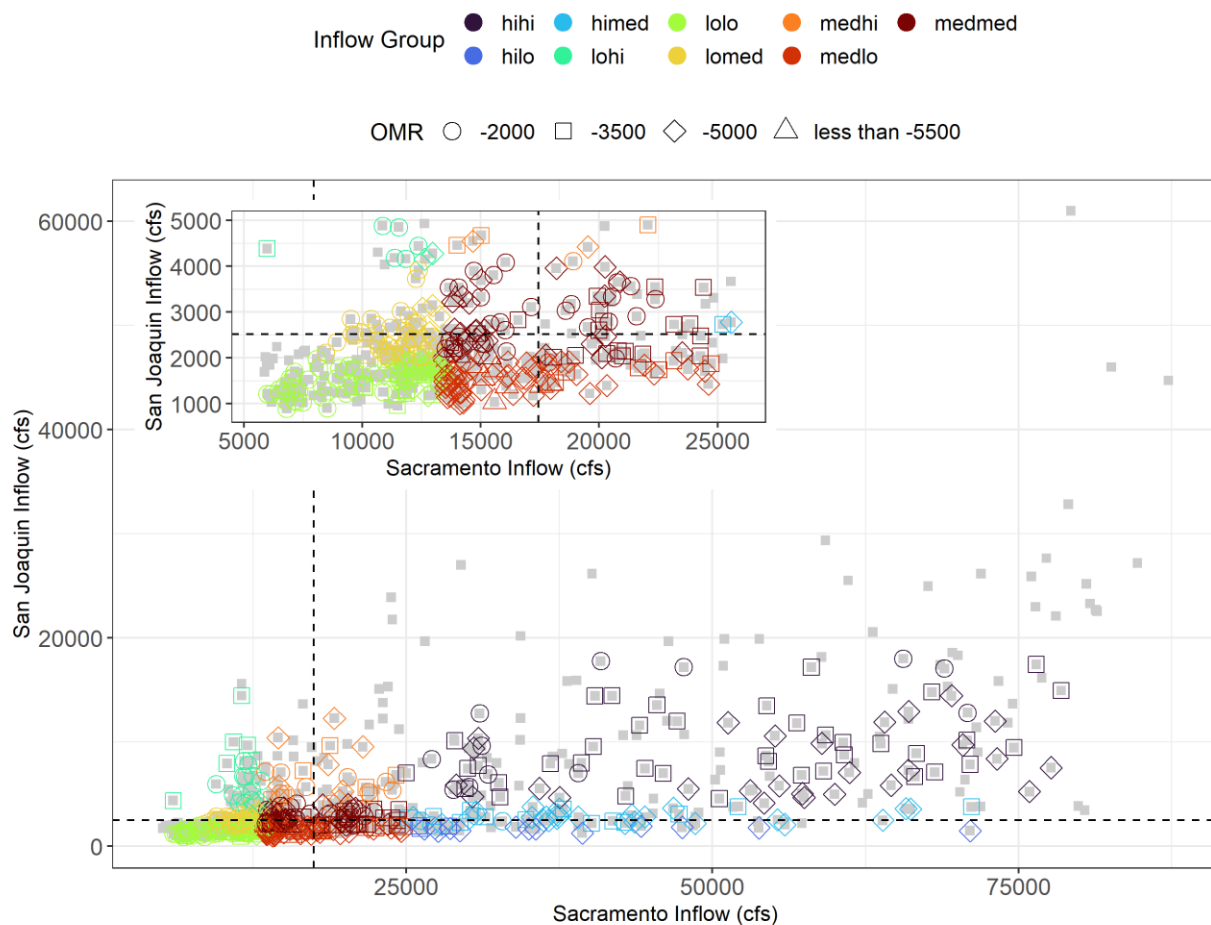


Figure I.3-3. Data categorized into Sacramento and San Joaquin River Inflow Groupings. Gray points represent all data. Points outlined in color indicate data points falling within OMR groupings, and used in subsequent modeling. Inset plot zooms in on lower inflow values for greater resolution. Points and inflow grouping are based Calsim 3 results from the No Action Alternative (NAA).

I.3.1.1.4 DSM2 Velocity Modeling and Post-Processing

In order to assess the potential for water project operations to influence hydrologic characteristics that affect survival and route entrainment, Delta hydrodynamic conditions were analyzed based on a comparative metric, proportion overlap, to capture channel level hydrodynamic details as a single number for color-scale mapping of Delta channels.

For each analysis, two DSM2 simulations must be run to isolate hydrologic alteration by exports: (1) alternative/component of interest and (2) alternative/component of interest without south Delta exports. The second simulation is required to assess the effect of pumping throughout the Delta in the alternative/component of interest. For both simulations (water year 1922 through 2021), hourly average velocity results are retrieved at Delta locations to assess the spatial influence of Delta pumping under various OMR flow conditions.

To assess the effect of pumping for a given inflow combination, the simulation results from the alternative/component of interest are reviewed to identify the periods (months) during which inflow falls within each category. Then, hourly velocity results from the scenario of interest and scenario of interest without south Delta exports are compared across the same set of inflow conditions.

I.3.1.1.5 Gaussian Kernel Density Estimation

The objective of the comparative metric is to summarize the water velocity time series for each channel and scenario such the channel-level comparison is captured in a single number. For the proportion overlap metric, kernel density estimates are calculated on each time series. The kernel density estimates represent a non-parametric smoothing of the empirical distribution of time series values. The proportion overlap of two kernel density estimates is calculated with the following steps: (1) calculate the total area under the curve (AUCt) as the sum of the AUC for each density estimate, (2) calculate the AUC of the overlapping portions (AUCo) of the two density distributions being compared, and (3) calculate the overlapping proportion of the density distributions as AUCo/AUCt. Proportion overlap is naturally bound by zero and one; a value of zero indicates no overlap and a value of one indicates complete overlap. Lower values of proportion overlap identify channels demonstrating larger differences in a scenario comparison. The plots demonstrate change to velocities at the locations listed in Table I.3-6.

Table I.3-6. Locations for Velocity KDE Plots

Locations
San Joaquin River downstream of Old River (Brandt Bridge)
Turner Cut
Columbia Cut
San Joaquin River at Prisoners Point
San Joaquin River at Jersey Point
Old River at Bacon Island
Old River at HWY 4
Middle River near Holt
Victoria Canal near Byron
San Joaquin River upstream of Old River
Old River at Head of Old River
Old River at Middle River
Grant Line Canal at Tracy Bridge
Old River near Tracy
Old River before Franks Tract
Fisherman's Cut
False River before Franks Tract
Threemile Slough
Mokelumne River
San Joaquin River downstream of Big Break
Sacramento River at Rio Vista
Sacramento River at Emmaton

The Gaussian Kernel Density Estimate (KDE) compares hourly velocities at a given location for the scenario of interest with and without Delta exports. An example KDE plot is presented in Figure I.3-4. Each figure presents: (1) location, (2) OMR bin of interest (either -2,000 cfs, -3,500 cfs or -5,000 cfs), (3) proportion of the simulation presented, (4) proportional overlap area of the Gaussian KDE curves, (5) differential of the median velocity between the two simulations, and (6) reference directional on the x-axis.

KDE of SJR at Jersey Point Velocity in Dec-Jun

OMR = -5000 cfs; Proportion of Simulation: 14%;
Proportional Overlap = 0.969; Velocity Differential = 0.1 fps

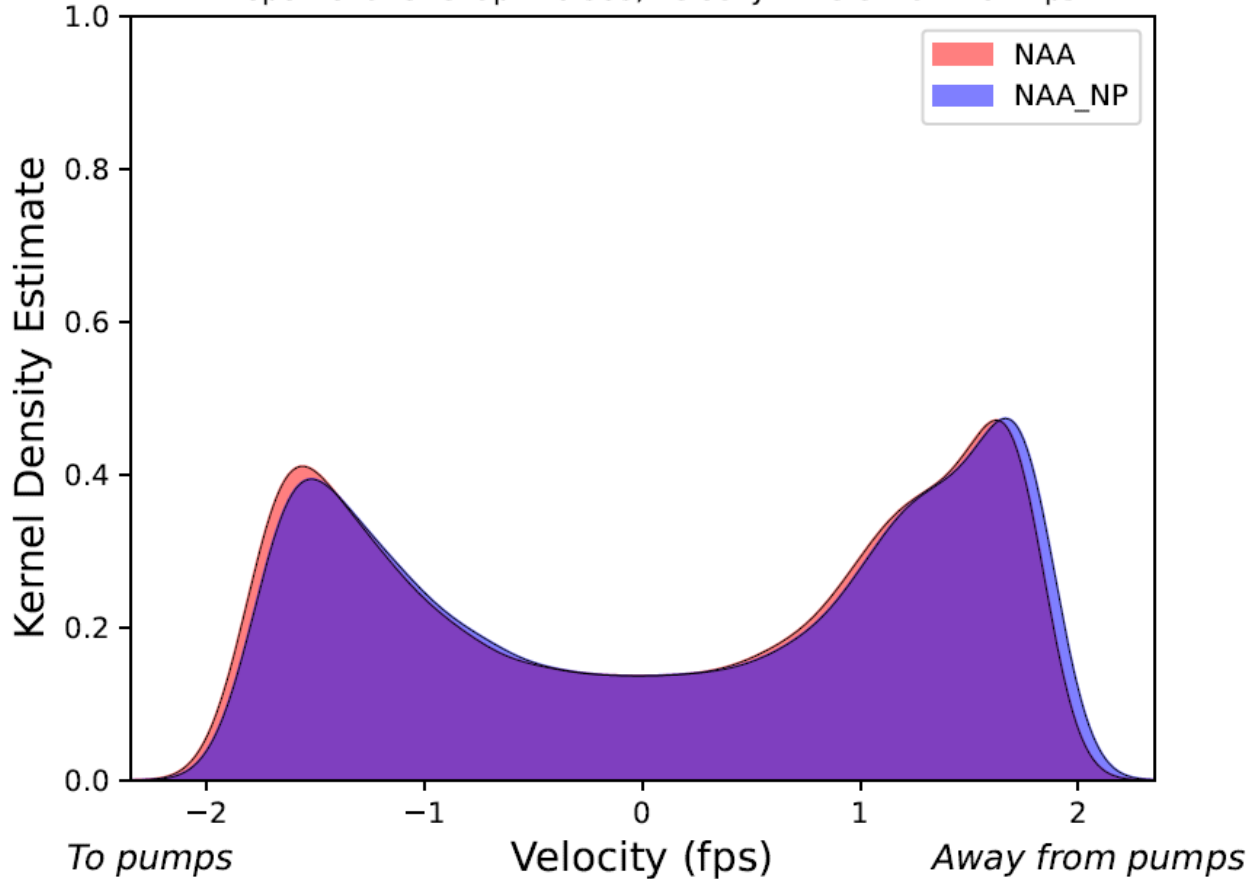


Figure I.3-4. Gaussian KDE of Velocity at San Joaquin River at Jersey Point in December through June with OMR of -5,000 cfs. Results apply to the No Action Alternative.

In Figure I.3-4, a proportional overlap value of 0.969 indicates that the distribution of velocity is similar under the NAA and NAA without Delta exports (NAA_NP) 96.9% of the time. A velocity differential value of 0.1 fps indicates that there is a 0.1 fps change in the median hourly average velocity between the scenario of interest with- and w/out pumps.

The proportional overlap value and velocity differential explain the change in the velocity distribution and the magnitude to which the velocities have changed, respectively. For example, in Figure I.3-5 (below), when OMR flows are -5,000 cfs at Old River at Middle River, the proportional overlap value is 0.809 and the velocity differential is 0.14 fps. The lower value in proportional overlap (compared with Figure I.3-4) indicates a larger difference in velocity distribution. However, the velocity differential is only 0.14 fps, a small change in median velocities. Together, these values indicate that the KDE curves may be different, but the actual change to velocity at that location is relatively small.

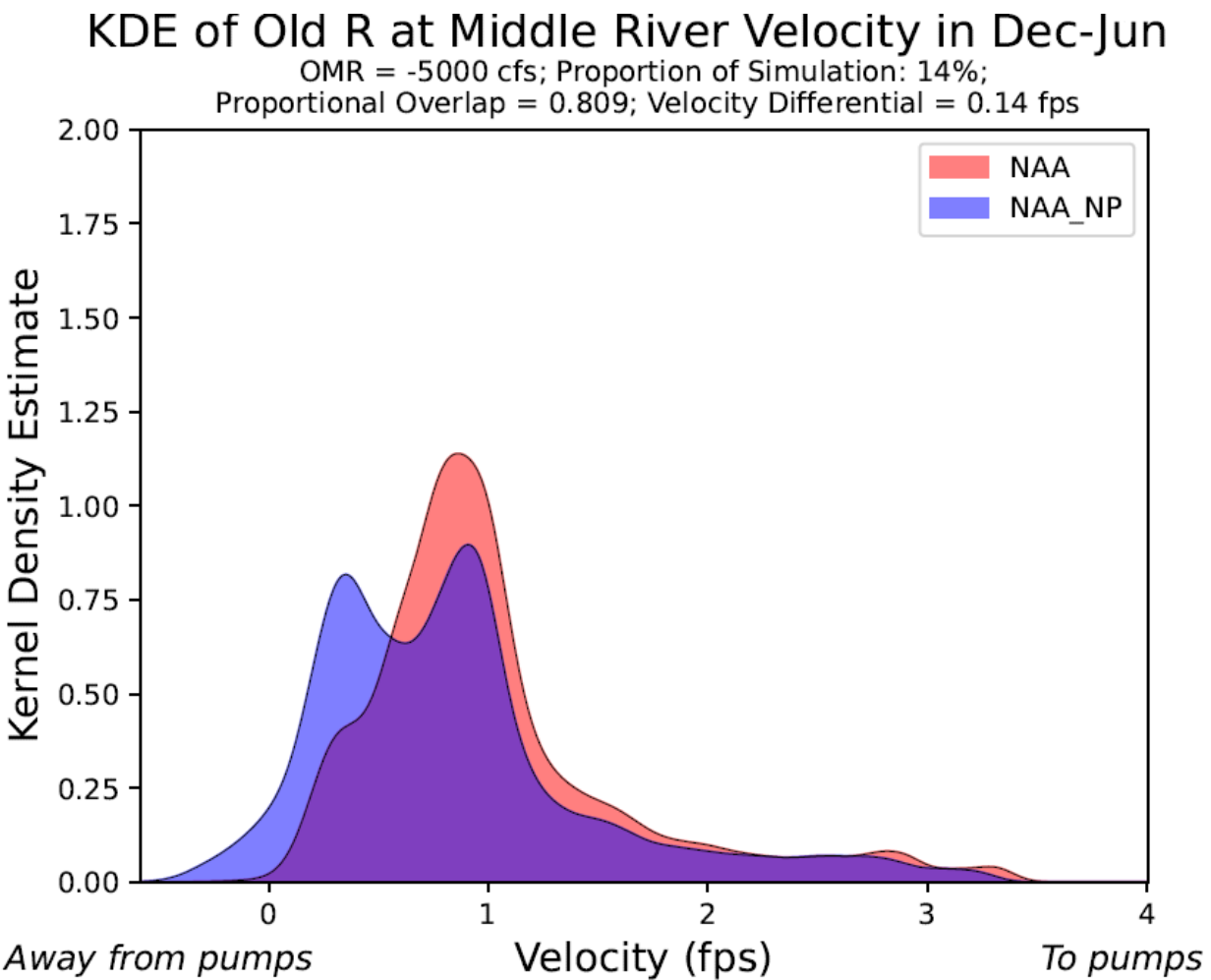


Figure I.3-5. Gaussian KDE of Velocity at Old River at Middle River in December through June with OMR of -5,000 cfs. Results apply to the No Action Alternative.

I.3.1.6 Gaussian KDE Proportional Overlap Contour Maps

For each inflow group, the proportional overlap of the hourly average velocity Gaussian KDEs for the scenario of interest with and without Delta exports at each location in the Delta are compared in each OMR bin.

Contour maps are used to visualize the outlining of the Delta export zone of influence for each condition as described above. Contours of 0.75 are selected to represent areas experiencing high and medium frequency of alteration from pumping. In order to reduce the noise in contour lines, DSM2 nodes that were sufficiently different from neighboring nodes to create isolated contours at several OMR flows were removed (nodes 146, 147, 148, 206, 242, 246, 432, 433, 434 for inflow contour maps). It was unclear whether the values associated with these DSM2 nodes were artifacts of the model output and/or assumptions, or due to unique hydrodynamics characteristics at each node location.

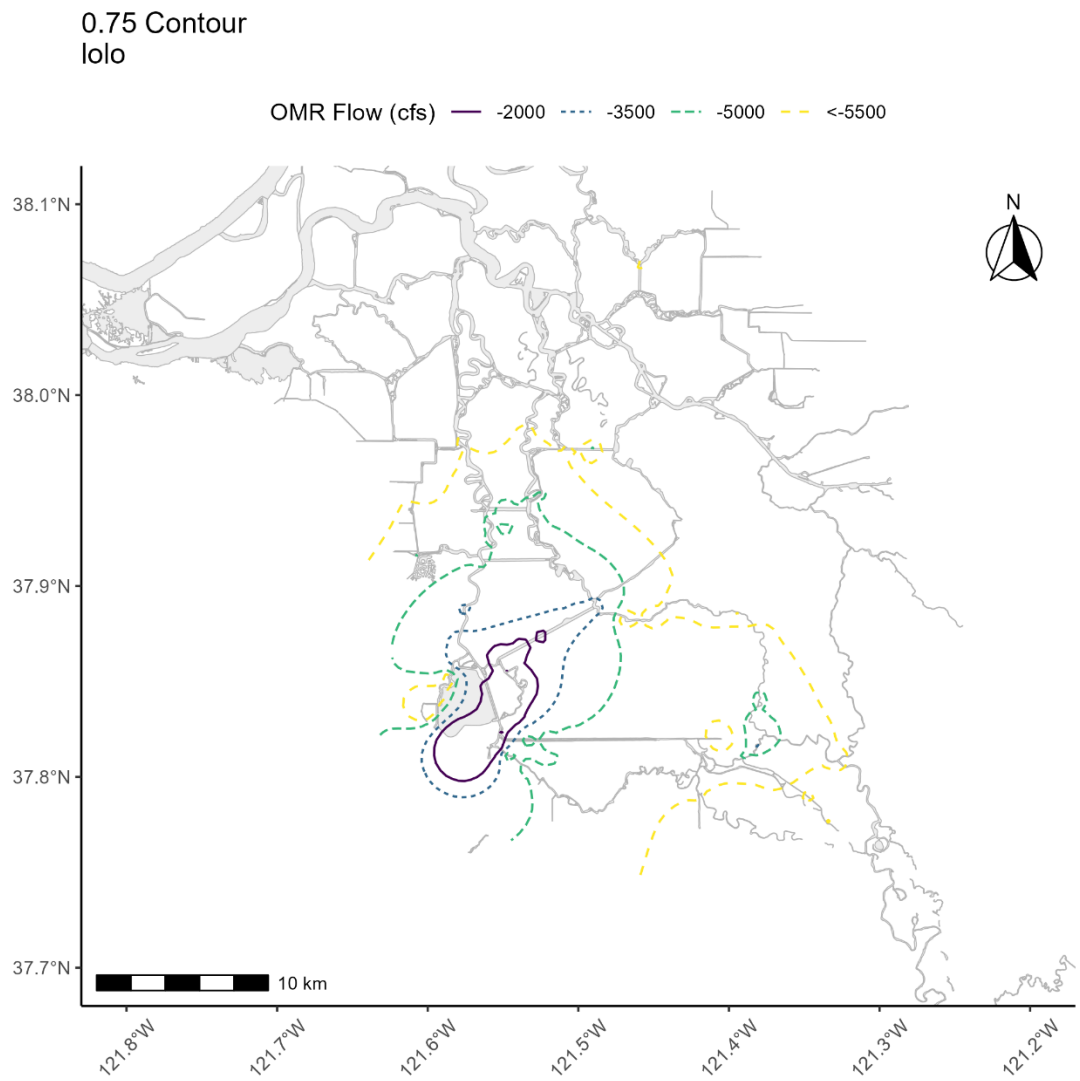


Figure I.3-6. Example 0.75 contour map for the lolo inflow group.

I.3.1.1.7 Channel length associated with ZOI

The proportion of DSM grid altered is also used as a metric to evaluate OMR influence at high, medium, and low pumping influence for each inflow group. Data are filtered to nodes with <25% proportion overlap (high alteration from pumping), 25-75% proportion overlap (medium alteration from pumping), and >75% proportion overlap (low alteration from pumping). For each inflow group and OMR bin, known lengths between DSM2 nodes are used to calculate summed channel length altered under high, medium, and low alteration from pumping. Summed channel length under each condition is divided by total DSM2 grid channel length to obtain the proportion of the DSM2 grid that was altered. Proportion of altered channel length is then plotted for each alternative by inflow group and OMR bin. Proportion of channel length altered for nodes experiencing medium alteration from pumping are also visualized separately to demonstrate for each alternative how patterns change by inflow group, OMR bin. Note that DSM2 nodes that differed from neighboring nodes sufficiently were removed (Removed nodes: 146, 147, 148, 206, 242, 246, 432, 433, 434). It is unclear whether the values associated with these DSM2 nodes are artifacts of the model output and/or assumptions, or due to unique hydrodynamics characteristics at that node location.

I.3.1.2 Assumptions / Uncertainty / Caveats

Proportional overlap thresholds for low, medium, high proportion overlap and values chosen for contour visualization were selected based on frequency thresholds in the BA. Patterns may differ depending on the threshold selected.

While the study hypothesizes that lower proportional overlap values (higher alteration from pumping) lead to higher likelihood of altering fish movements, the proportional overlap values do not reflect the magnitude of velocity differences, only that there were differences. Thus, two locations with the same value of proportional overlap might experience very different magnitudes of velocity difference. These figures also do not directly reflect biological implications, as velocity differences are not being analyzed, and there is no comparison with values of velocity change that would alter fish movements.

Contour maps have been mapped across land to visualize the relative spatial extent of the Delta export zone of influence at each OMR flow. Reclamation assumes changes in the Delta's channels and channel configuration (e.g., new channels constructed) would impact regional hydrodynamics, and therefore the Delta export zone of influence would need to be recalculated. In other words, this map does not suggest that a new channel added within the current Delta export zone of influence would have the same impacts of pumping as existing waterways within that contour. The addition of new waterways would require an update to the current DSM2 models and recalculation of the Delta export zone of influence.

While channel length is a useful metric for calculating the extent of hydrologic influence from pumping, width and depth can also alter the hydrodynamic extent of pumping influence. These variables were not considered for this analysis.

Seasonal tidal influence can play a role in hydrodynamics, and was not taken into account for this analysis.

The primary contrasts within and between alternatives are based on the estimated overlap in velocity distributions at DSM2 nodes when facilities are and are not exporting water (i.e., pumping and no pumping). However, it is important to note that the estimated distribution of velocities under ‘pumping’ and ‘no pumping’ conditions contains time periods when no pumping is occurring in either condition because pumping is not continuous under the alternatives. The analysis does not consider the number of pumping hours in a given inflow-OMR grouping.

Sample sizes vary among different inflow groups and OMR bins (Table I.3-4). While all combinations with data were visualized, the amount of certainty and variability in a given result may differ widely depending on the sample size.

I.3.1.3 Code and Data Repository

Code for inflow grouping, contour maps, and channel length plots are available at:

<https://github.com/BDO-Science/contour-zone-of-influence>. Files also available upon request.

See readme at: https://github.com/BDO-Science/contour-zone-of-influence/blob/main/README_zoi.txt for information about the files used to generate results for Delta Exports Zone of Influence.

I.3.2 Results

With the methodology described above, results were prepared: (1) KDE plots of hourly velocities at -2000, -3500, -5000, and less than -5500 cfs OMR conditions for the different inflow groups as specific locations, (2) contour maps of proportional overlap by month with different OMR conditions, and (3) proportion of channel lengths altered under differing inflow and OMR conditions.

The Gaussian KDE plots, contour maps, and channel length plots demonstrate the effects of pumping under a range of OMR flow conditions. Several factors affect the proportional overlap and velocity differential values, including proximity to the pumps, orientation of the flow (relative to the pumps), influence of riverine flow, and preexisting flow/velocity patterns in the channel. Each location and output parameter (proportional overlap and velocity differential) must be examined to understand the influence of pumping at a given location.

I.3.2.1 Gaussian Kernel Density Estimation

Plots of velocity KDE for each alternative under different OMRs at three locations are presented below as examples. The three locations at which the KDE plots are presented are Turner Cut, San Joaquin River at Jersey Point, and Old River at Middle River (0). At each location, several plots (one for each OMR bin) are included. As the regulatory environment changes in the scenarios of interest, the number of OMR bins associated with each analysis changes.

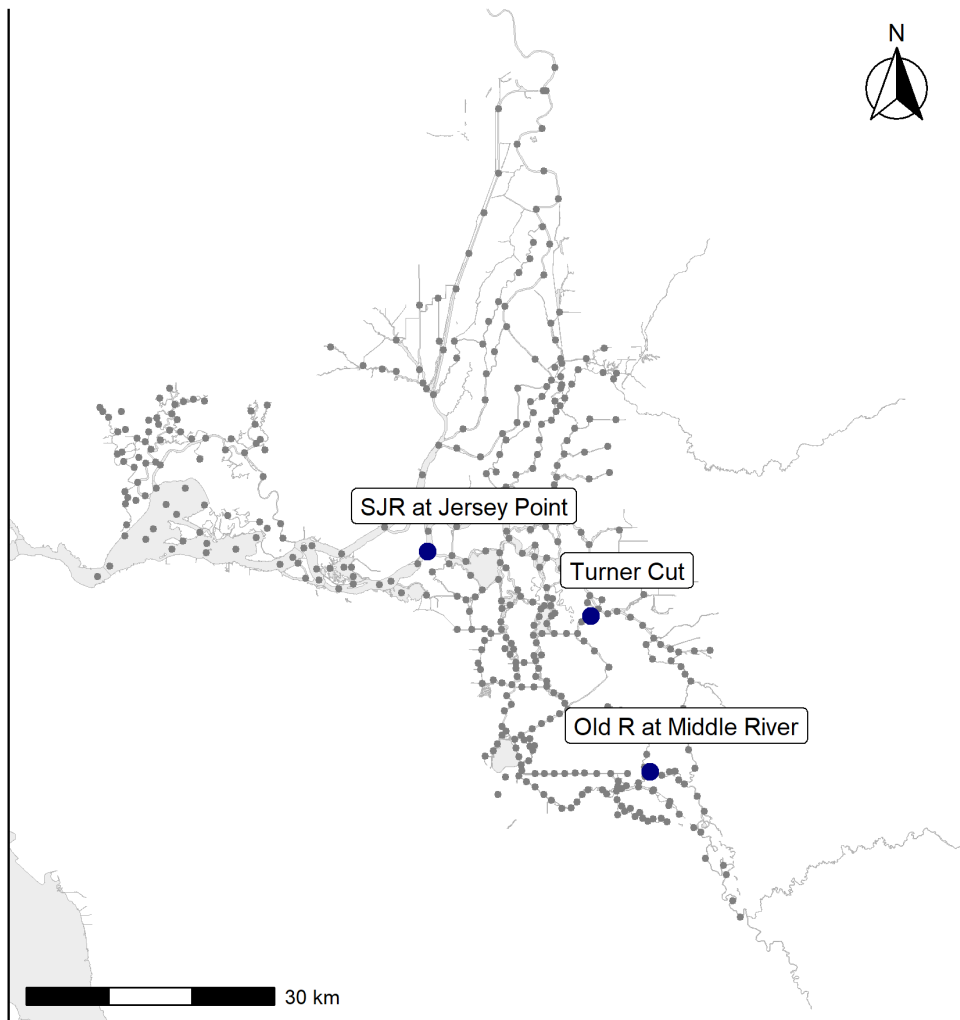


Figure I.3-7. Map of Stations Used for Kernel Density Estimate (KDE) Plot Examples. Small gray points indicate all nodes in DSM2 grid. Large navy points indicate stations selected for KDE plot examples below.

I.3.2.1.1 KDE plots for No Action Alternative:

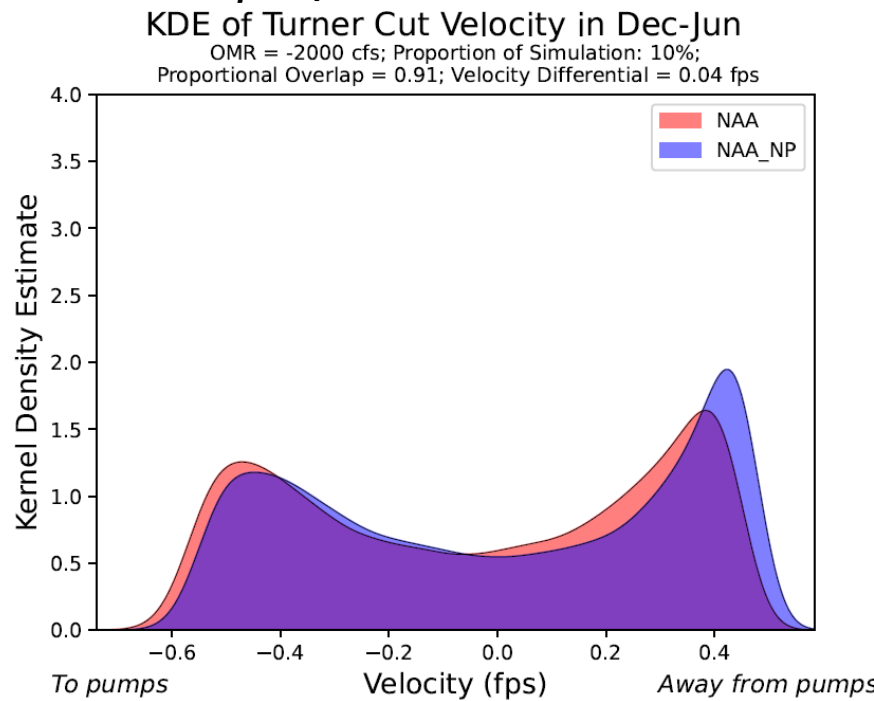


Figure I.3-8. Gaussian KDE of Velocity at Turner Cut in December through June with OMR of -2,000 cfs. Results apply to the No Action Alternative.

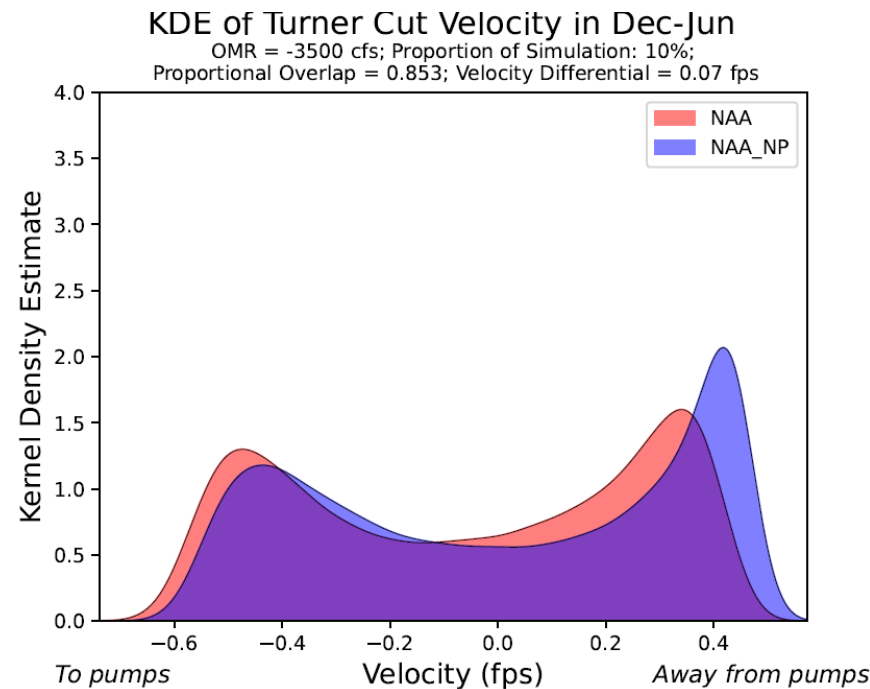


Figure I.3-9. Gaussian KDE of Velocity at Turner Cut in December through June with OMR of -3,500 cfs. Results apply to the No Action Alternative.

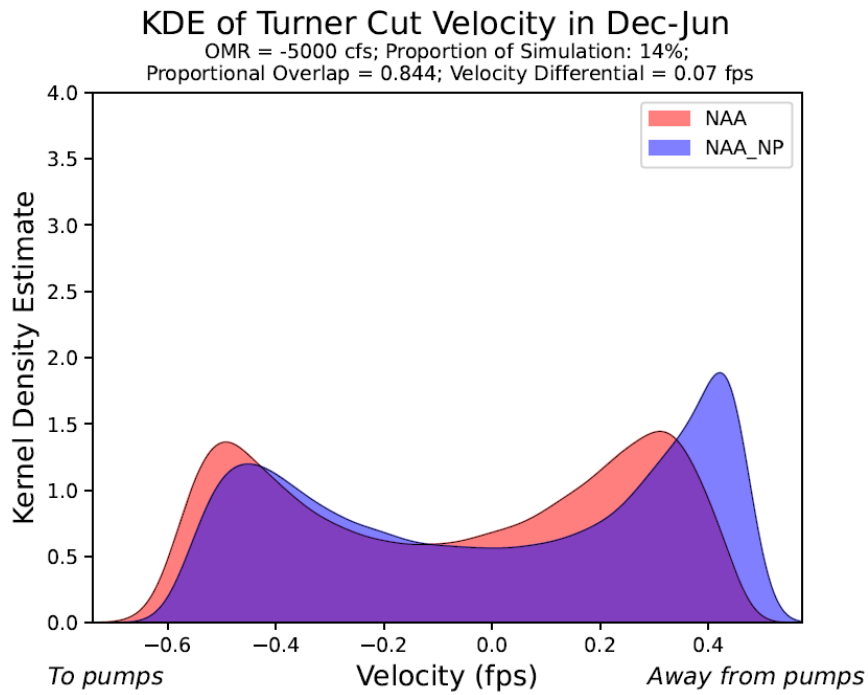


Figure I.3-10. Gaussian KDE of Velocity at Turner Cut in December through June with OMR of -5,000 cfs. Results apply to the No Action Alternative.

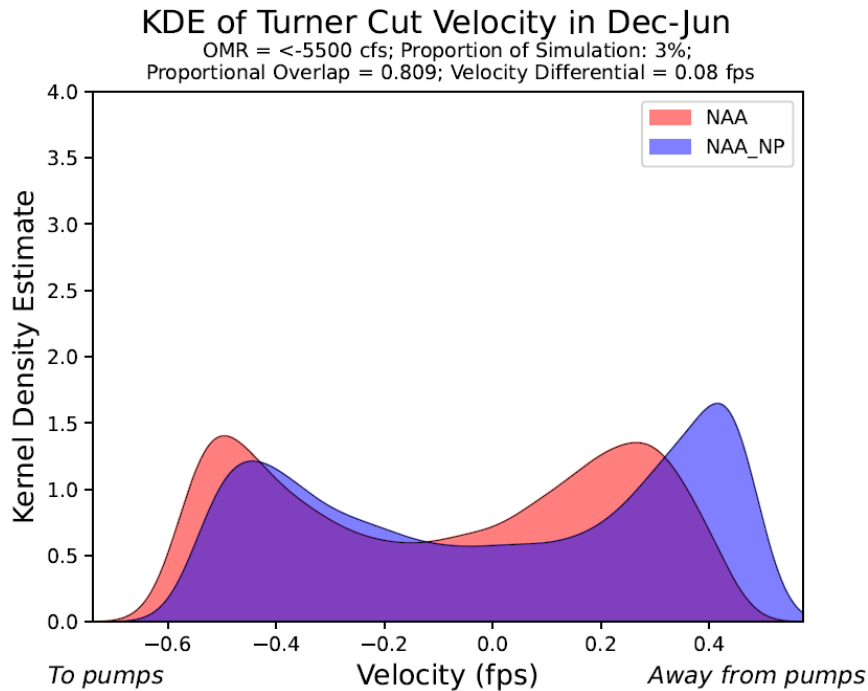


Figure I.3-11. Gaussian KDE of Velocity at Turner Cut in December through June with OMR < -5,500 cfs. Results apply to the No Action Alternative.

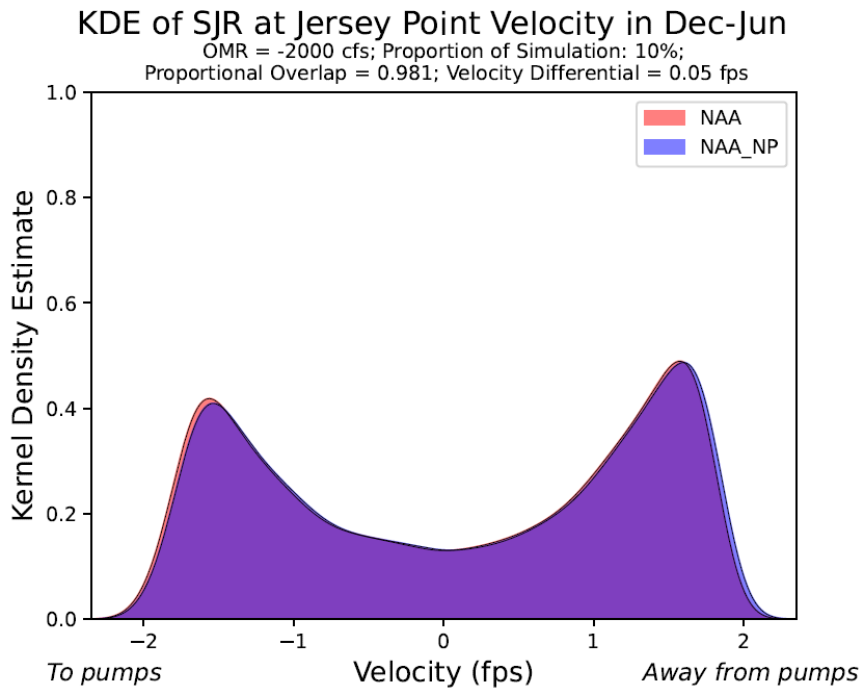


Figure I.3-12. Gaussian KDE of Velocity at San Joaquin River at Jersey Point in December through June with OMR of -2,000 cfs. Results apply to the No Action Alternative.

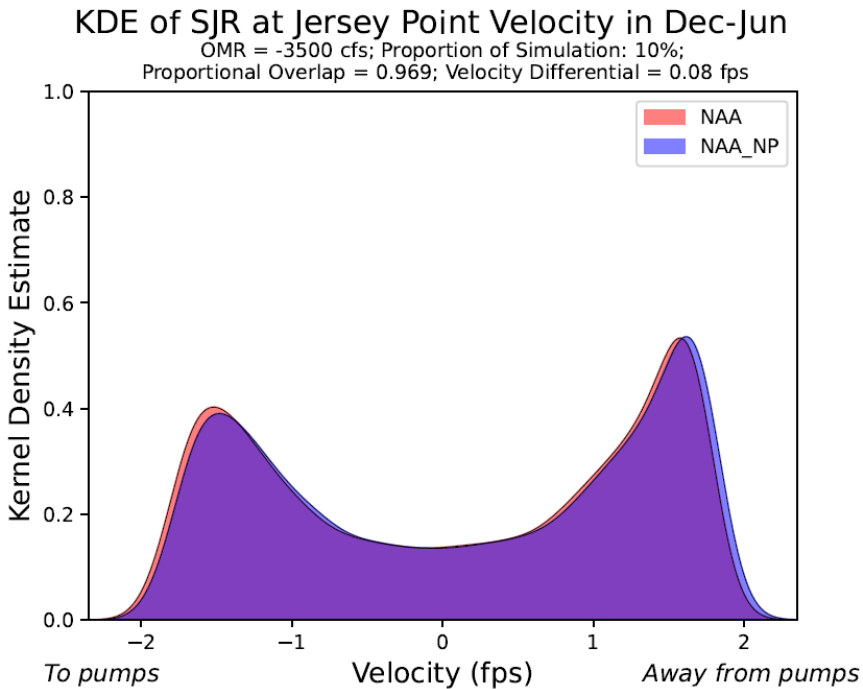


Figure I.3-13. Gaussian KDE of Velocity at San Joaquin River at Jersey Point in December through June with OMR of -3,500 cfs. Results apply to the No Action Alternative.

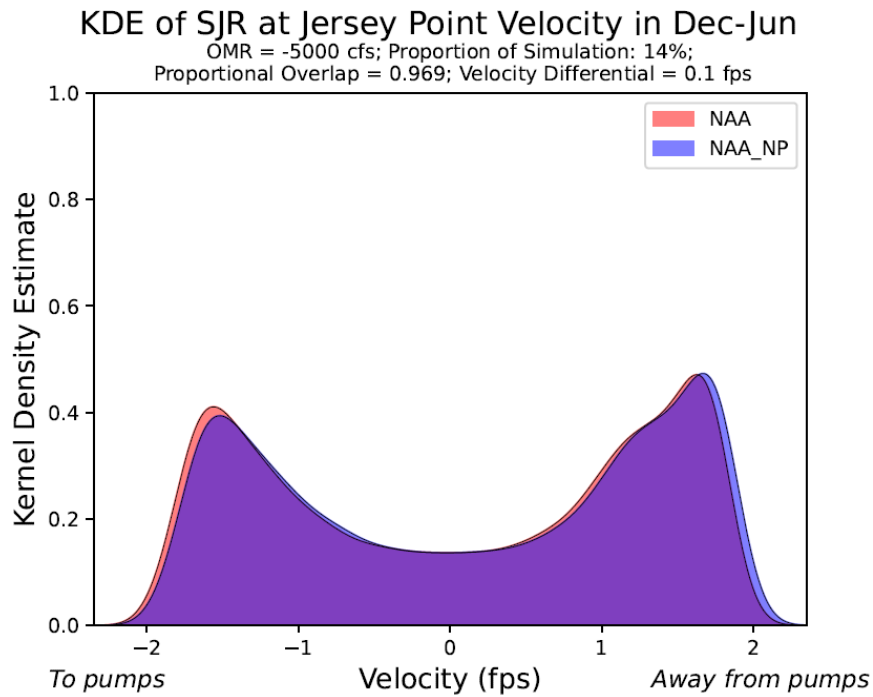


Figure I.3-14. Gaussian KDE of Velocity at San Joaquin River at Jersey Point in December through June with OMR of -5,000 cfs. Results apply to the No Action Alternative.

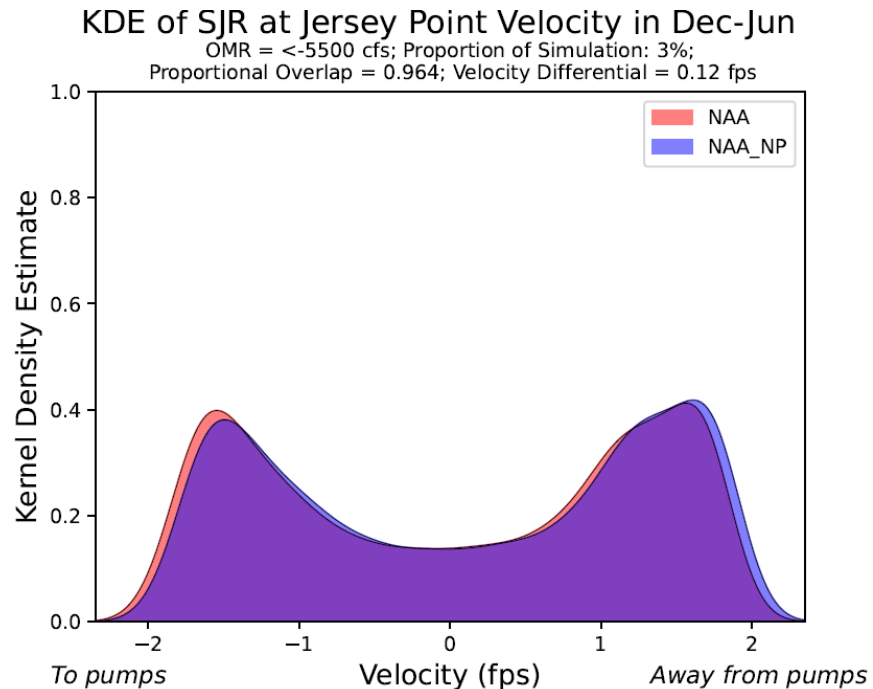


Figure I.3-15. Gaussian KDE of Velocity at San Joaquin River at Jersey Point in December through June with OMR < -5,500 cfs. Results apply to the No Action Alternative.

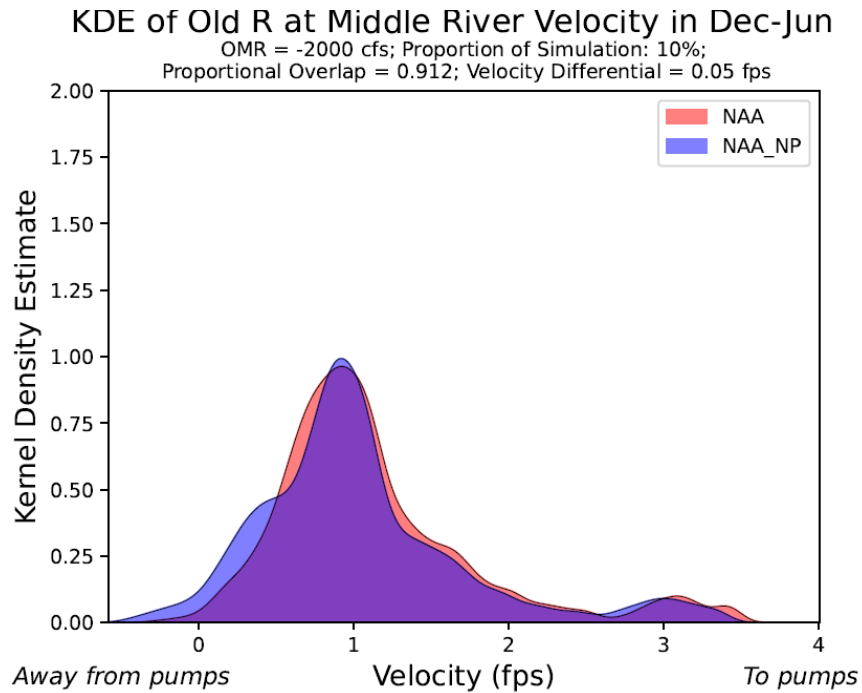


Figure I.3-16. Gaussian KDE of Velocity at Old River at Middle River in December through June with OMR of -2,000 cfs. Results apply to the No Action Alternative.

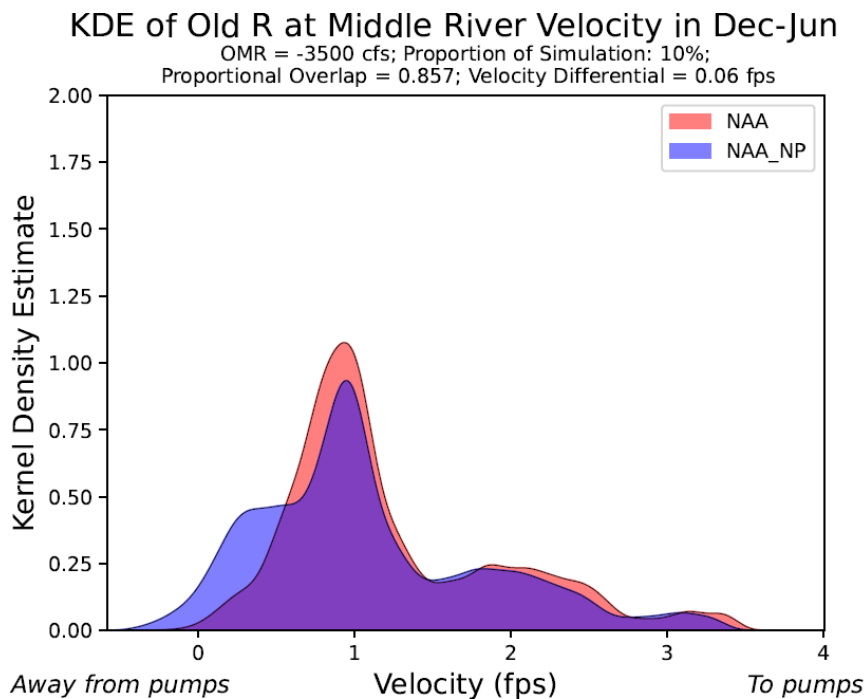


Figure I.3-17. Gaussian KDE of Velocity at Old River at Middle River in December through June with OMR of -3,500 cfs. Results apply to the No Action Alternative.

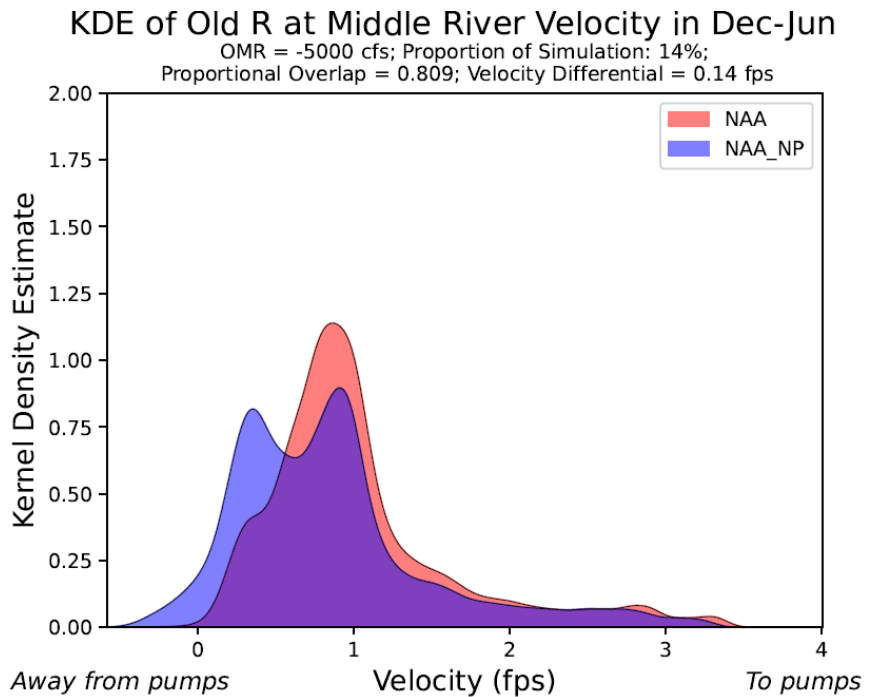


Figure 3-18. Gaussian KDE of Velocity at Old River at Middle River in December through June with OMR of -5,000 cfs. Results apply to the No Action Alternative.

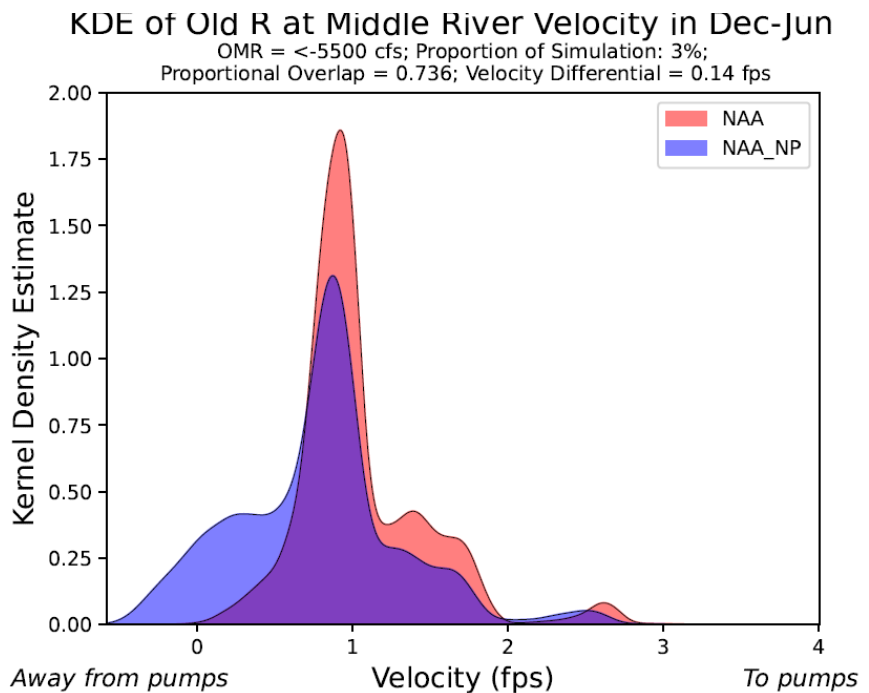


Figure I.3-19. Gaussian KDE of Velocity at Old River at Middle River in December through June with OMR < -5,500 cfs. Results apply to the No Action Alternative.

I.3.2.1.2 KDE plots for Alt1 alternative:

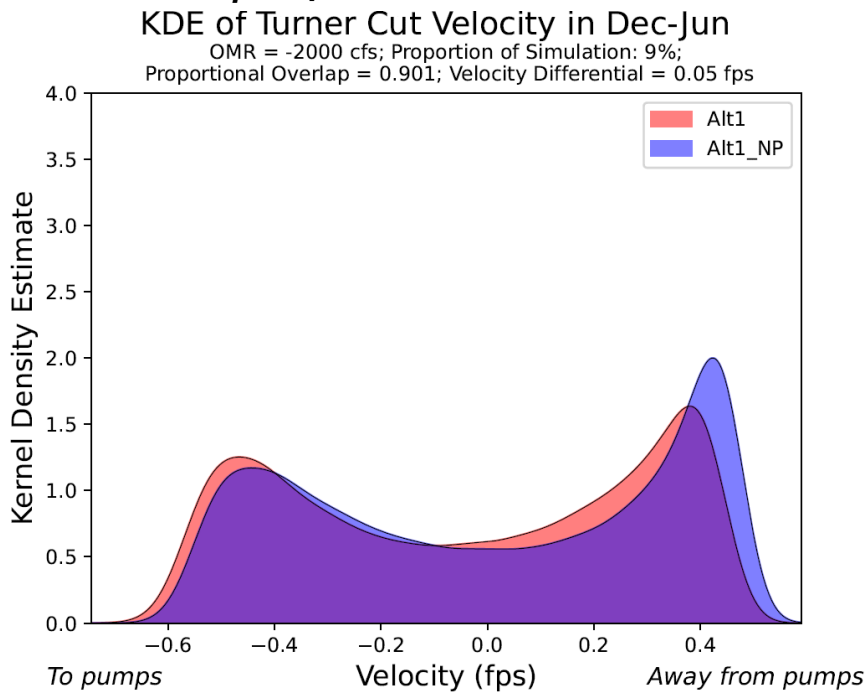


Figure I.3-20. Gaussian KDE of Velocity at Turner Cut in December through June with OMR of -2,000 cfs. Results apply to the Alt1 alternative.

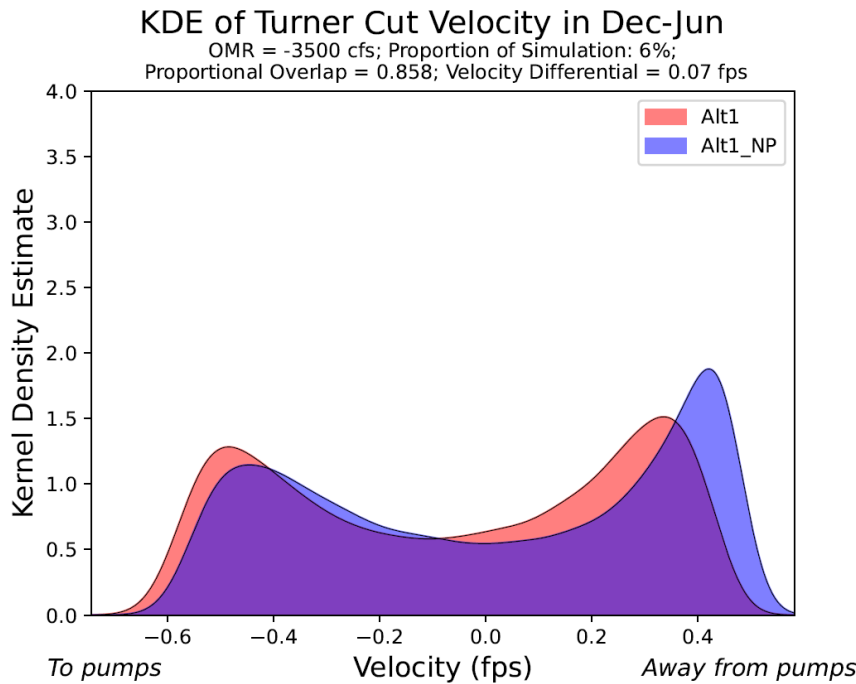


Figure I.3-21. Gaussian KDE of Velocity at Turner Cut in December through June with OMR of -3,500 cfs. Results apply to the Alt1 alternative.

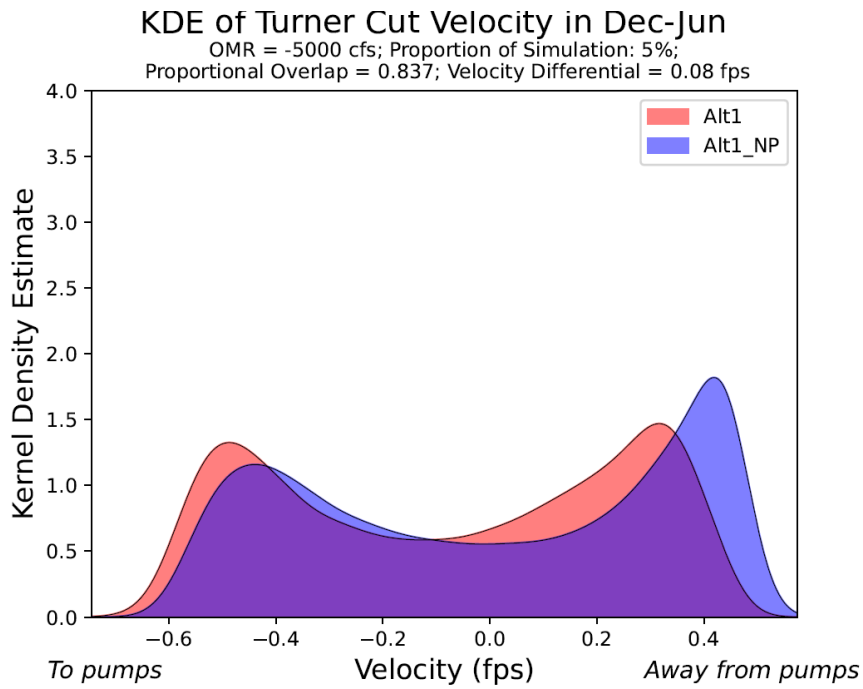


Figure I.3-22. Gaussian KDE of Velocity at Turner Cut in December through June with OMR of -5,000 cfs. Results apply to the Alt1 alternative.

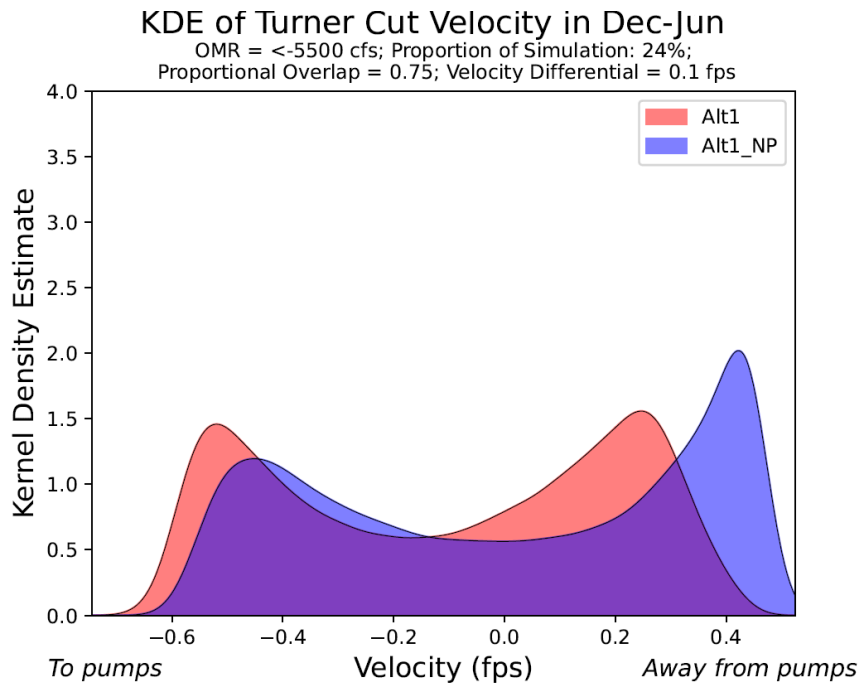


Figure I.3-23. Gaussian KDE of Velocity at Turner Cut in December through June with OMR < -5,500 cfs. Results apply to the Alt1 alternative.

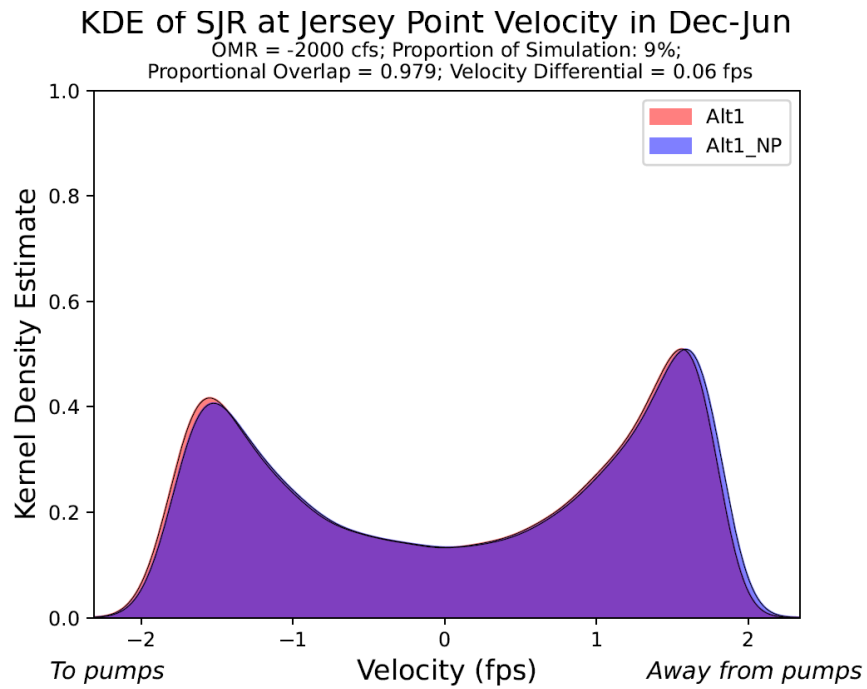


Figure I.3-24. Gaussian KDE of Velocity at San Joaquin River at Jersey Point in December through June with OMR of -2,000 cfs. Results apply to the Alt1 alternative.

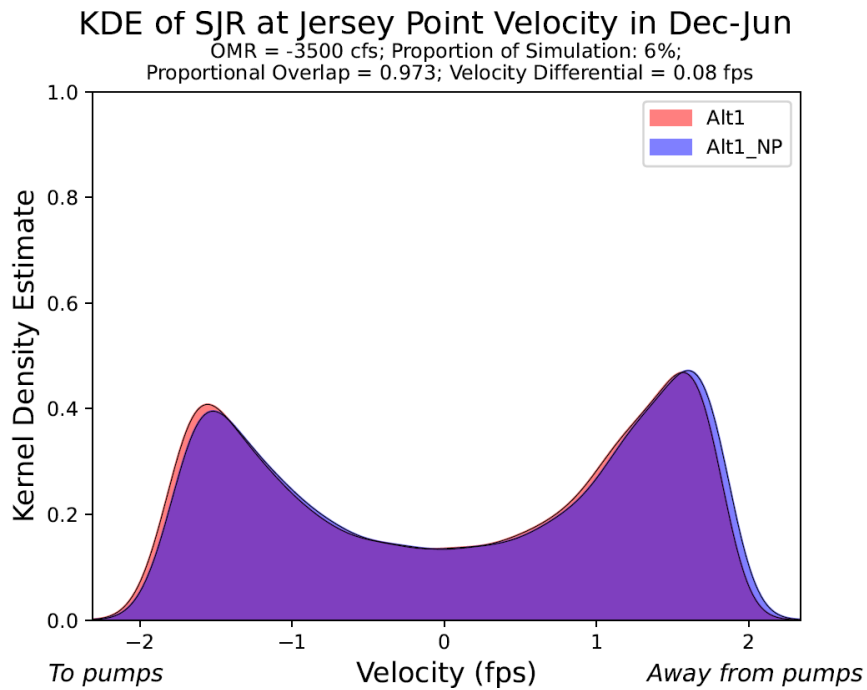


Figure I.3-25. Gaussian KDE of Velocity at San Joaquin River at Jersey Point in December through June with OMR of -3,500 cfs. Results apply to the Alt1 alternative.

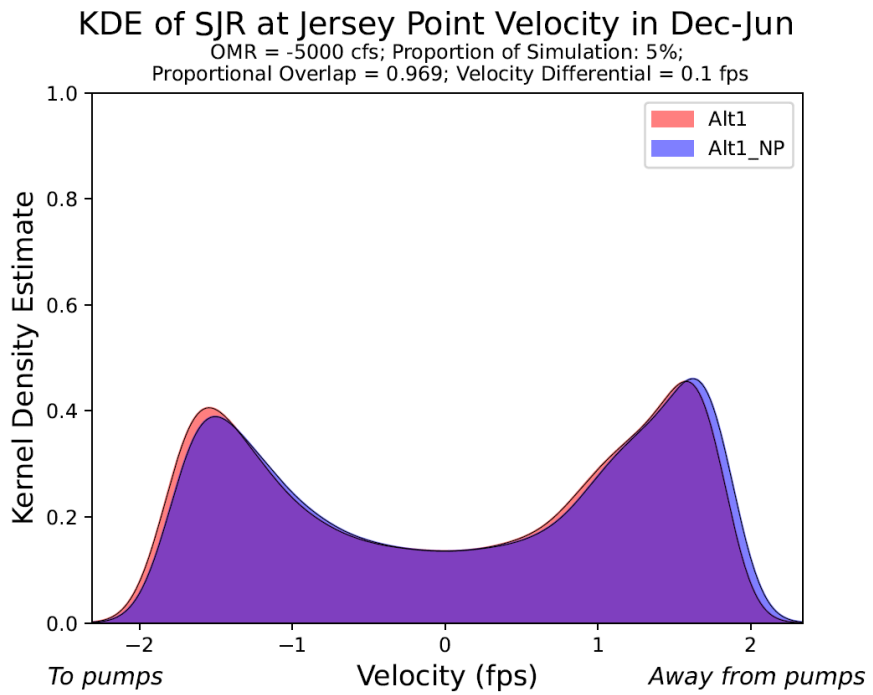


Figure I.3-26. Gaussian KDE of Velocity at San Joaquin River at Jersey Point in December through June with OMR of -5,000 cfs. Results apply to the Alt1 alternative.

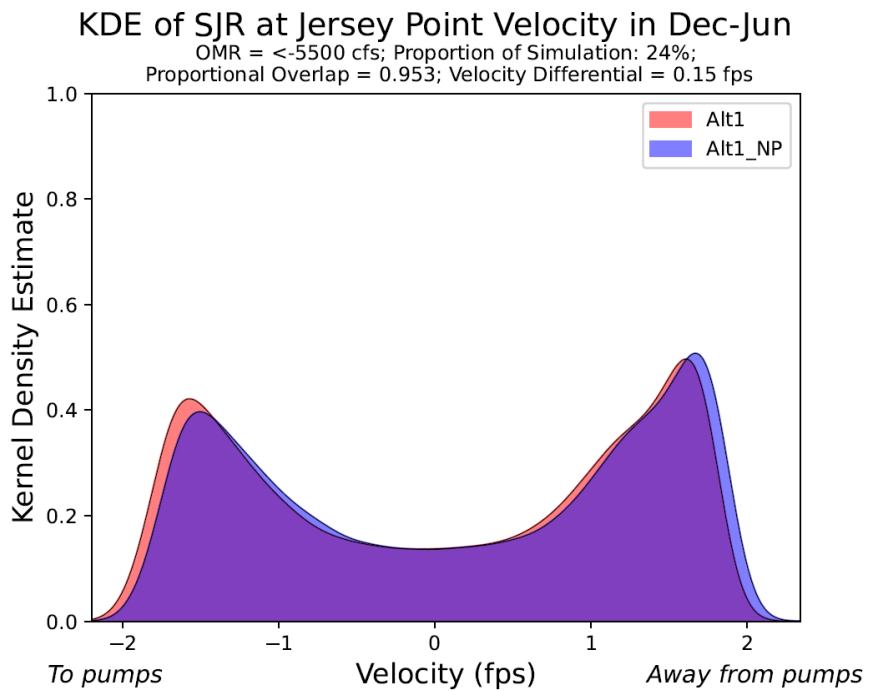


Figure I.3-27. Gaussian KDE of Velocity at San Joaquin River at Jersey Point in December through June with OMR < -5,500 cfs. Results apply to the Alt1 alternative.

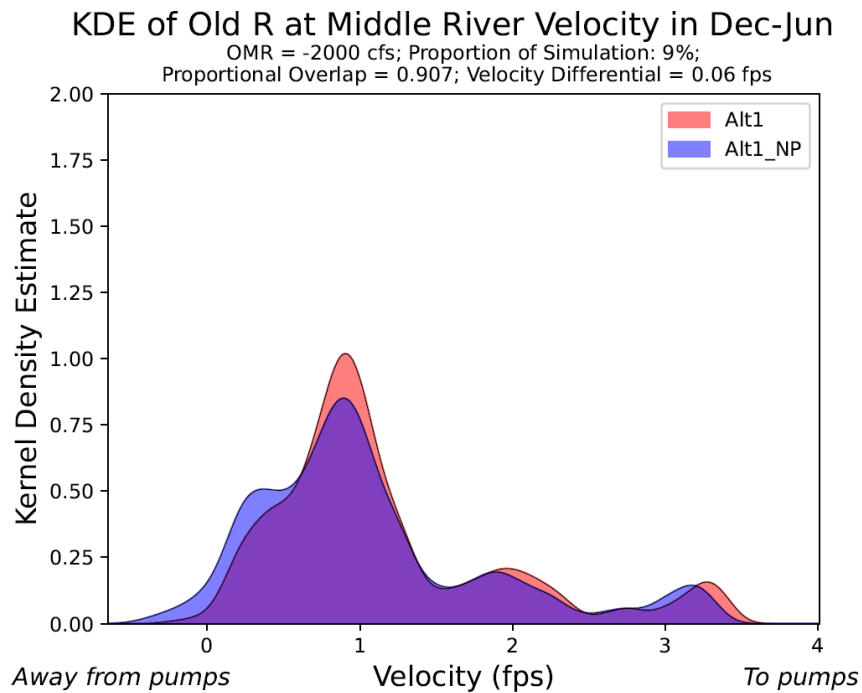


Figure I.3-28. Gaussian KDE of Velocity at Old River at Middle River in December through June with OMR of -2,000 cfs. Results apply to the Alt1 alternative.

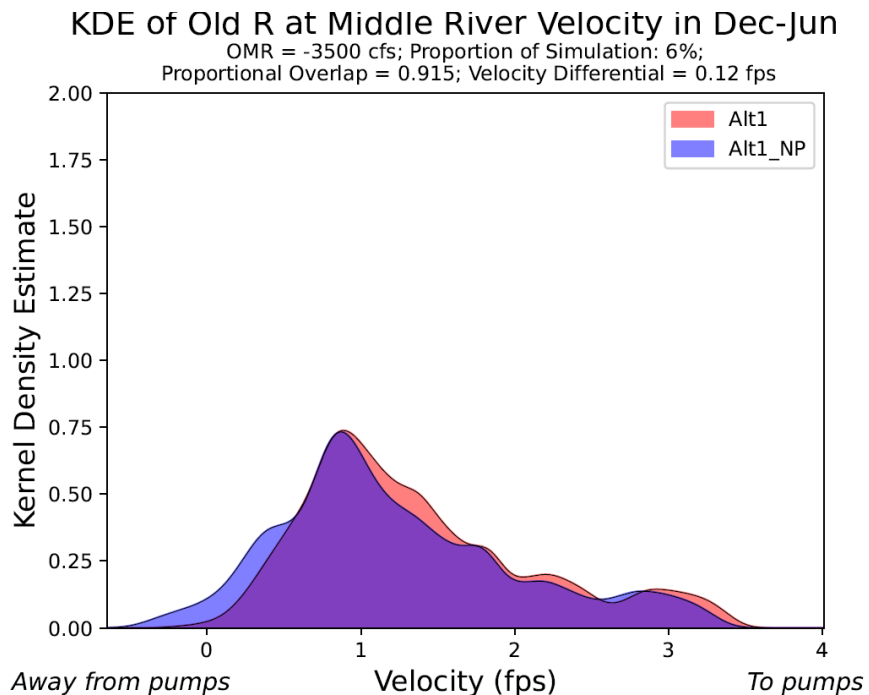


Figure I.3-29. Gaussian KDE of Velocity at Old River at Middle River in December through June with OMR of -3,500 cfs. Results apply to the Alt1 alternative.

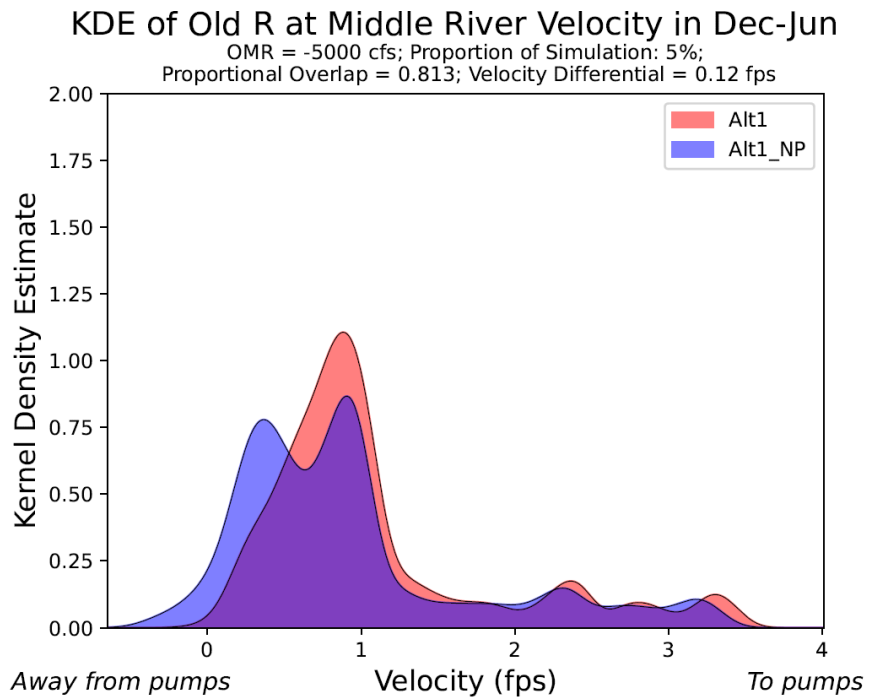


Figure I.3-30. Gaussian KDE of Velocity at Old River at Middle River in December through June with OMR of -5,000 cfs. Results apply to the Alt1 alternative.

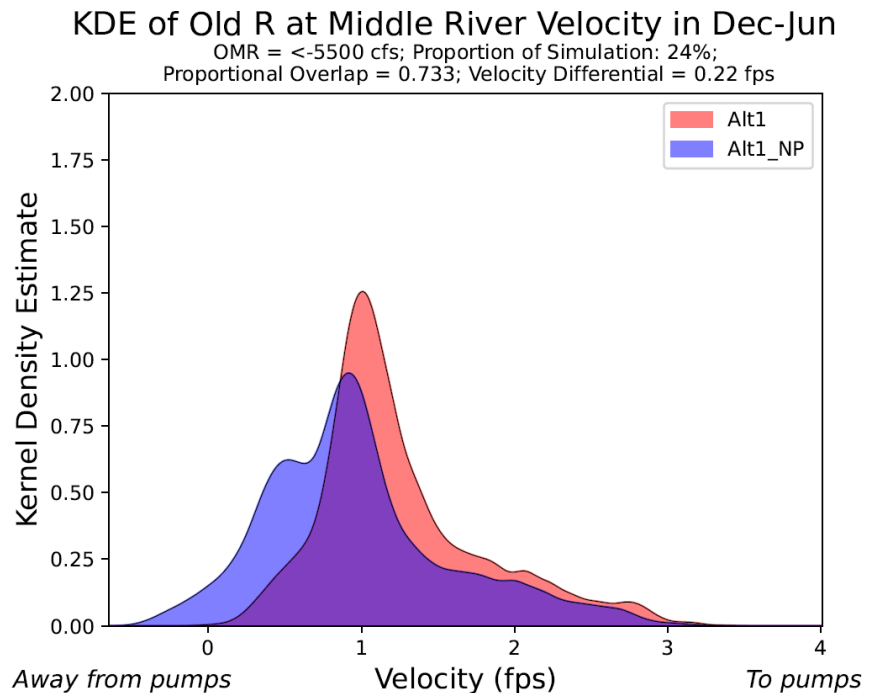


Figure I.3-31. Gaussian KDE of Velocity at Old River at Middle River in December through June with OMR < -5,500 cfs. Results apply to the Alt1 alternative.

I.3.2.1.3 KDE plots for Alt2v1woTUCP alternative:

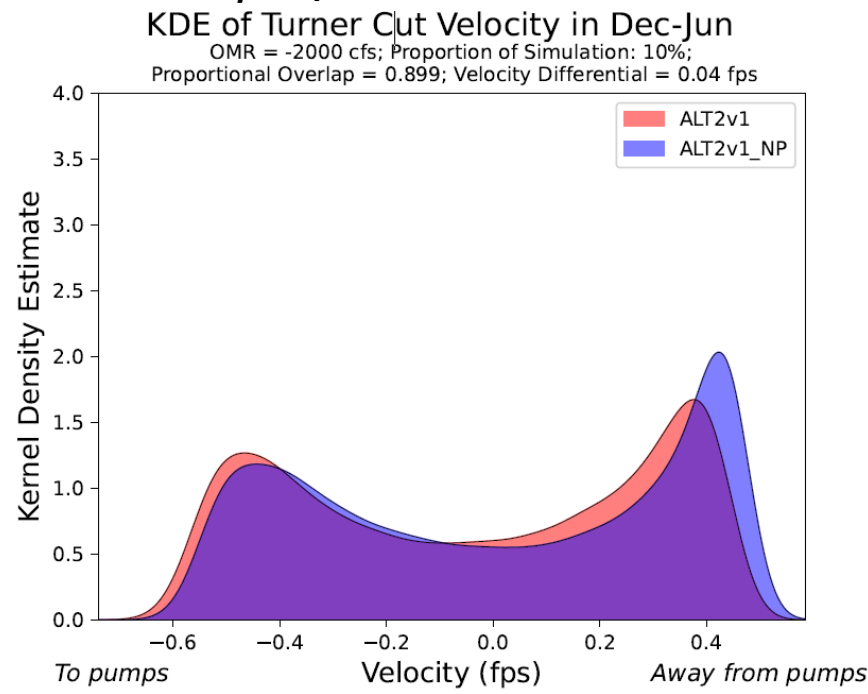


Figure I.3-32. Gaussian KDE of Velocity at Turner Cut in December through June with OMR of -2,000 cfs. Results apply to the Alt2v1woTUCP alternative.

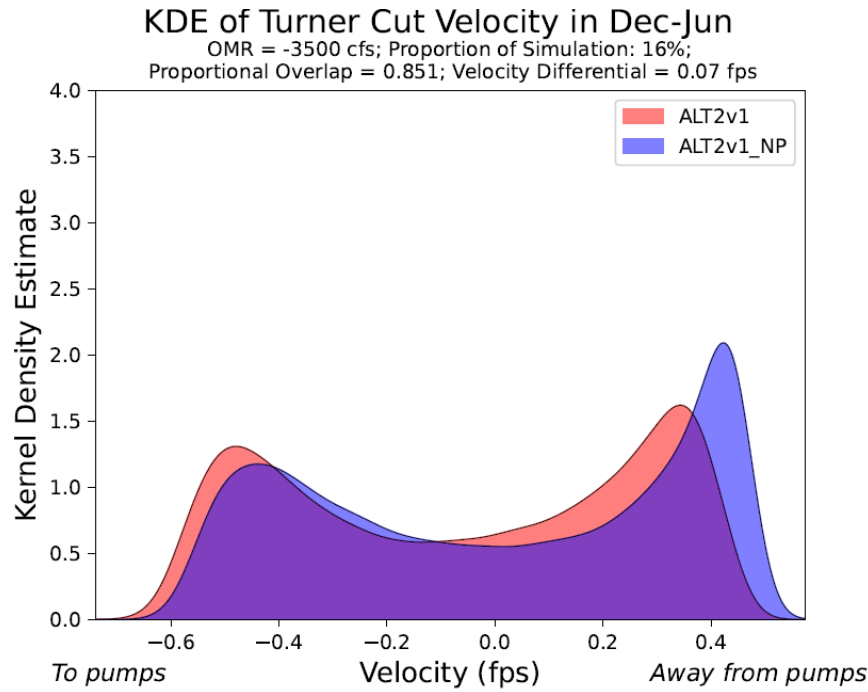


Figure I.3-33. Gaussian KDE of Velocity at Turner Cut in December through June with OMR of -3,500 cfs. Results apply to the Alt2v1woTUCP alternative.

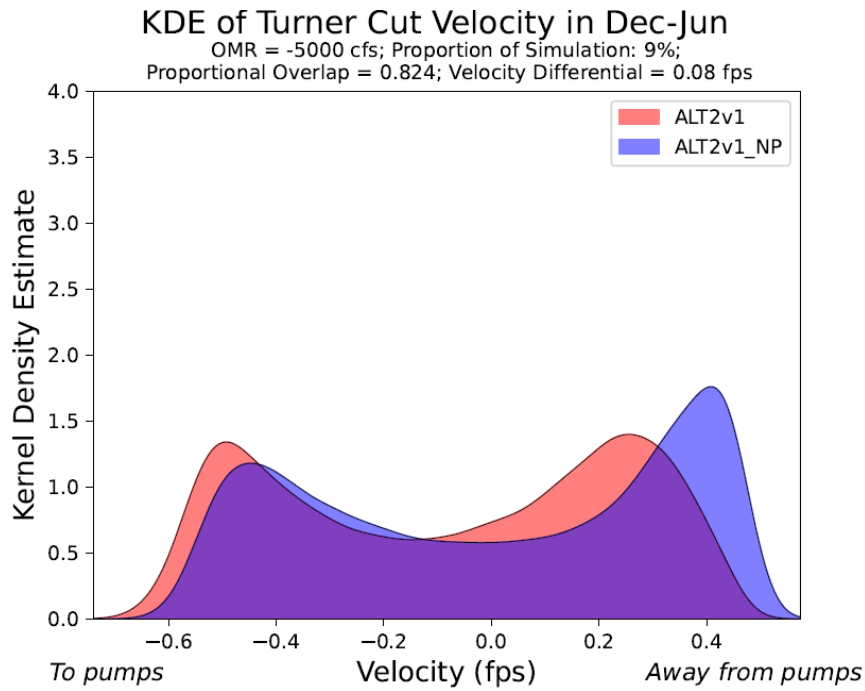


Figure I.3-34. Gaussian KDE of Velocity at Turner Cut in December through June with OMR of -5,000 cfs. Results apply to the Alt2v1woTUCP alternative.

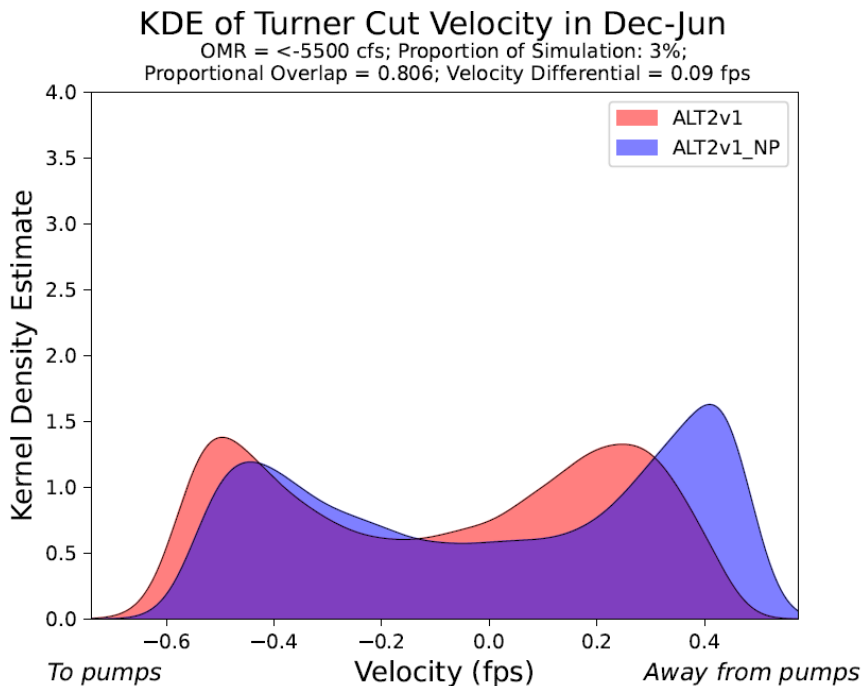


Figure I.3-35. Gaussian KDE of Velocity at Turner Cut in December through June with OMR < -5,500 cfs. Results apply to the Alt2v1woTUCP alternative.

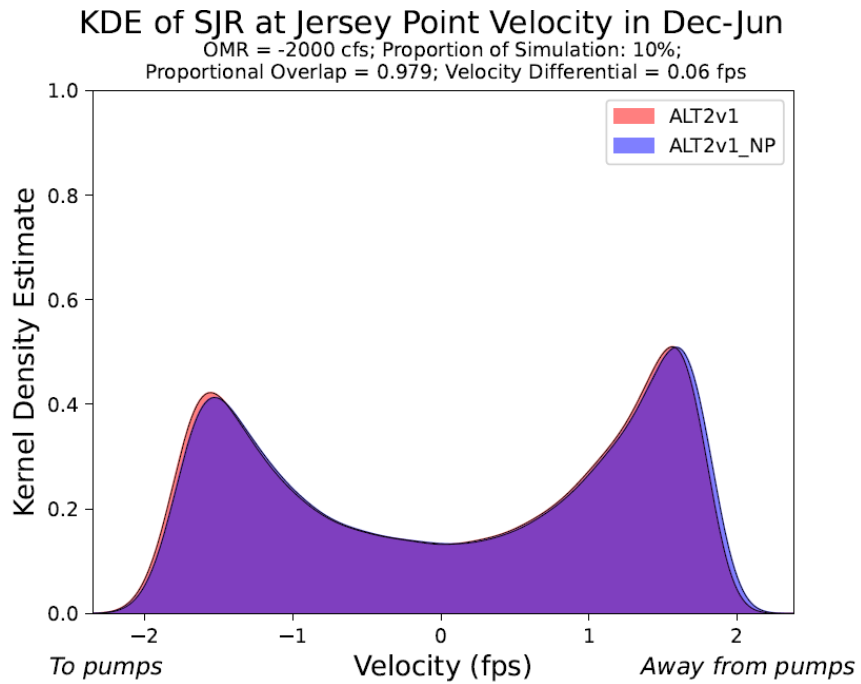


Figure I.3-36. Gaussian KDE of Velocity at San Joaquin River at Jersey Point in December through June with OMR of -2,000 cfs. Results apply to the Alt2v1woTUCP alternative.

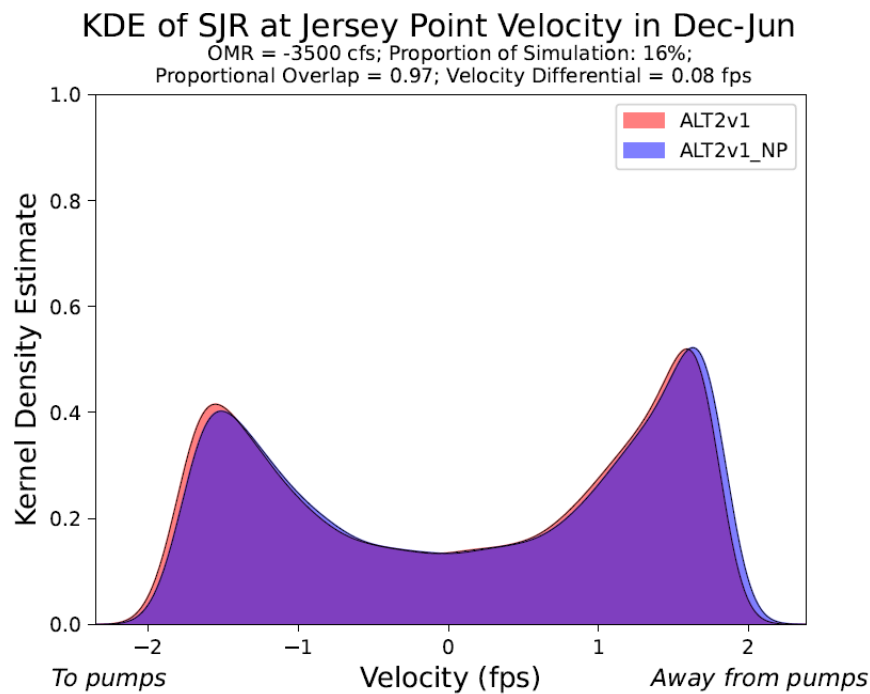


Figure I.3-37. Gaussian KDE of Velocity at San Joaquin River at Jersey Point in December through June with OMR of -3,500 cfs. Results apply to the Alt2v1woTUCP alternative.

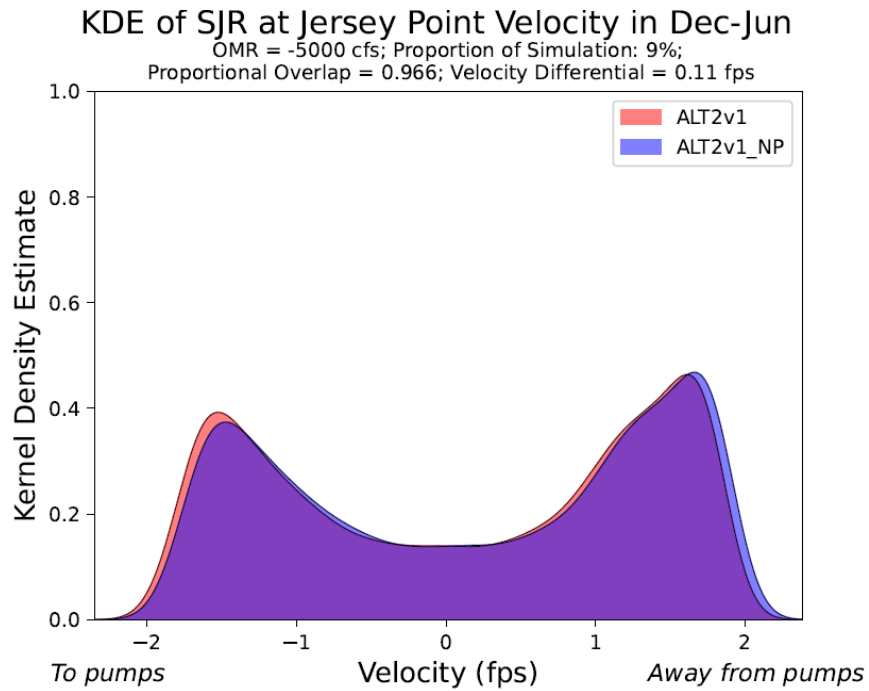


Figure I.3-38. Gaussian KDE of Velocity at San Joaquin River at Jersey Point in December through June with OMR of -5,000 cfs. Results apply to the Alt2v1woTUCP alternative.

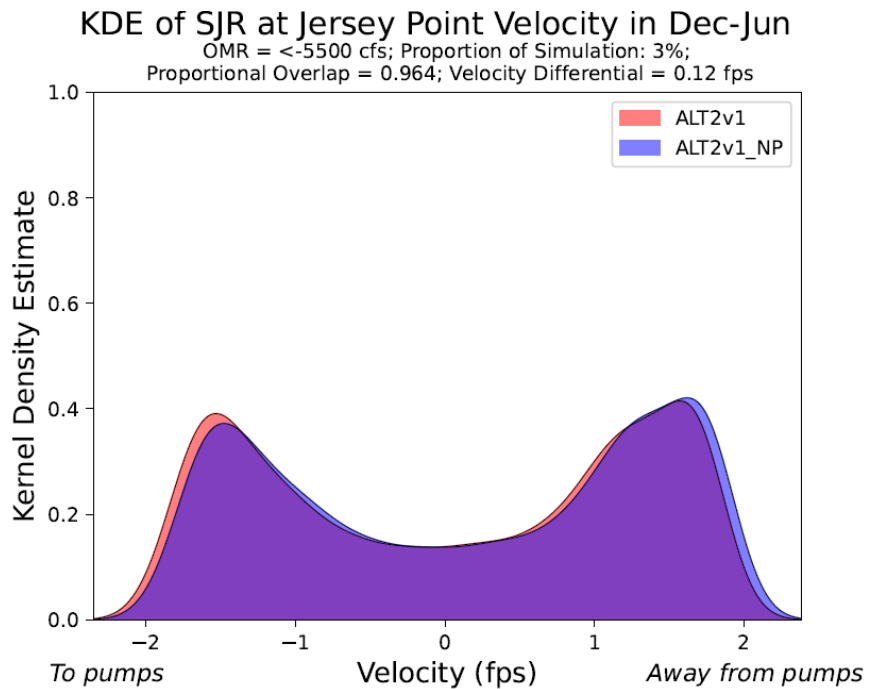


Figure I.3-39. Gaussian KDE of Velocity at San Joaquin River at Jersey Point in December through June with OMR < -5,500 cfs. Results apply to the Alt2v1woTUCP alternative.

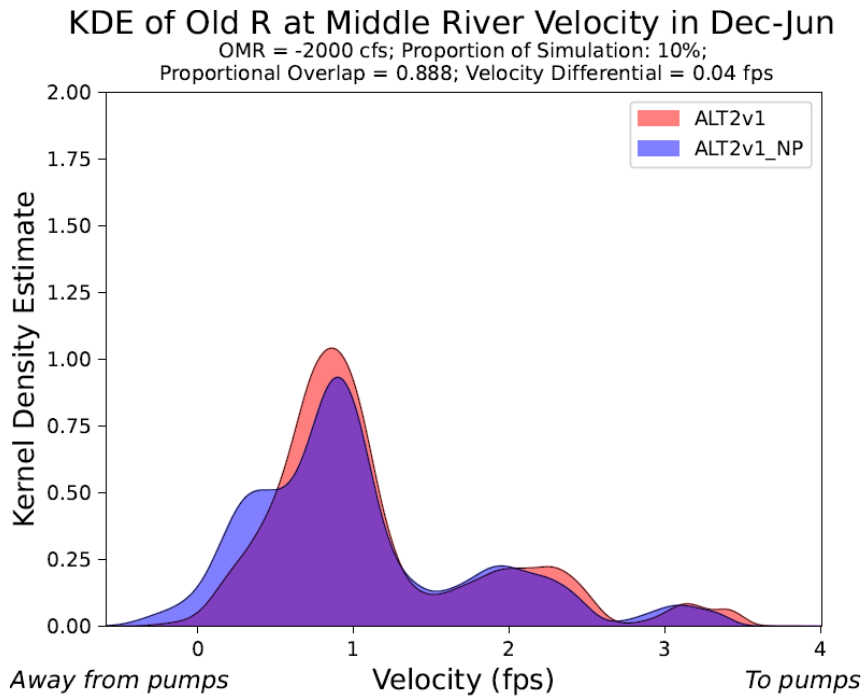


Figure I.3-40. Gaussian KDE of Velocity at Old River at Middle River in December through June with OMR of -2,000 cfs. Results apply to the Alt2v1woTUCP alternative.

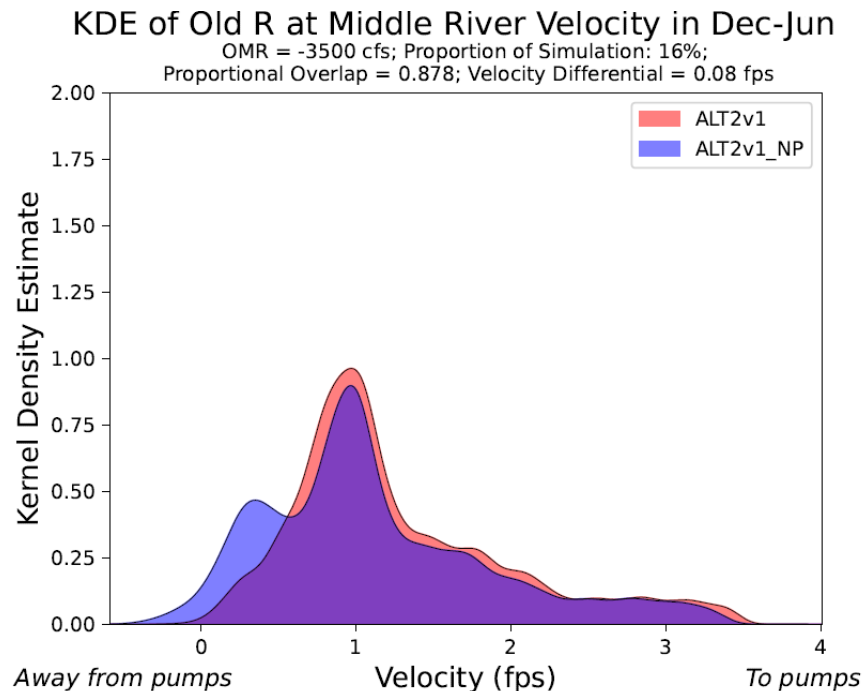


Figure I.3-41. Gaussian KDE of Velocity at Old River at Middle River in December through June with OMR of -3,500 cfs. Results apply to the Alt2v1woTUCP alternative.

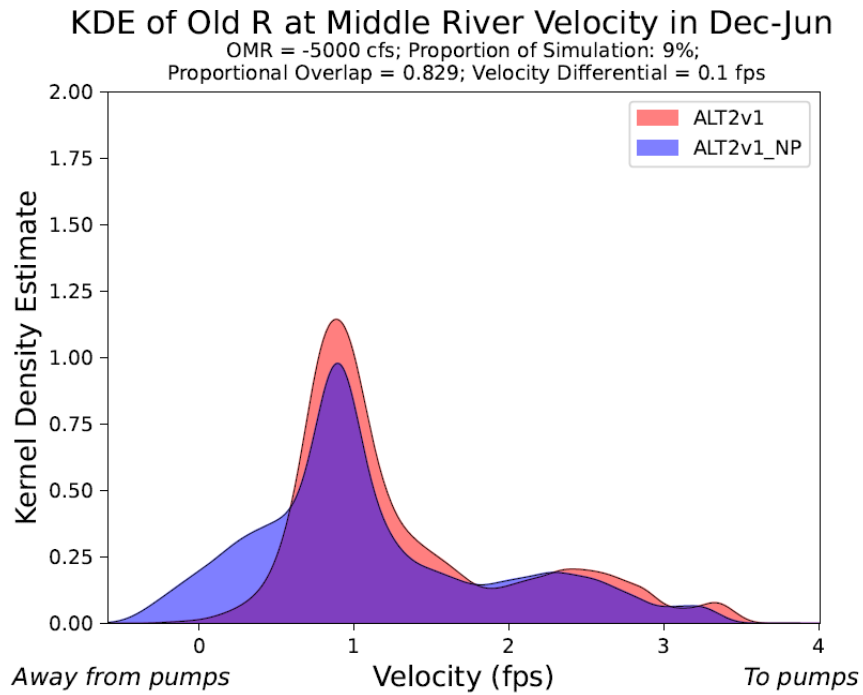


Figure I.3-42. Gaussian KDE of Velocity at Old River at Middle River in December through June with OMR of -5,000 cfs. Results apply to the Alt2v1woTUCP alternative.

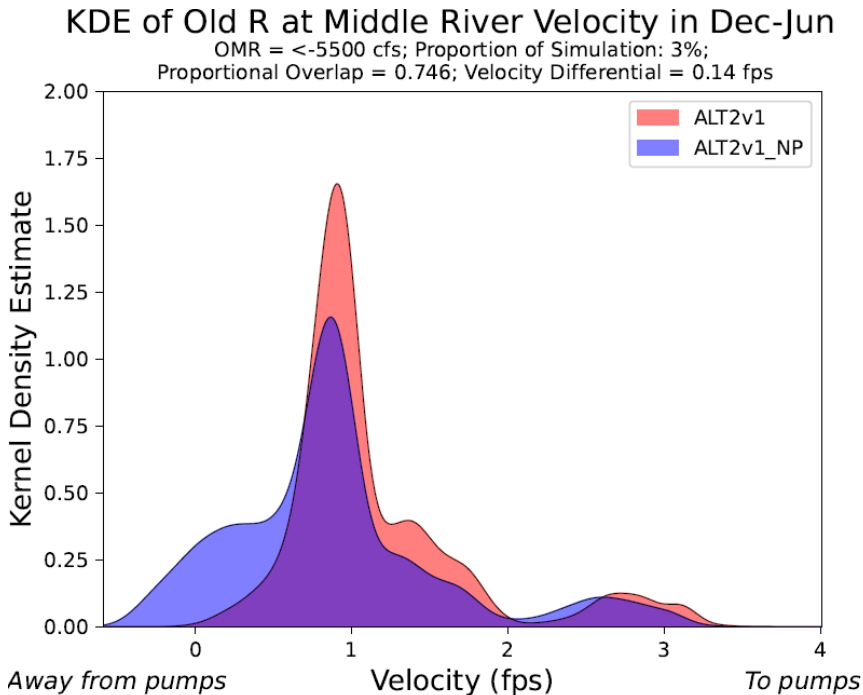


Figure I.3-43. Gaussian KDE of Velocity at Old River at Middle River in December through June with OMR < -5,500 cfs. Results apply to the Alt2v1woTUCP alternative.

I.3.2.1.4 KDE plots for Alt2v2woTUCP alternative:

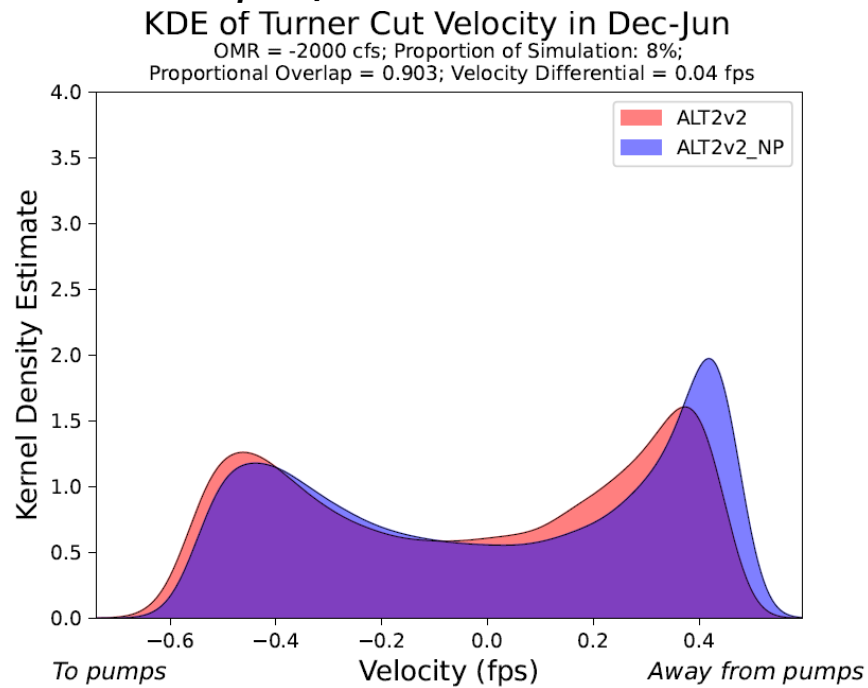


Figure I.3-44. Gaussian KDE of Velocity at Turner Cut in December through June with OMR of -2,000 cfs. Results apply to the Alt2v2woTUCP alternative.

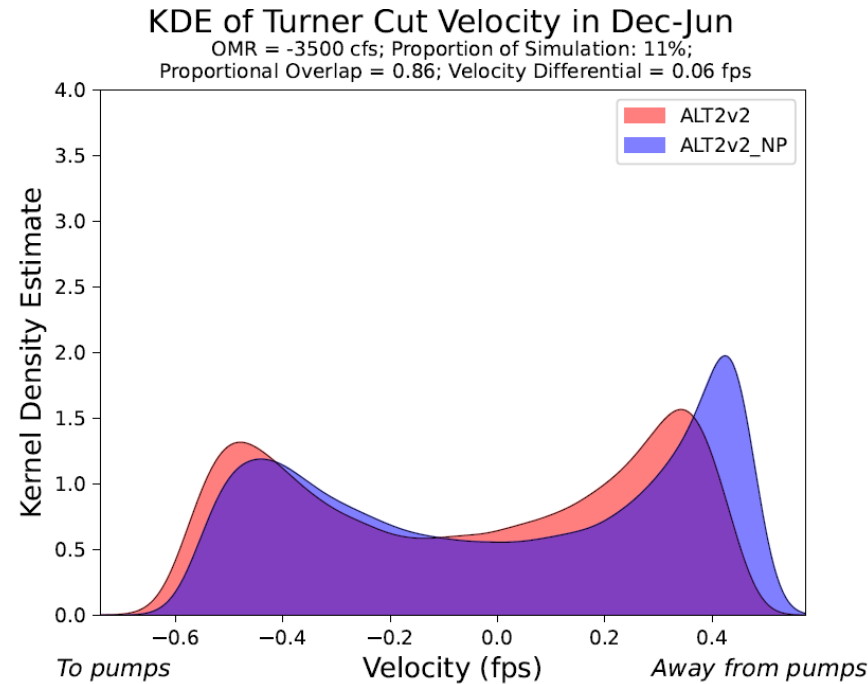


Figure I.3-45. Gaussian KDE of Velocity at Turner Cut in December through June with OMR of -3,500 cfs. Results apply to the Alt2v2woTUCP alternative.

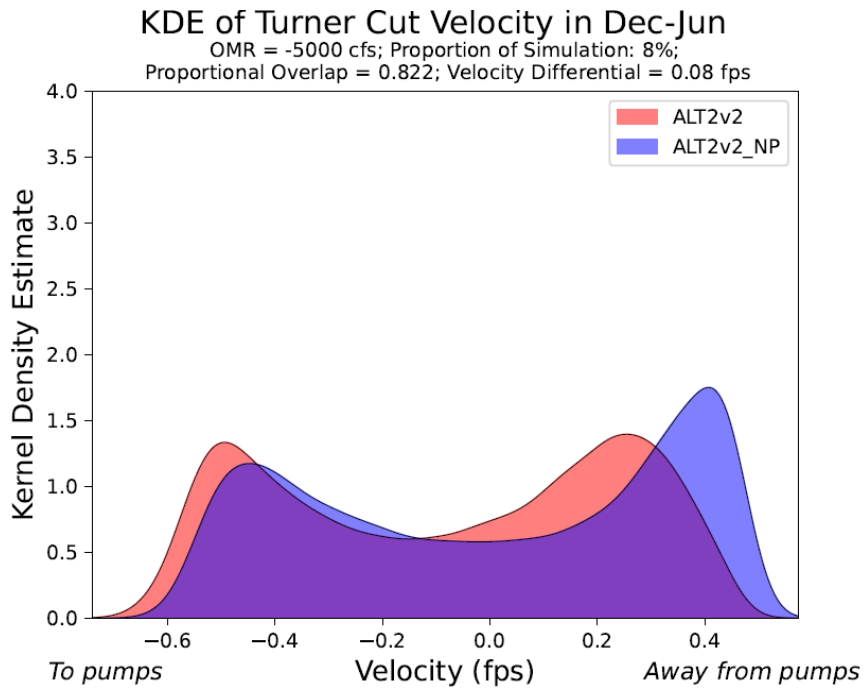


Figure I.3-46. Gaussian KDE of Velocity at Turner Cut in December through June with OMR of -5,000 cfs. Results apply to the Alt2v2woTUCP alternative.

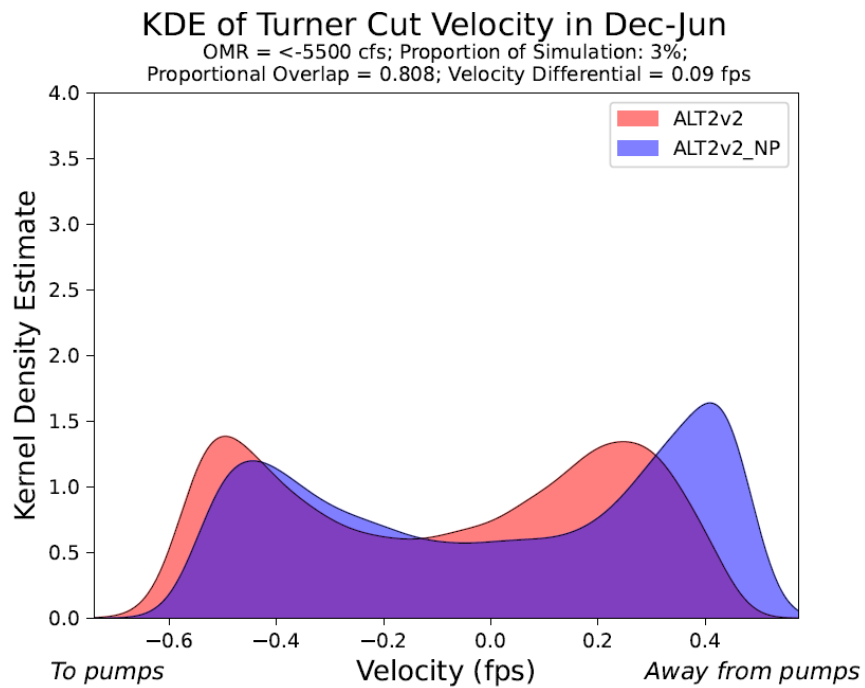


Figure I.3-47. Gaussian KDE of Velocity at Turner Cut in December through June with OMR < -5,500 cfs. Results apply to the Alt2v2woTUCP alternative.

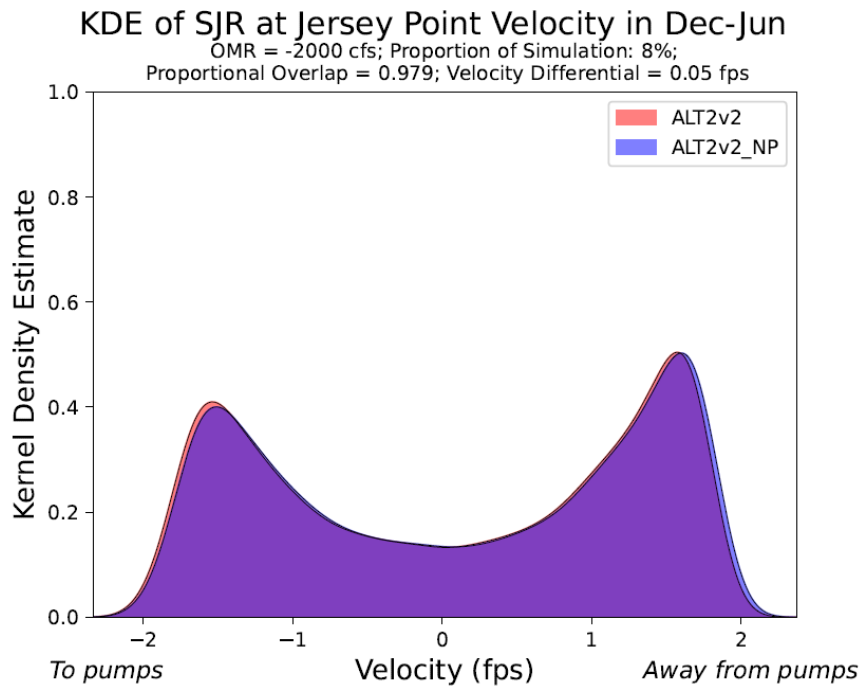


Figure I.3-48. Gaussian KDE of Velocity at San Joaquin River at Jersey Point in December through June with OMR of -2,000 cfs. Results apply to the Alt2v2woTUCP alternative.

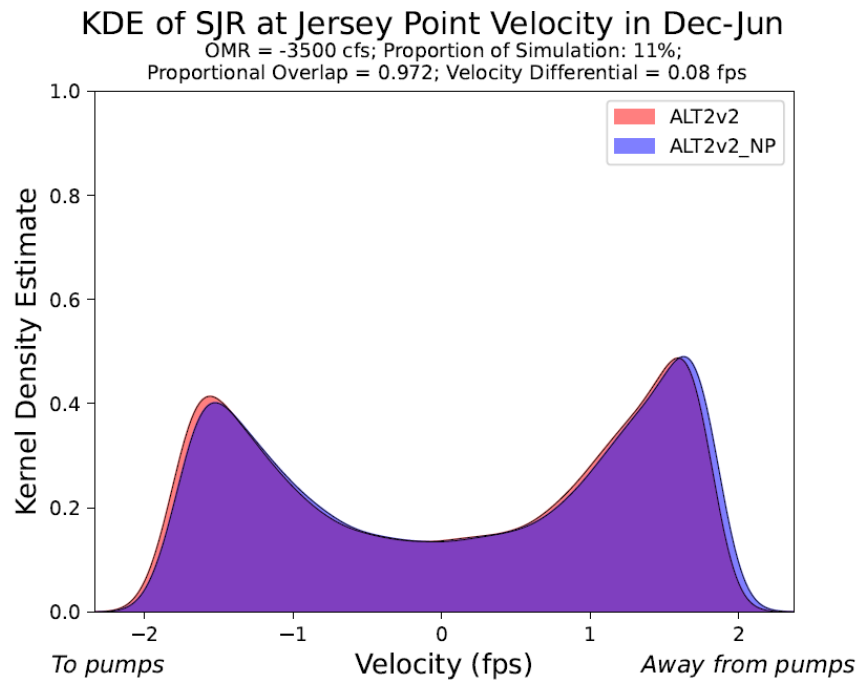


Figure I.3-49. Gaussian KDE of Velocity at San Joaquin River at Jersey Point in December through June with OMR of -3,500 cfs. Results apply to the Alt2v2woTUCP alternative.

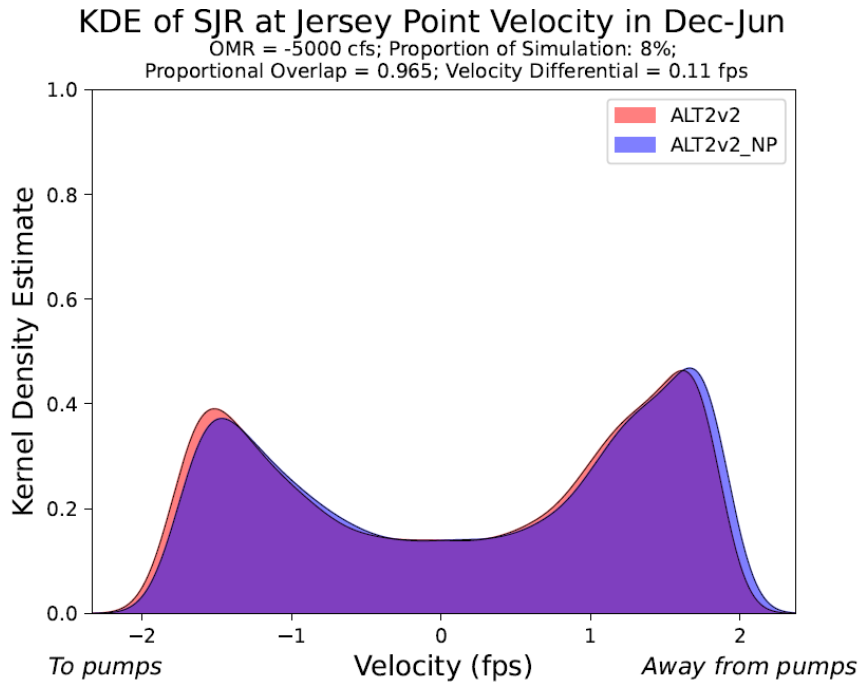


Figure I.3-50. Gaussian KDE of Velocity at San Joaquin River at Jersey Point in December through June with OMR of -5,000 cfs. Results apply to the Alt2v2woTUCP alternative.

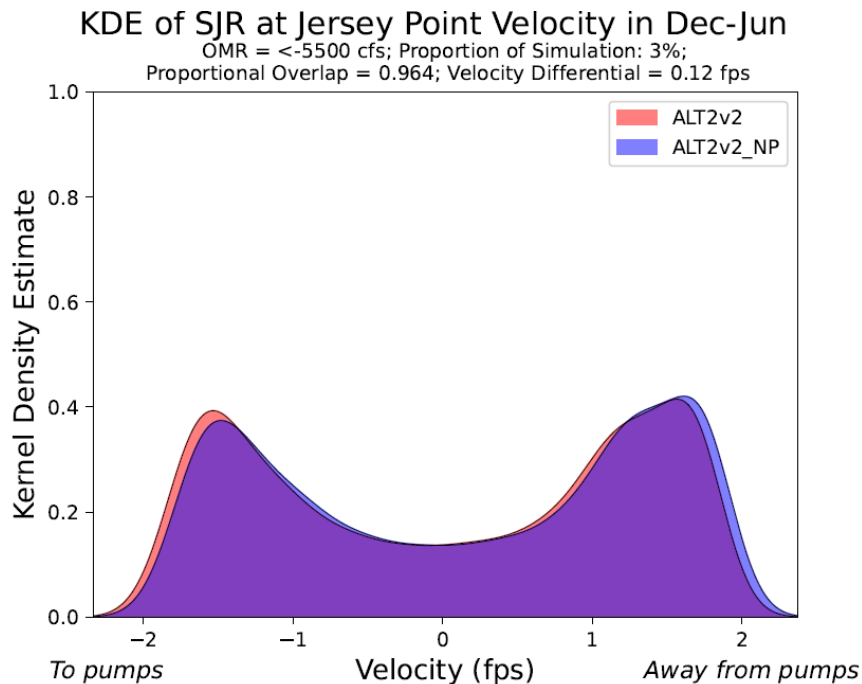


Figure I.3-51. Gaussian KDE of Velocity at San Joaquin River at Jersey Point in December through June with OMR < -5,500 cfs. Results apply to the Alt2v2woTUCP alternative.

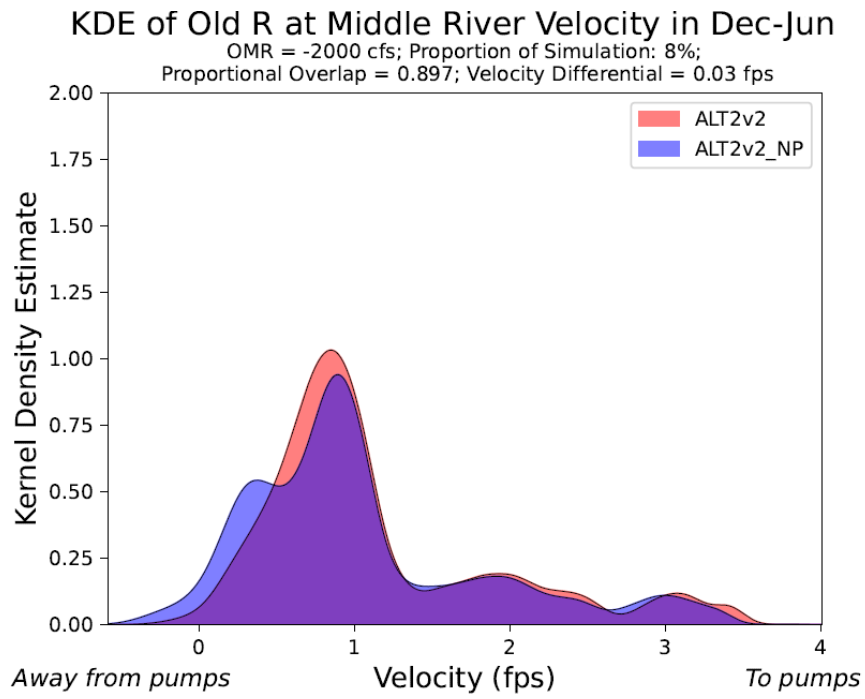


Figure I.3-52. Gaussian KDE of Velocity at Old River at Middle River in December through June with OMR of -2,000 cfs. Results apply to the Alt2v2woTUCP alternative.

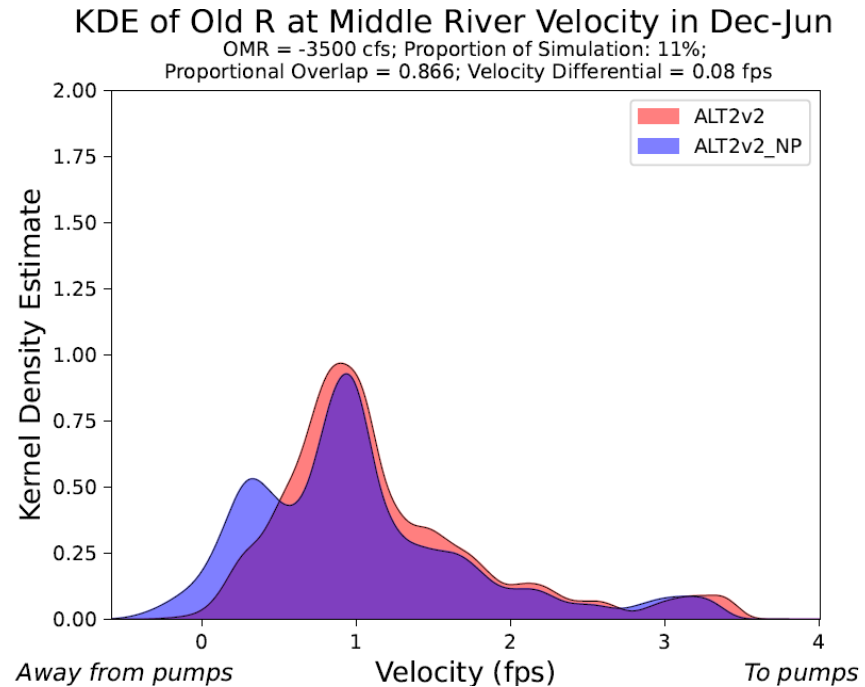


Figure I.3-53. Gaussian KDE of Velocity at Old River at Middle River in December through June with OMR of -3,500 cfs. Results apply to the Alt2v2woTUCP alternative.

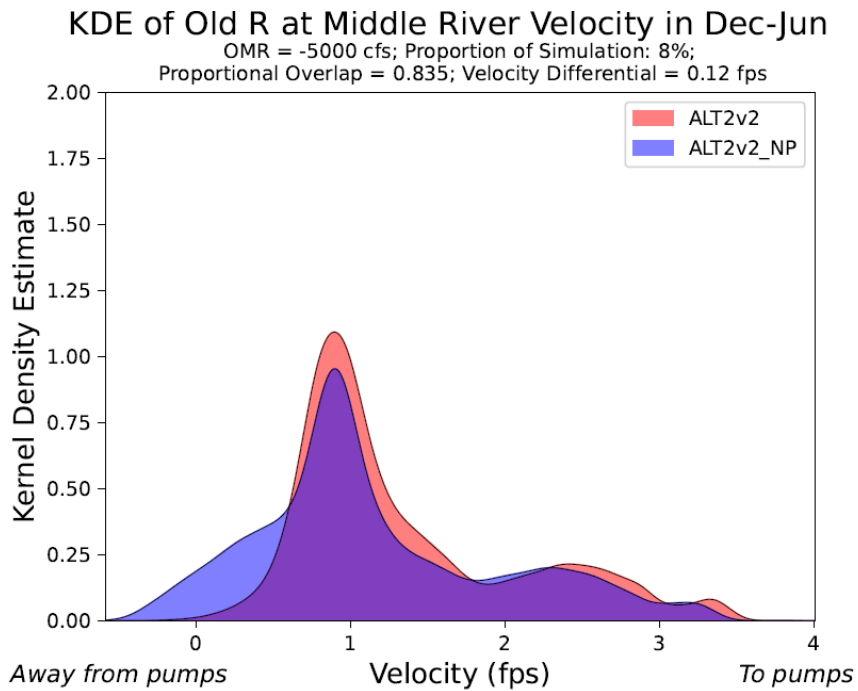


Figure I.3-54. Gaussian KDE of Velocity at Old River at Middle River in December through June with OMR of -5,000 cfs. Results apply to the Alt2v2woTUCP alternative.

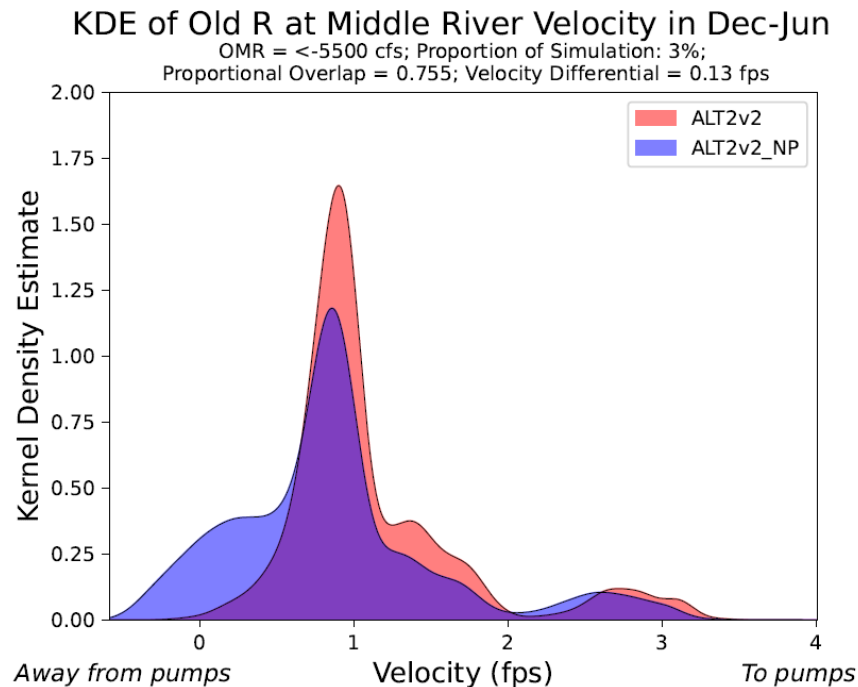


Figure I.3-55. Gaussian KDE of Velocity at Old River at Middle River in December through June with OMR < -5,500 cfs. Results apply to the Alt2v2woTUCP alternative.

I.3.2.1.5 KDE plots for Alt2v3woTUCP alternative:

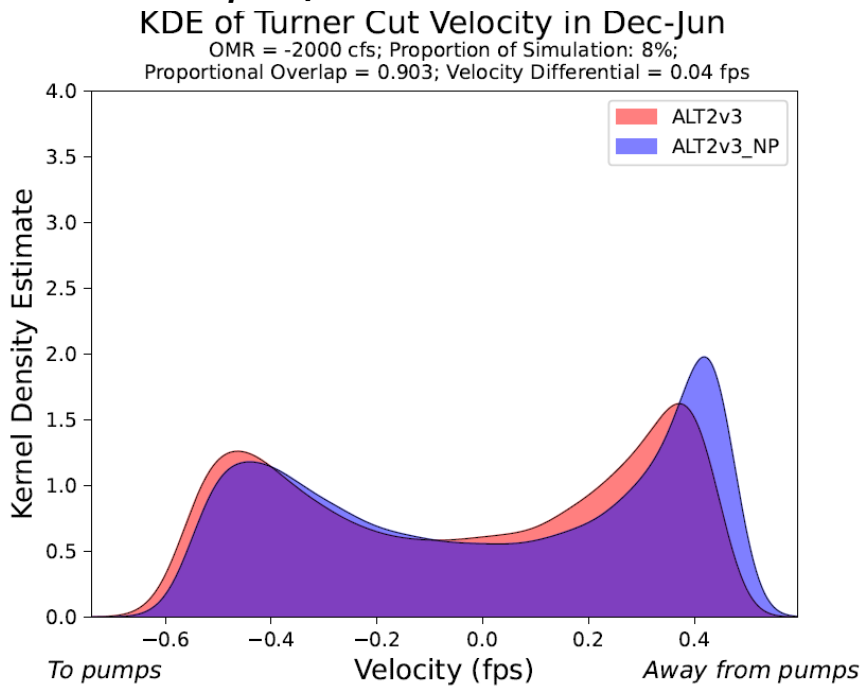


Figure I.3-56. Gaussian KDE of Velocity at Turner Cut in December through June with OMR of -2,000 cfs. Results apply to the Alt2v3woTUCP alternative.

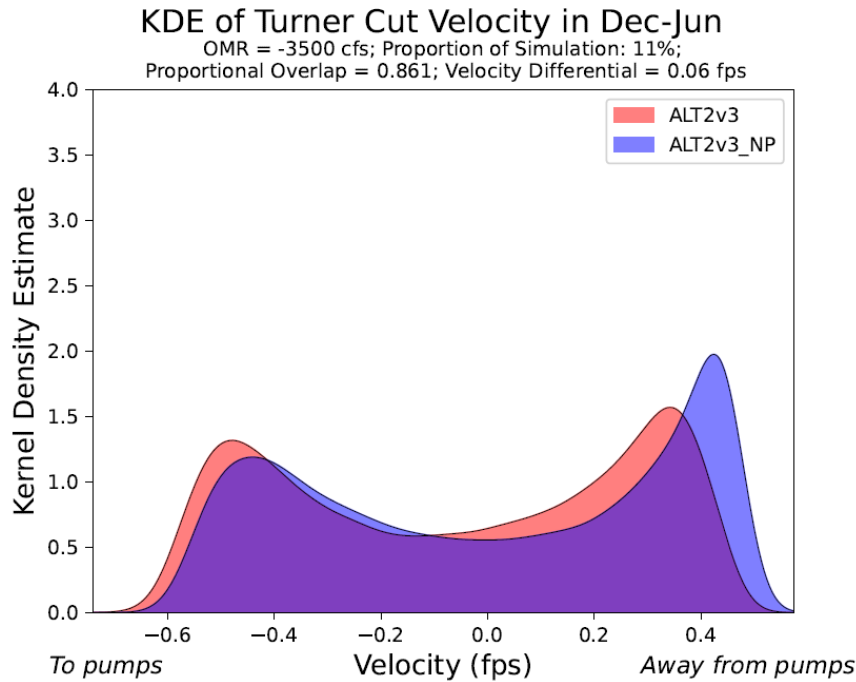


Figure I.3-57. Gaussian KDE of Velocity at Turner Cut in December through June with OMR of -3,500 cfs. Results apply to the Alt2v3woTUCP alternative.

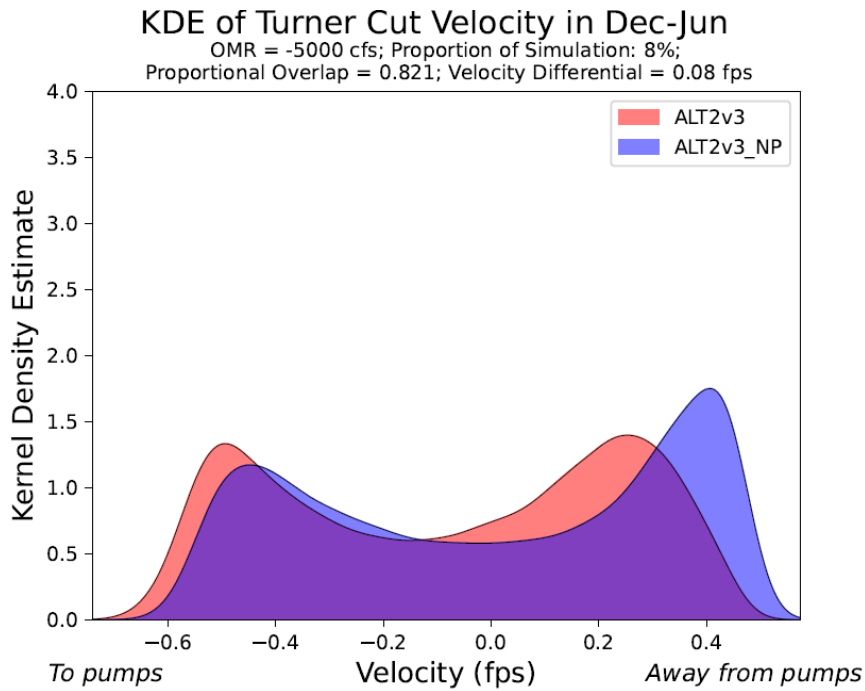


Figure I.3-58. Gaussian KDE of Velocity at Turner Cut in December through June with OMR of -5,000 cfs. Results apply to the Alt2v3woTUCP alternative.

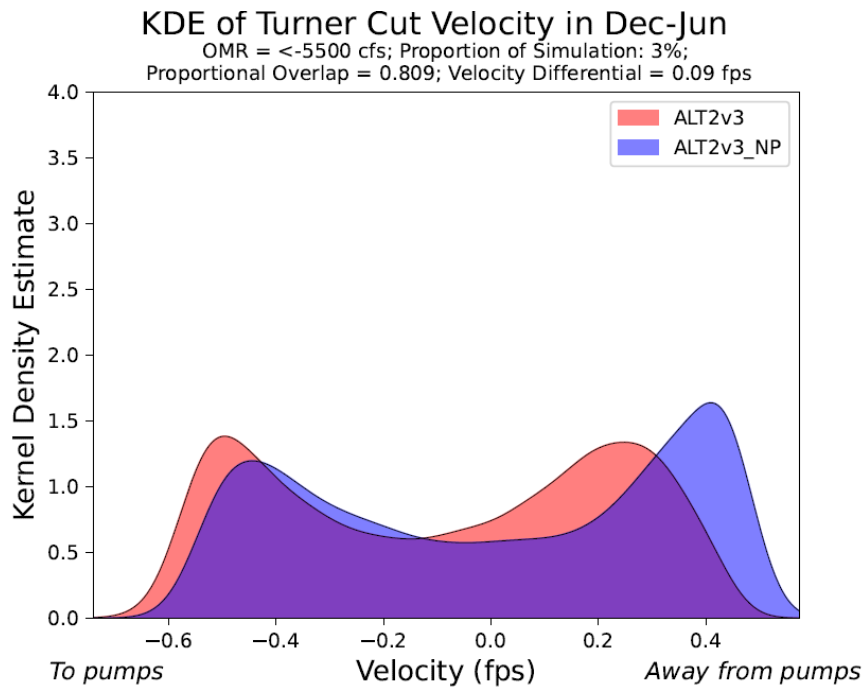


Figure I.3-59. Gaussian KDE of Velocity at Turner Cut in December through June with OMR < -5,500 cfs. Results apply to the Alt2v3woTUCP alternative.

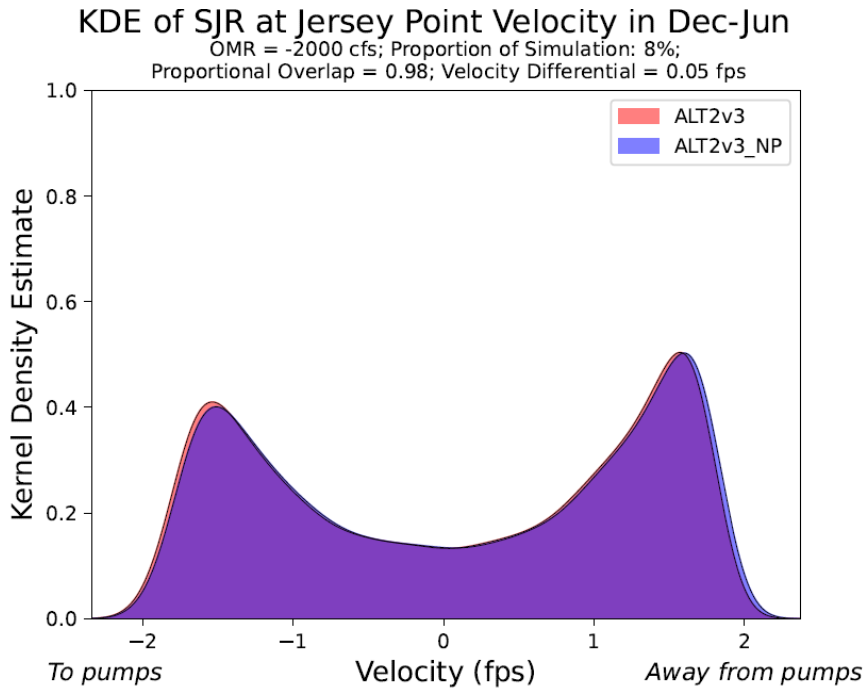


Figure I.3-60. Gaussian KDE of Velocity at San Joaquin River at Jersey Point in December through June with OMR of -2,000 cfs. Results apply to the Alt2v3woTUCP alternative.

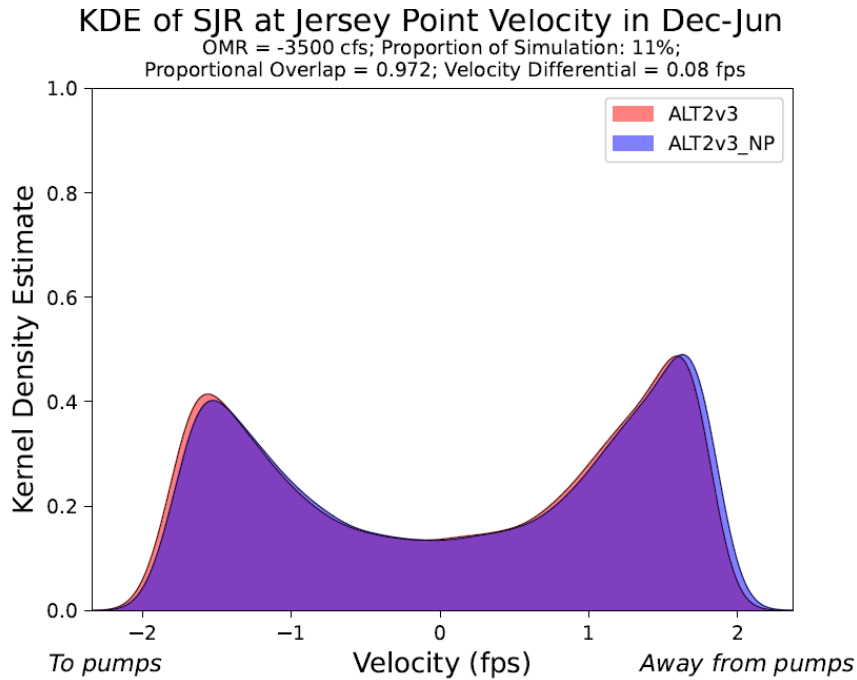


Figure I.3-61. Gaussian KDE of Velocity at San Joaquin River at Jersey Point in December through June with OMR of -3,500 cfs. Results apply to the Alt2v3woTUCP alternative.

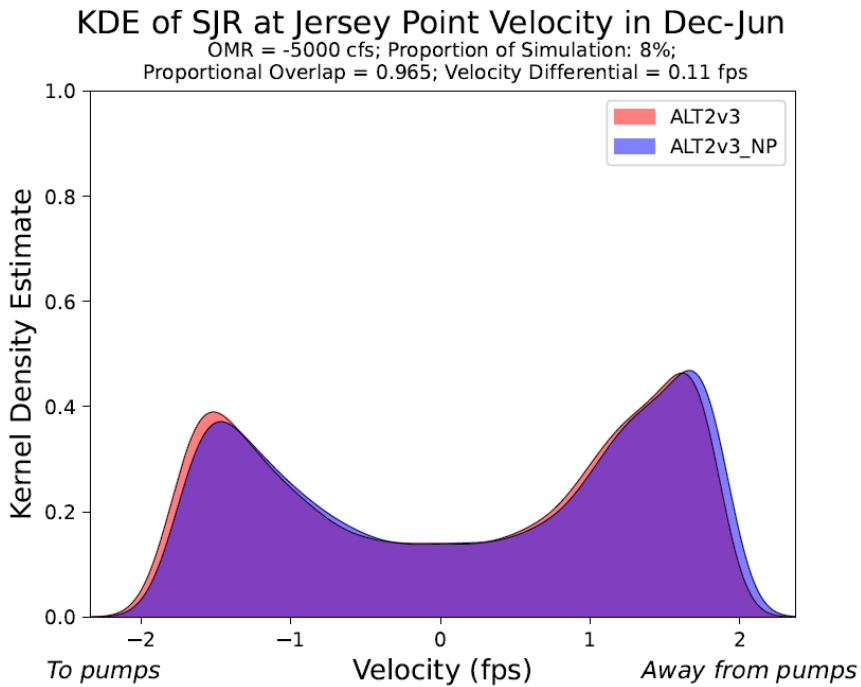


Figure I.3-62. Gaussian KDE of Velocity at San Joaquin River at Jersey Point in December through June with OMR of -5,000 cfs. Results apply to the Alt2v3woTUCP alternative.

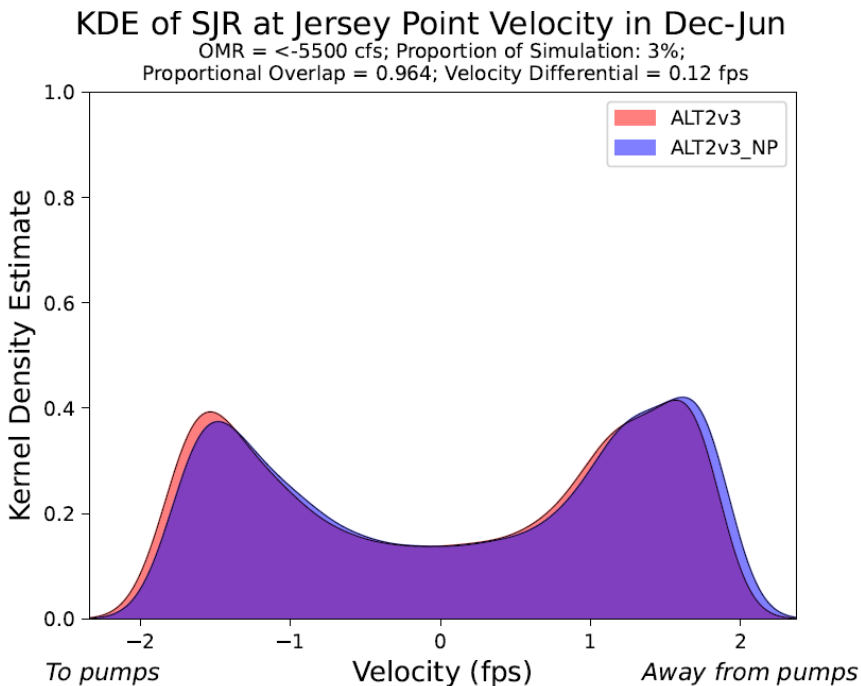


Figure I.3-63. Gaussian KDE of Velocity at San Joaquin River at Jersey Point in December through June with OMR < -5,500 cfs. Results apply to the Alt2v3woTUCP alternative.

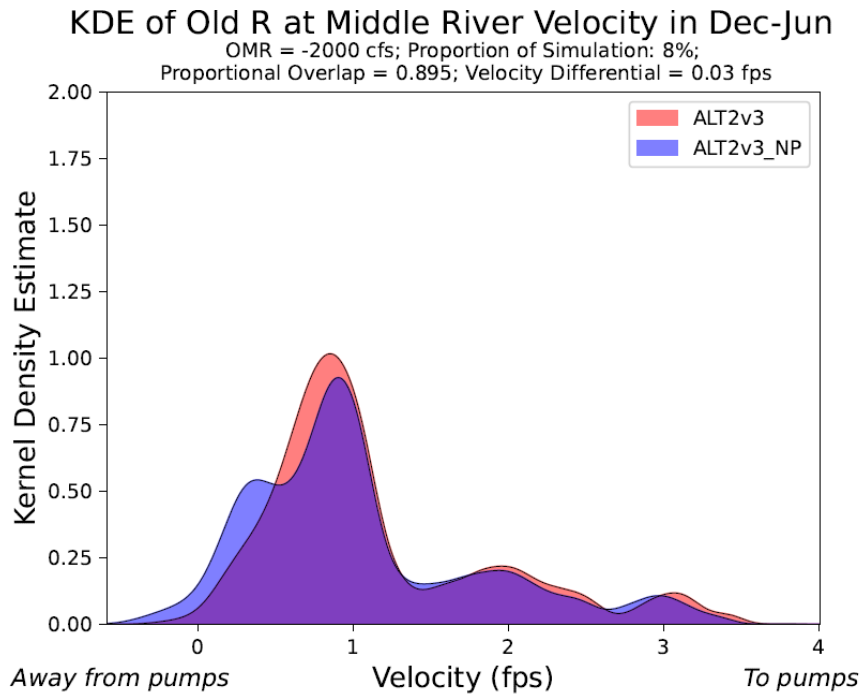


Figure I.3-64. Gaussian KDE of Velocity at Old River at Middle River in December through June with OMR of -2,000 cfs. Results apply to the Alt2v3woTUCP alternative.

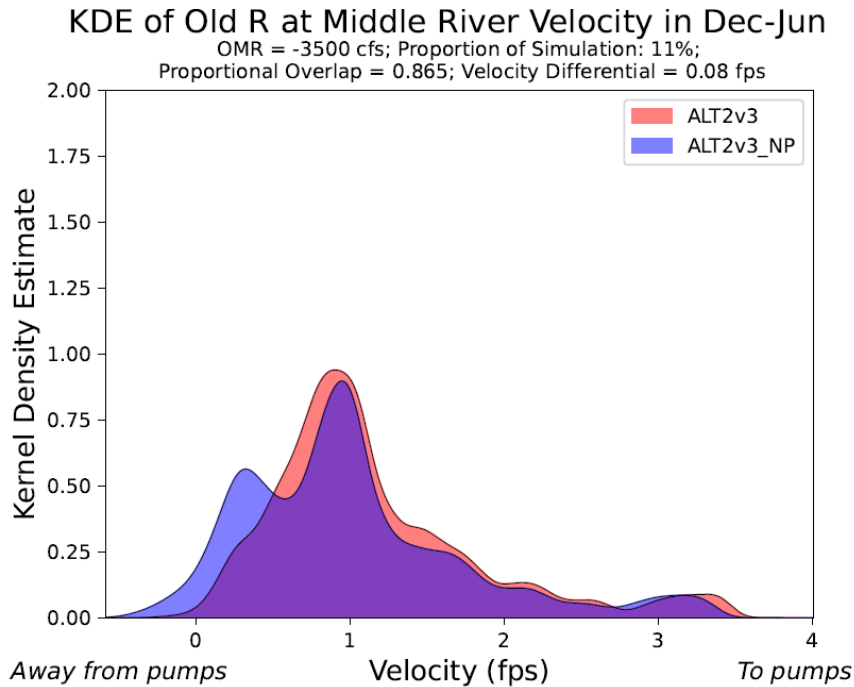


Figure I.3-65. Gaussian KDE of Velocity at Old River at Middle River in December through June with OMR of -3,500 cfs. Results apply to the Alt2v3woTUCP alternative.

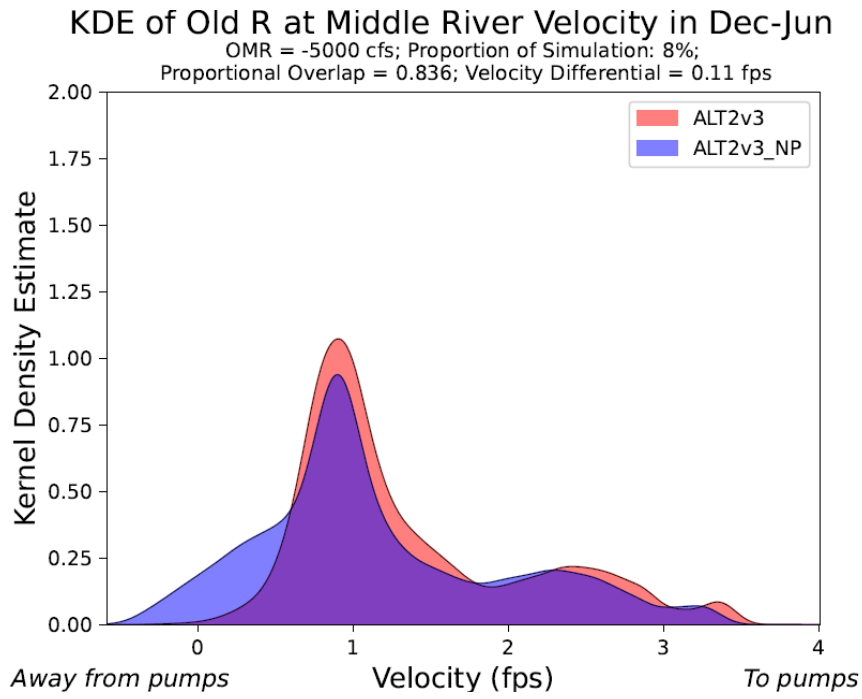


Figure I.3-66. Gaussian KDE of Velocity at Old River at Middle River in December through June with OMR of -5,000 cfs. Results apply to the Alt2v3woTUCP alternative.

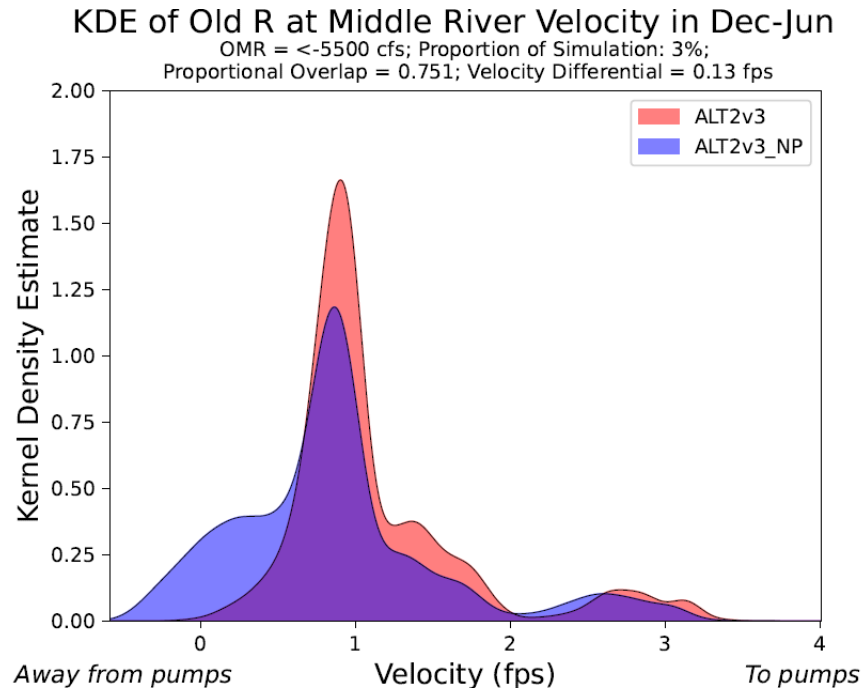


Figure I.3-67. Gaussian KDE of Velocity at Old River at Middle River in December through June with OMR < -5,500 cfs. Results apply to the Alt2v3woTUCP alternative.

I.3.2.1.6 KDE plots for Alt2v1wTUCP alternative:

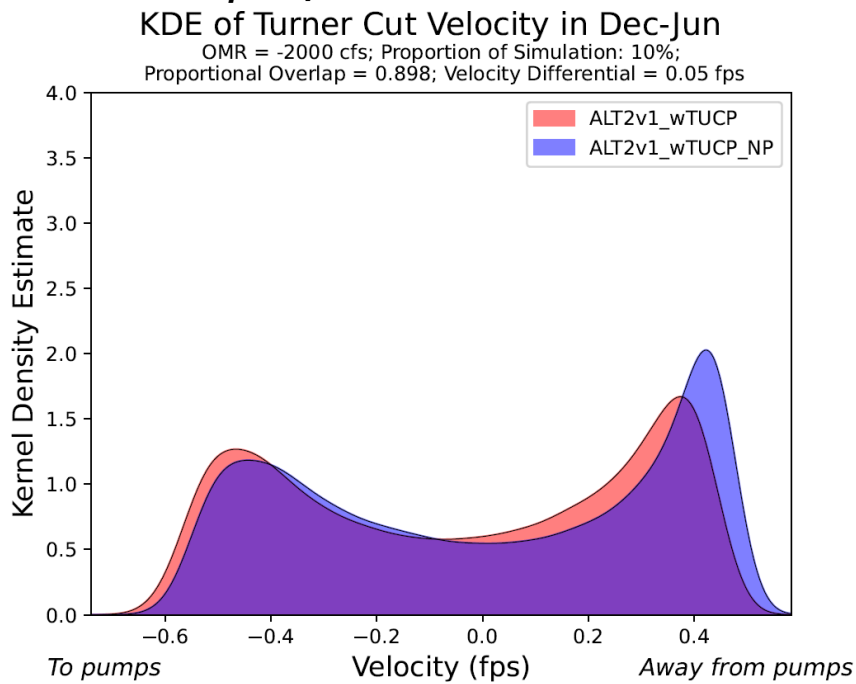


Figure I.3-68. Gaussian KDE of Velocity at Turner Cut in December through June with OMR of -2,000 cfs. Results apply to the Alt2v1wTUCP alternative.

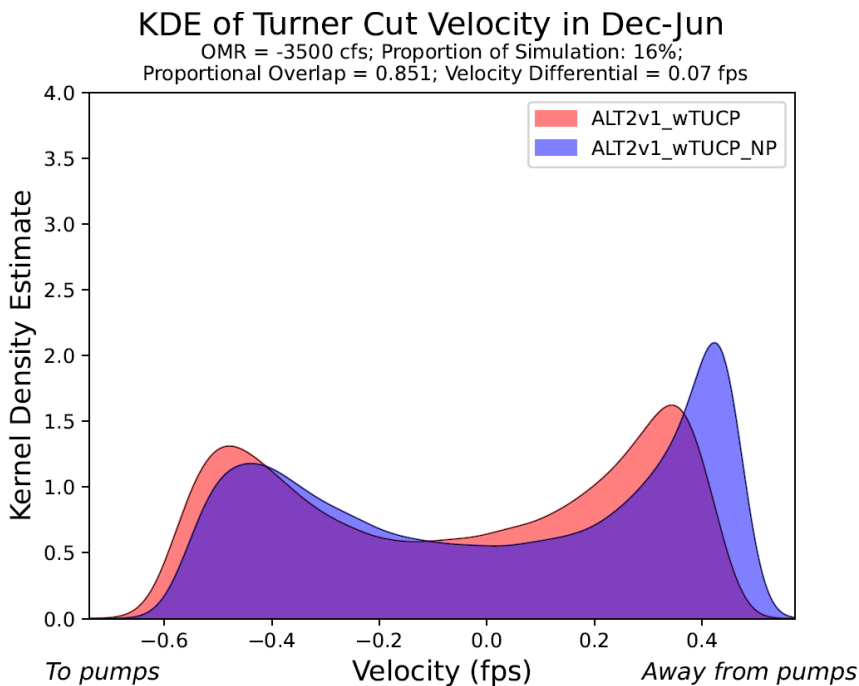


Figure I.3-69. Gaussian KDE of Velocity at Turner Cut in December through June with OMR of -3,500 cfs. Results apply to the Alt2v1wTUCP alternative.

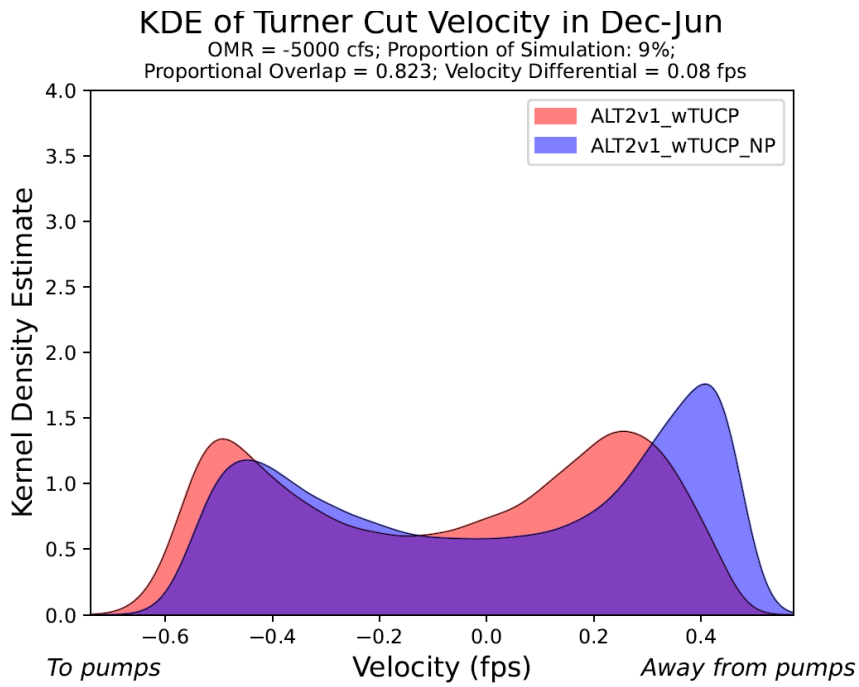


Figure I.3-70. Gaussian KDE of Velocity at Turner Cut in December through June with OMR of -5,000 cfs. Results apply to the Alt2v1wTUCP alternative.

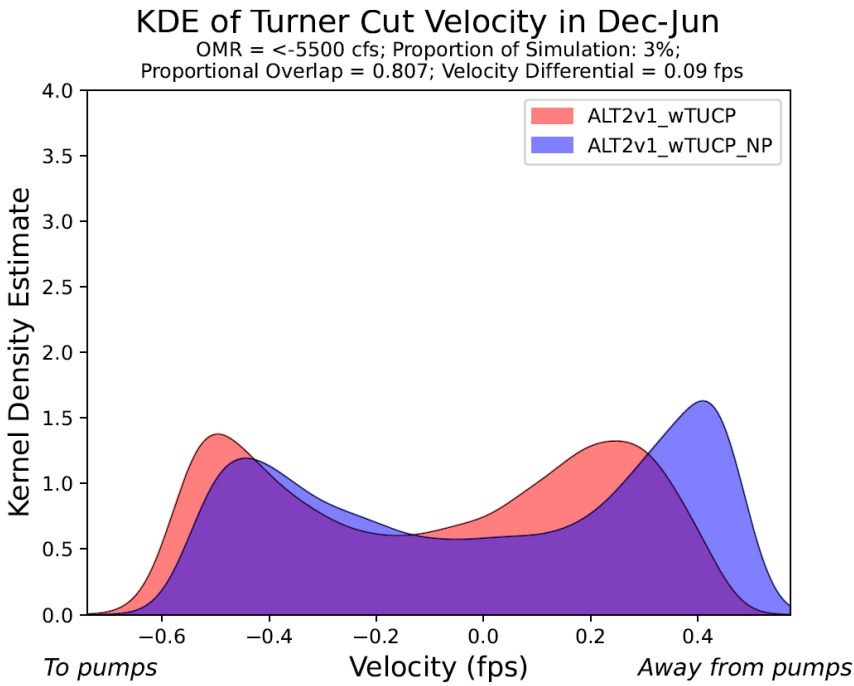


Figure I.3-71. Gaussian KDE of Velocity at Turner Cut in December through June with OMR < -5,500 cfs. Results apply to the Alt2v1wTUCP alternative.

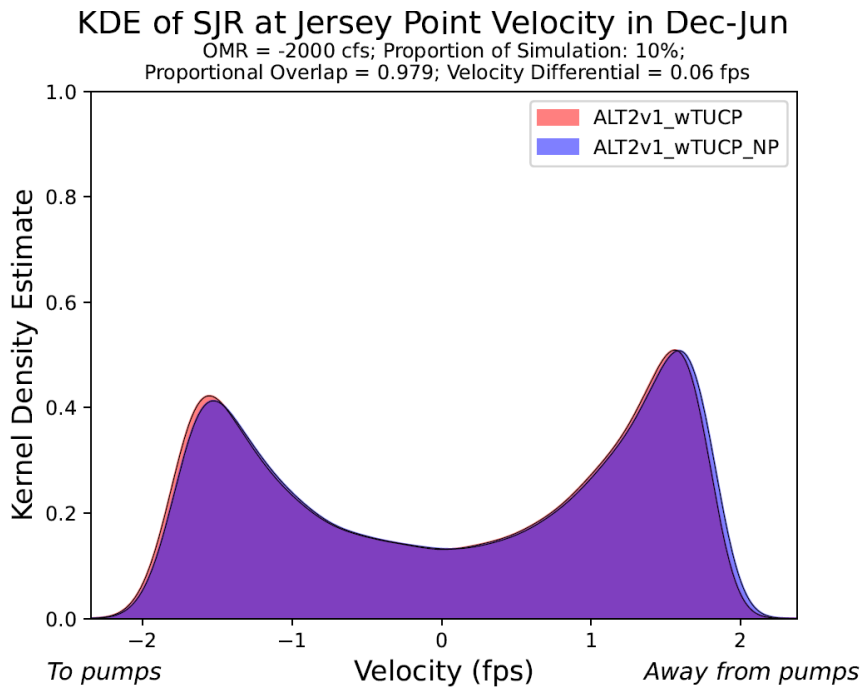


Figure I.3-72. Gaussian KDE of Velocity at San Joaquin River at Jersey Point in December through June with OMR of -2,000 cfs. Results apply to the Alt2v1wTUCP alternative.

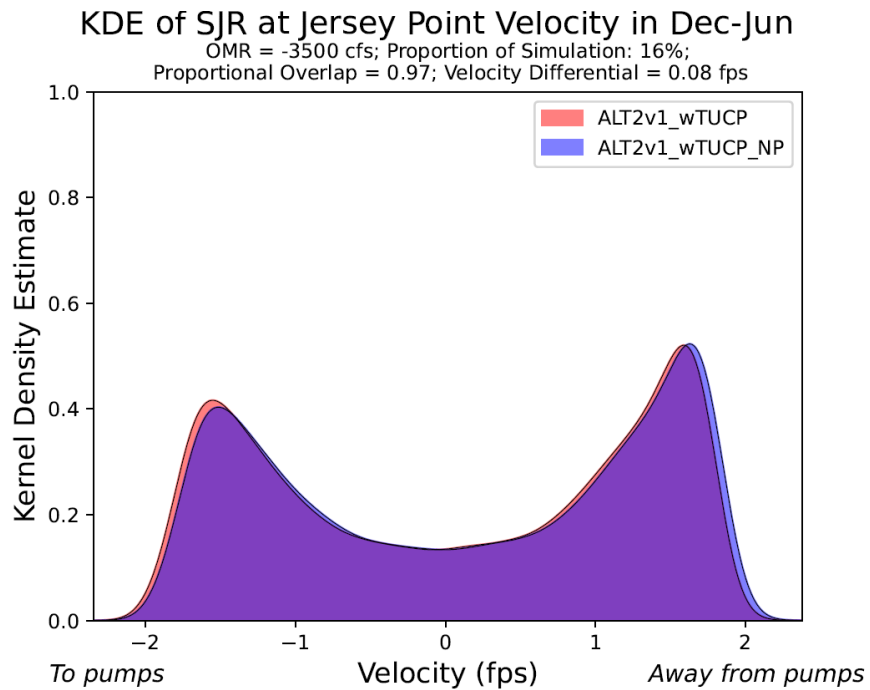


Figure I.3-73. Gaussian KDE of Velocity at San Joaquin River at Jersey Point in December through June with OMR of -3,500 cfs. Results apply to the Alt2v1wTUCP alternative.

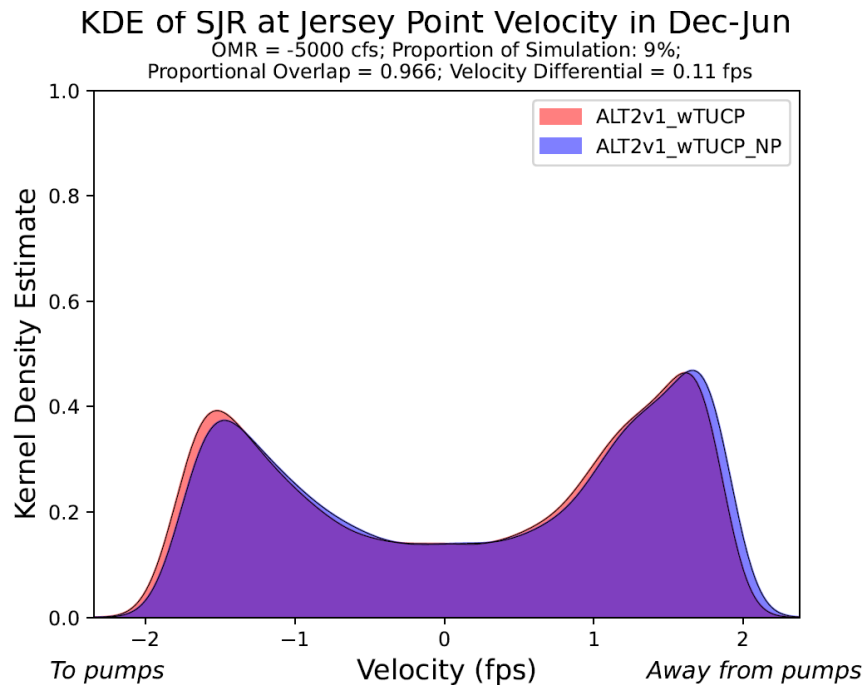


Figure I.3-74. Gaussian KDE of Velocity at San Joaquin River at Jersey Point in December through June with OMR of -5,000 cfs. Results apply to the Alt2v1wTUCP alternative.

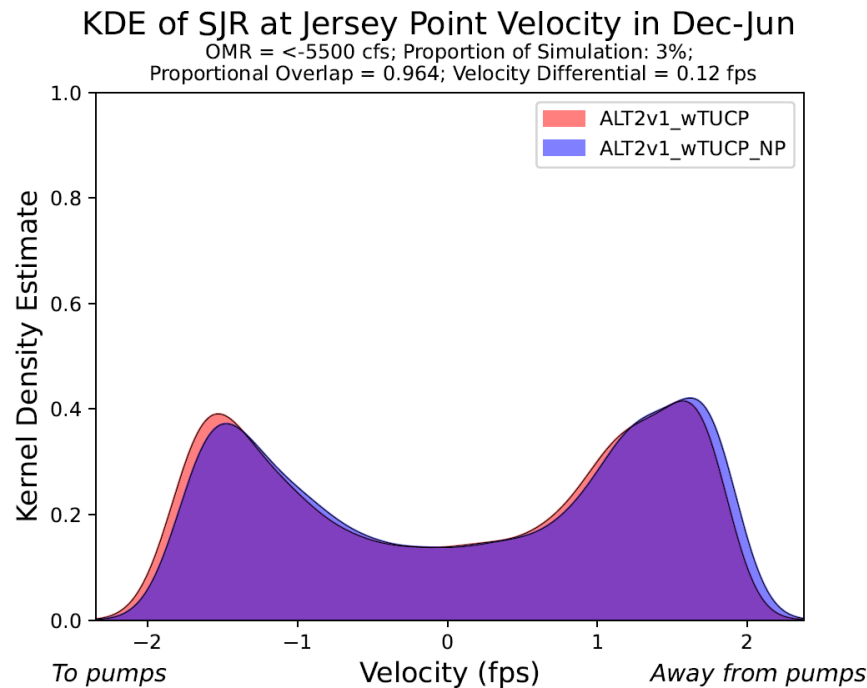


Figure I.3-75. Gaussian KDE of Velocity at San Joaquin River at Jersey Point in December through June with OMR < -5,500 cfs. Results apply to the Alt2v1wTUCP alternative.

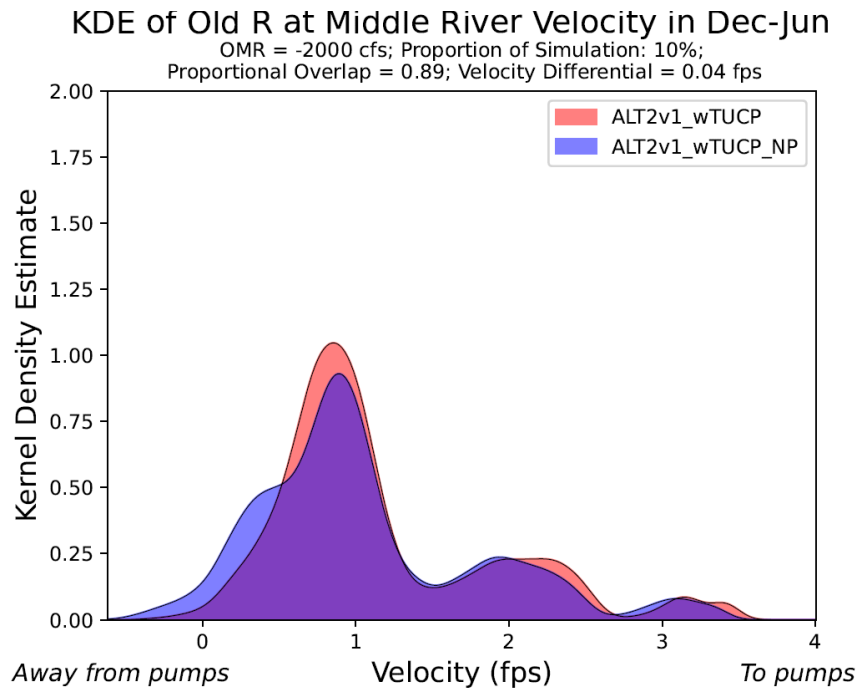


Figure I.3-76. Gaussian KDE of Velocity at Old River at Middle River in December through June with OMR of -2,000 cfs. Results apply to the Alt2v1wTUCP alternative.

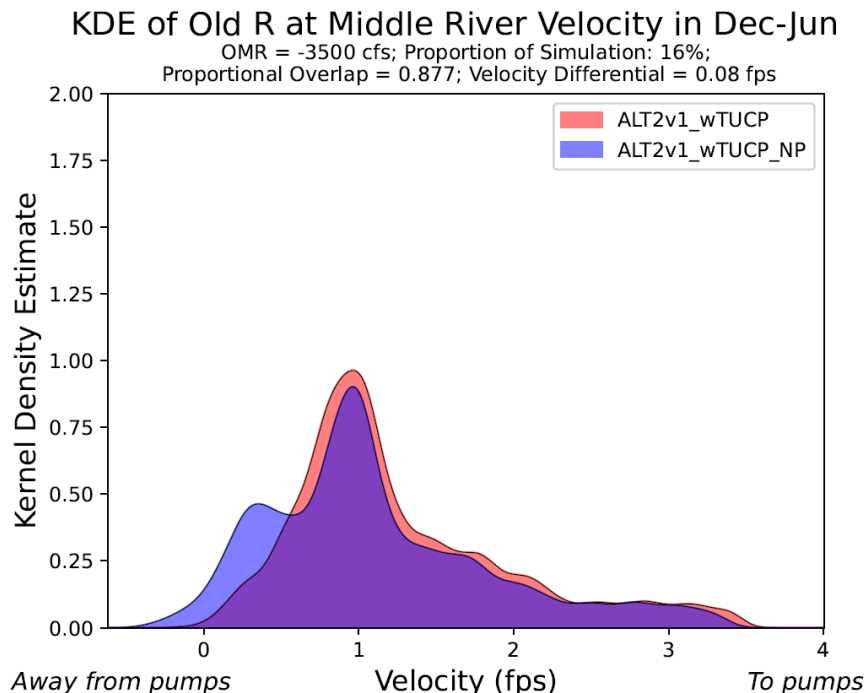


Figure I.3-77. Gaussian KDE of Velocity at Old River at Middle River in December through June with OMR of -3,500 cfs. Results apply to the Alt2v1wTUCP alternative.

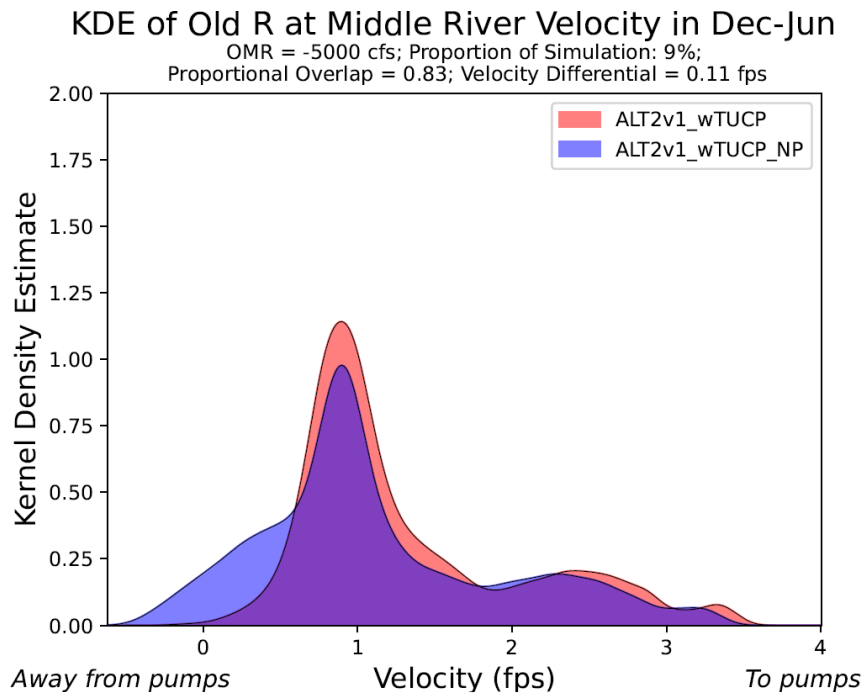


Figure I.3-78. Gaussian KDE of Velocity at Old River at Middle River in December through June with OMR of -5,000 cfs. Results apply to the Alt2v1wTUCP alternative.

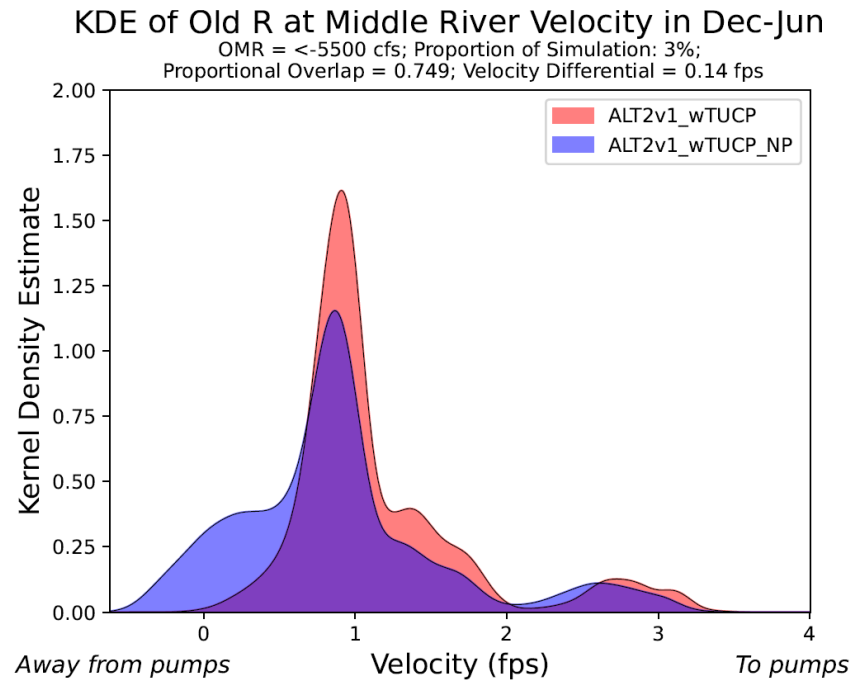


Figure I.3-79. Gaussian KDE of Velocity at Old River at Middle River in December through June with OMR < -5,500 cfs. Results apply to the Alt2v1wTUCP alternative.

I.3.2.1.7 KDE plots for Alt3 alternative:

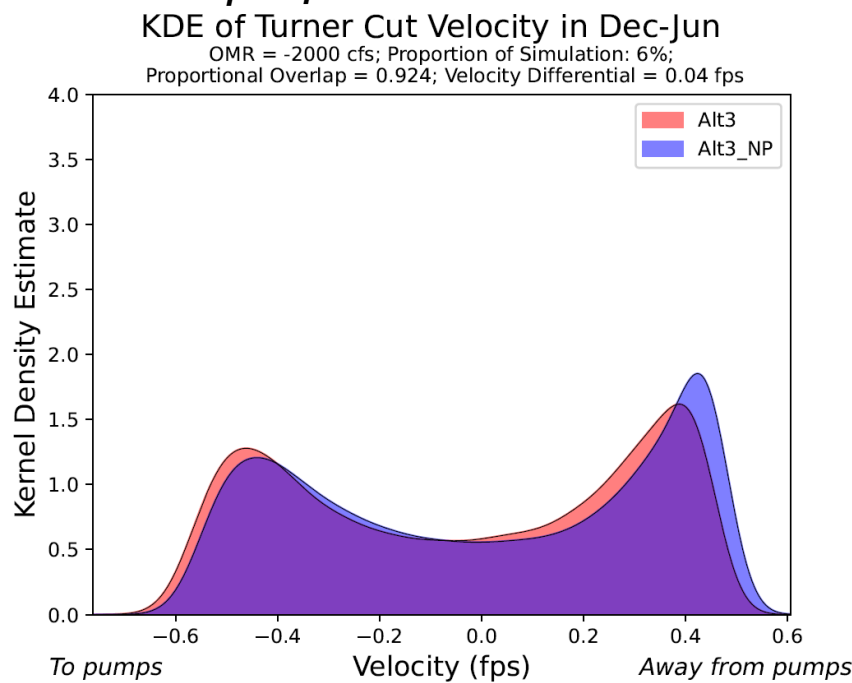


Figure I.3-80. Gaussian KDE of Velocity at Turner Cut in December through June with OMR of -2,000 cfs. Results apply to the Alt3 alternative.

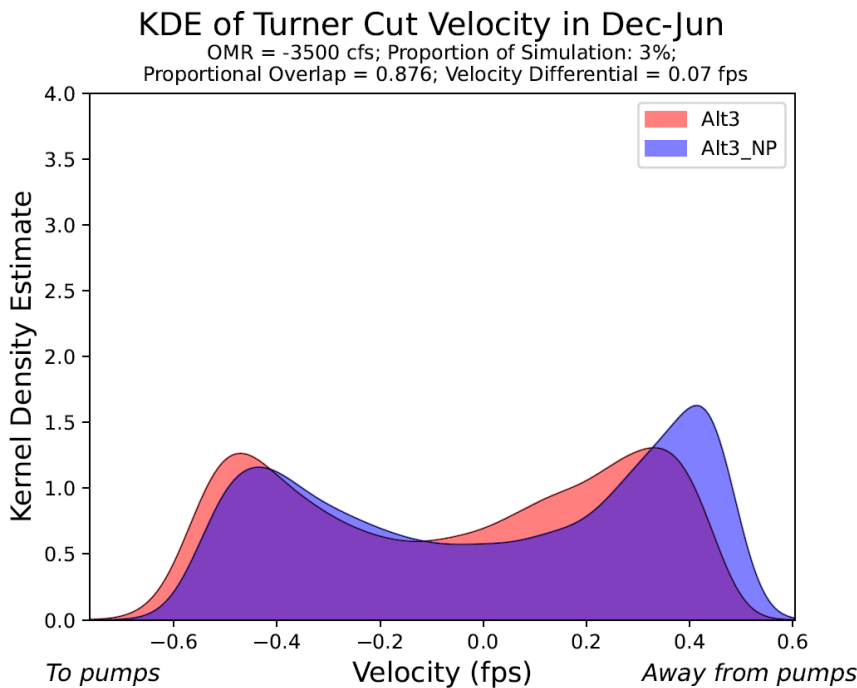


Figure I.3-81. Gaussian KDE of Velocity at Turner Cut in December through June with OMR of -3,500 cfs. Results apply to the Alt3 alternative.

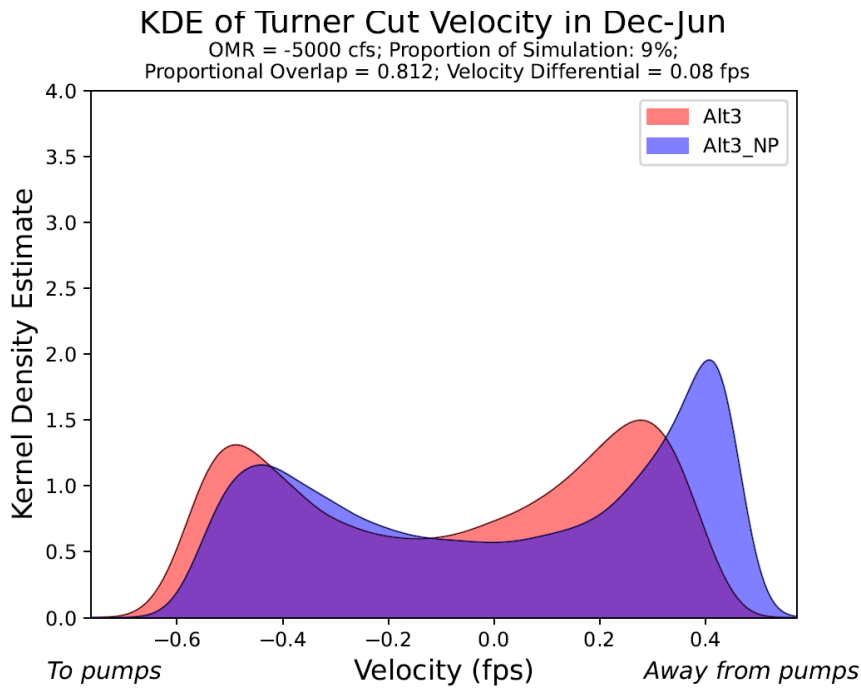


Figure I.3-82. Gaussian KDE of Velocity at Turner Cut in December through June with OMR of -5,000 cfs. Results apply to the Alt3 alternative.

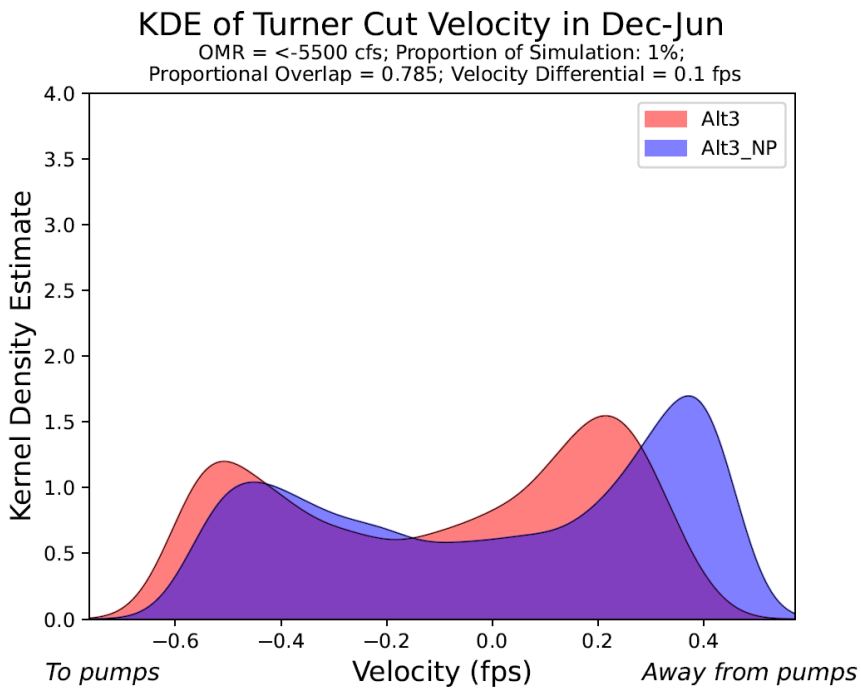


Figure I.3-83. Gaussian KDE of Velocity at Turner Cut in December through June with OMR < -5,500 cfs. Results apply to the Alt3 alternative.

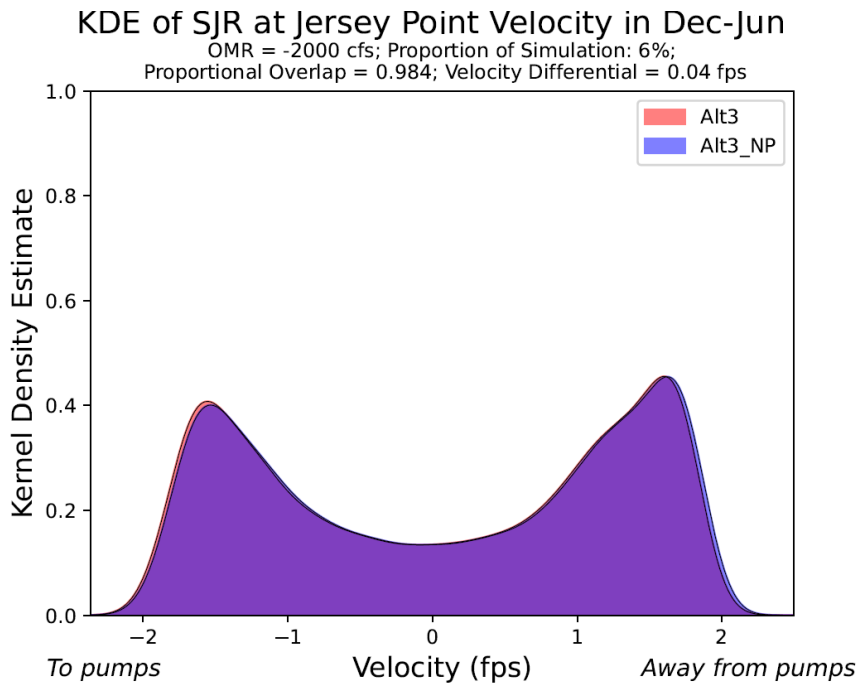


Figure I.3-84. Gaussian KDE of Velocity at San Joaquin River at Jersey Point in December through June with OMR of -2,000 cfs. Results apply to the Alt3 alternative.

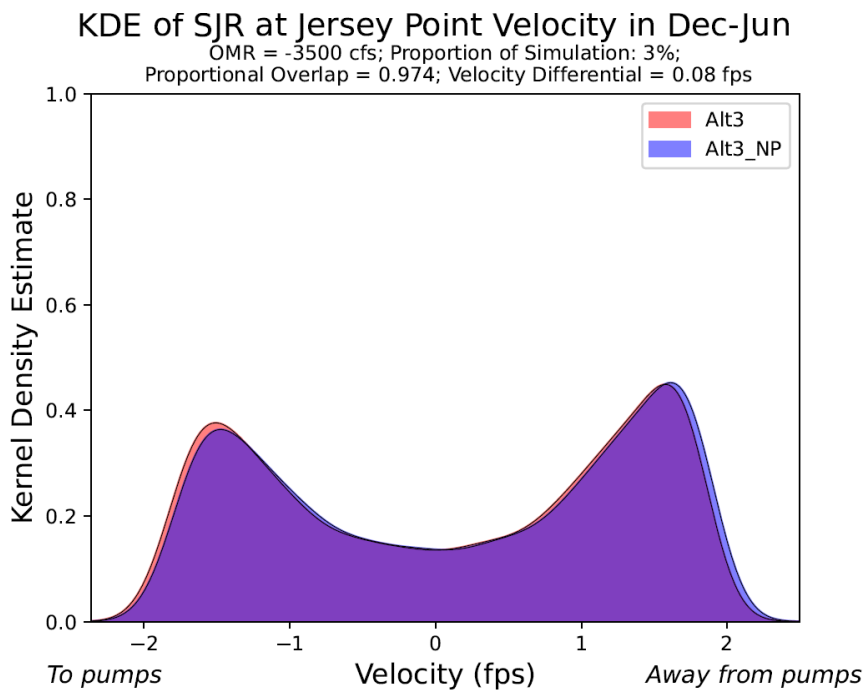


Figure I.3-85. Gaussian KDE of Velocity at San Joaquin River at Jersey Point in December through June with OMR of -3,500 cfs. Results apply to the Alt3 alternative.

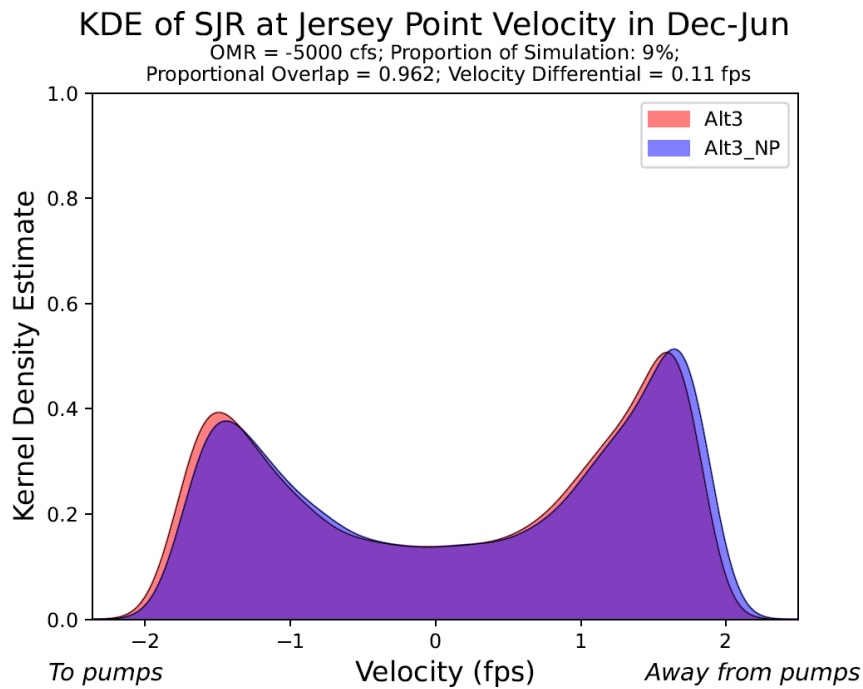


Figure I.3-86. Gaussian KDE of Velocity at San Joaquin River at Jersey Point in December through June with OMR of -5,000 cfs. Results apply to the Alt3 alternative.

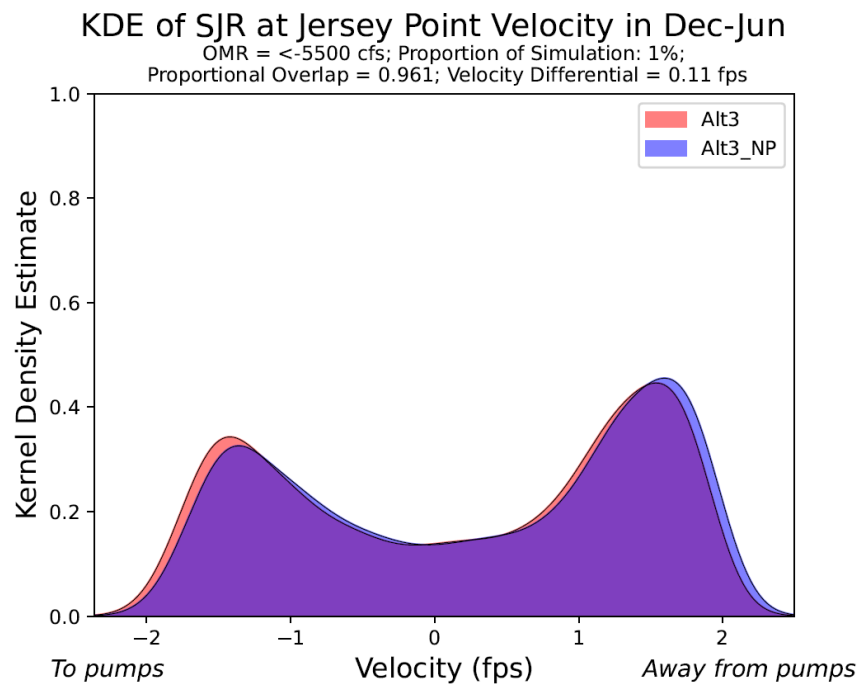


Figure I.3-87. Gaussian KDE of Velocity at San Joaquin River at Jersey Point in December through June with OMR < -5,500 cfs. Results apply to the Alt3 alternative.

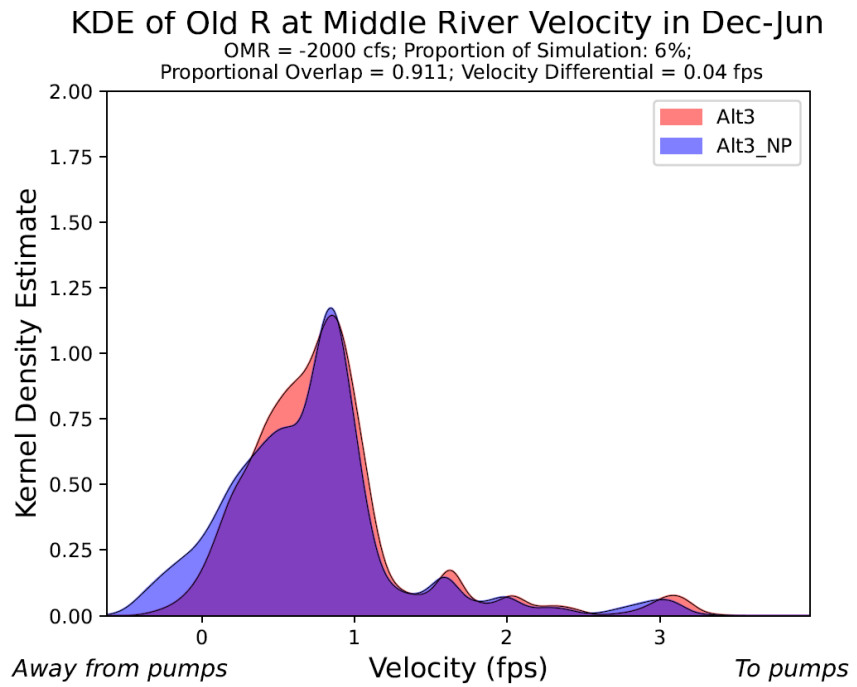


Figure I.3-88. Gaussian KDE of Velocity at Old River at Middle River in December through June with OMR of -2,000 cfs. Results apply to the Alt3 alternative.

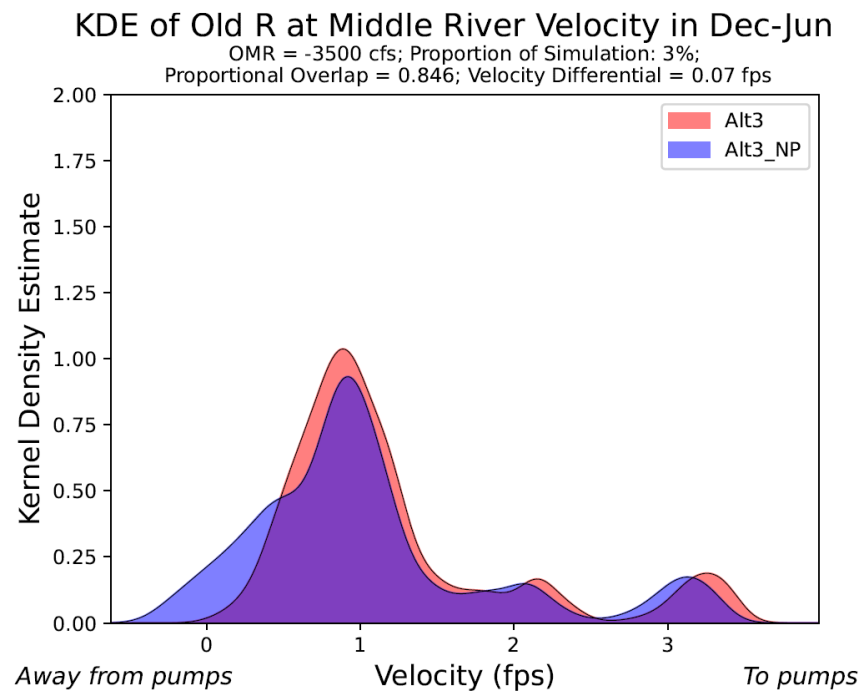


Figure I.3-89. Gaussian KDE of Velocity at Old River at Middle River in December through June with OMR of -3,500 cfs. Results apply to the Alt3 alternative.

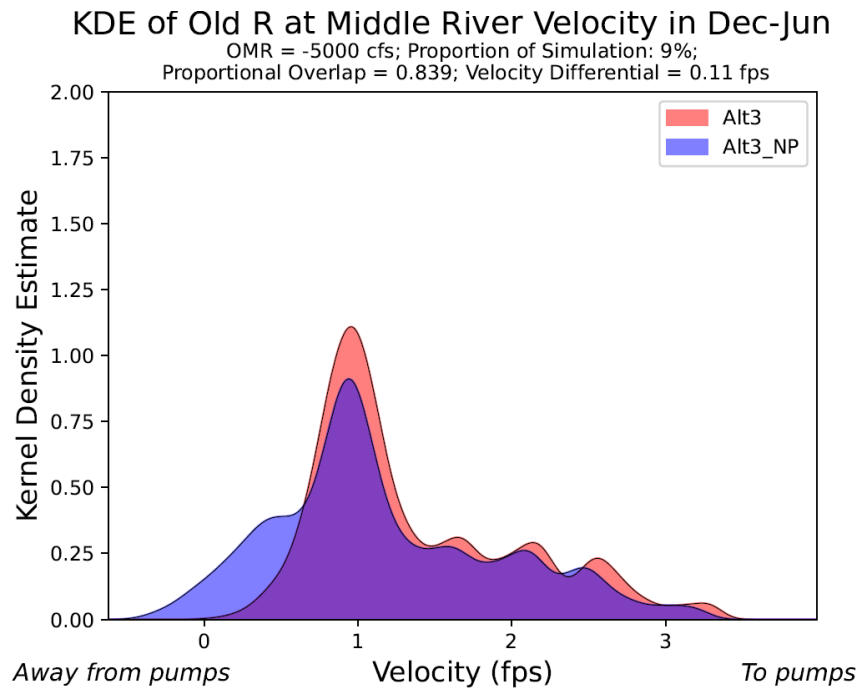


Figure I.3-90. Gaussian KDE of Velocity at Old River at Middle River in December through June with OMR of -5,000 cfs. Results apply to the Alt3 alternative.

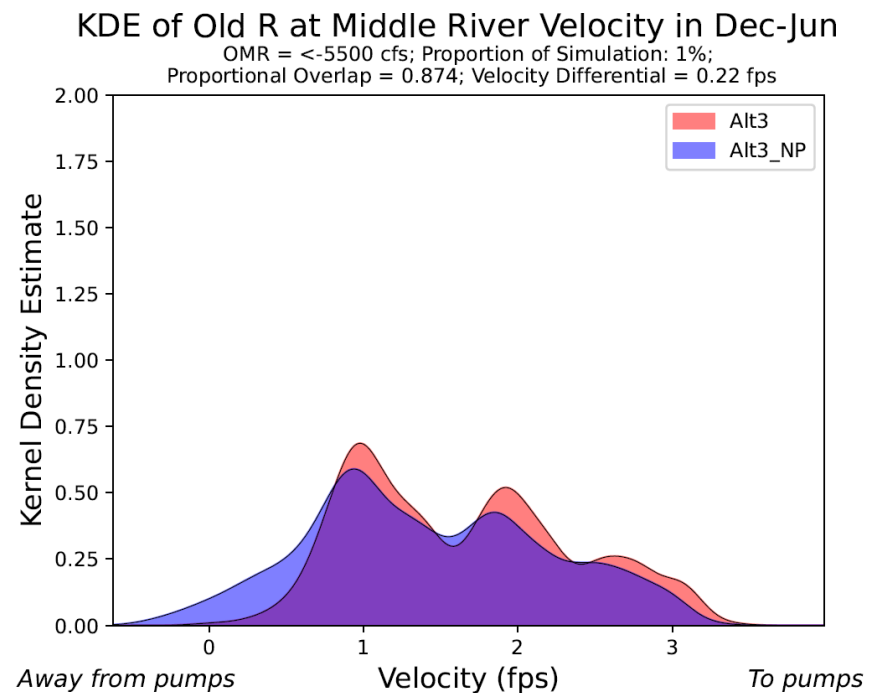


Figure I.3-91. Gaussian KDE of Velocity at Old River at Middle River in December through June with OMR < -5,500 cfs. Results apply to the Alt3 alternative.

I.3.2.1.8 KDE plots for Alt4 alternative:

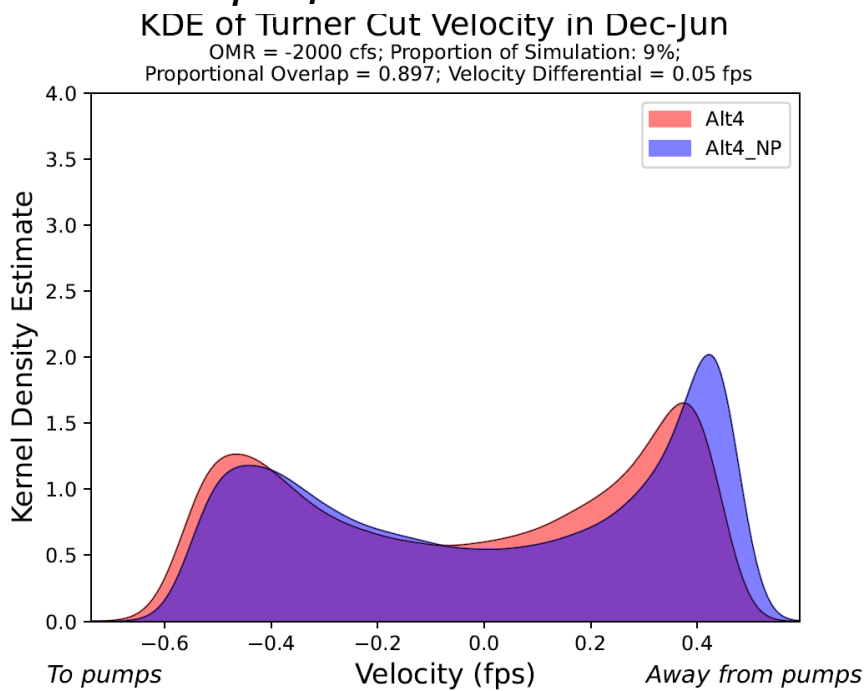


Figure I.3-92. Gaussian KDE of Velocity at Turner Cut in December through June with OMR of -2,000 cfs. Results apply to the Alt4 alternative.

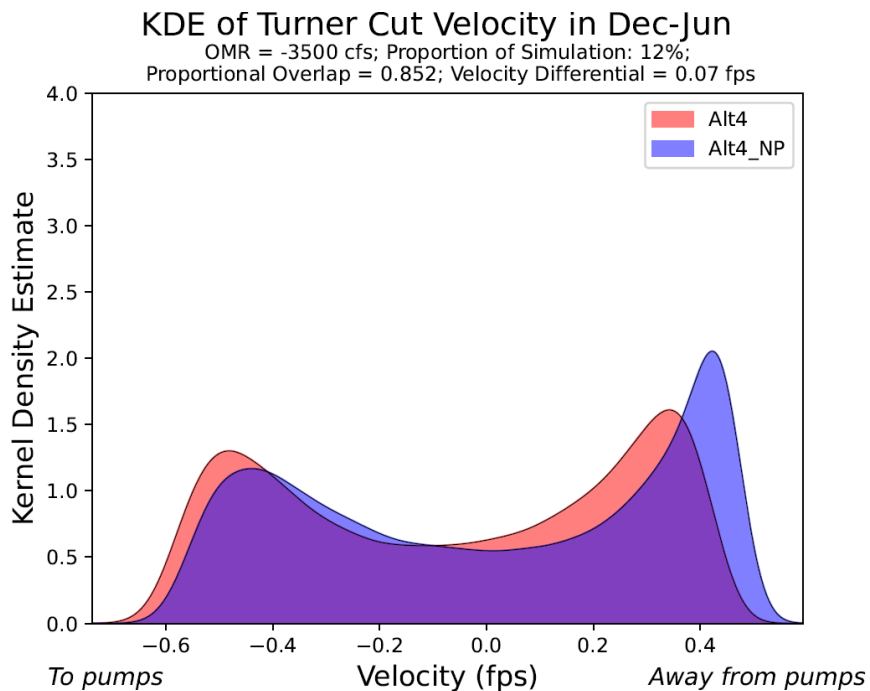


Figure I.3-93. Gaussian KDE of Velocity at Turner Cut in December through June with OMR of -3,500 cfs. Results apply to the Alt4 alternative.

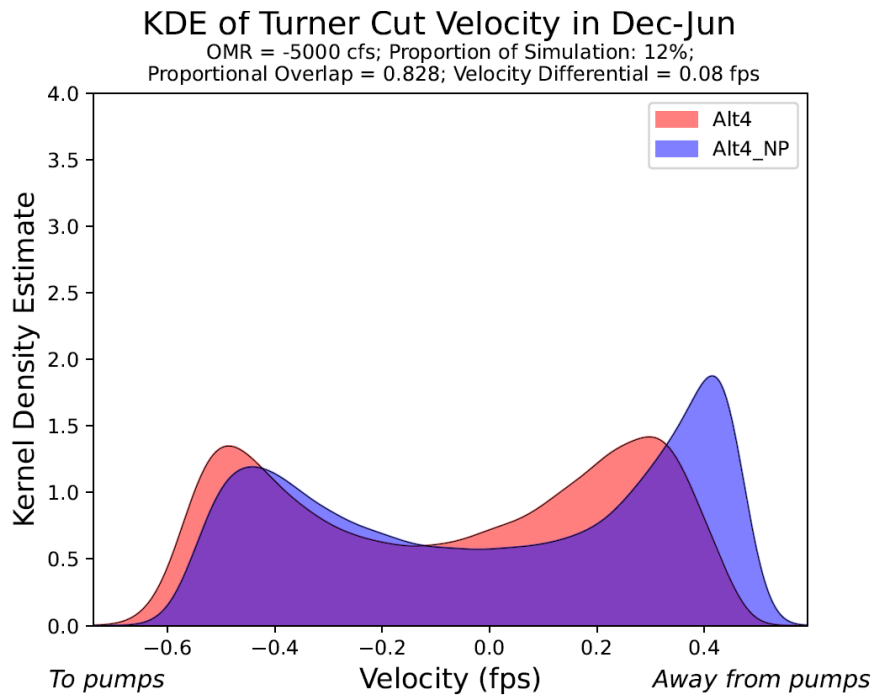


Figure I.3-94. Gaussian KDE of Velocity at Turner Cut in December through June with OMR of -5,000 cfs. Results apply to the Alt4 alternative.

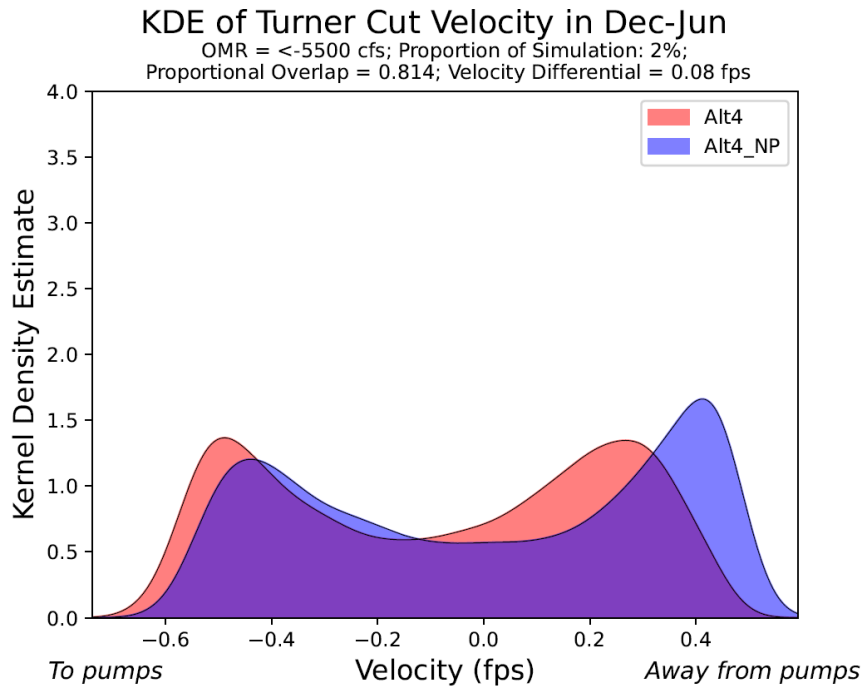


Figure I.3-95. Gaussian KDE of Velocity at Turner Cut in December through June with OMR < -5,500 cfs. Results apply to the Alt4 alternative.

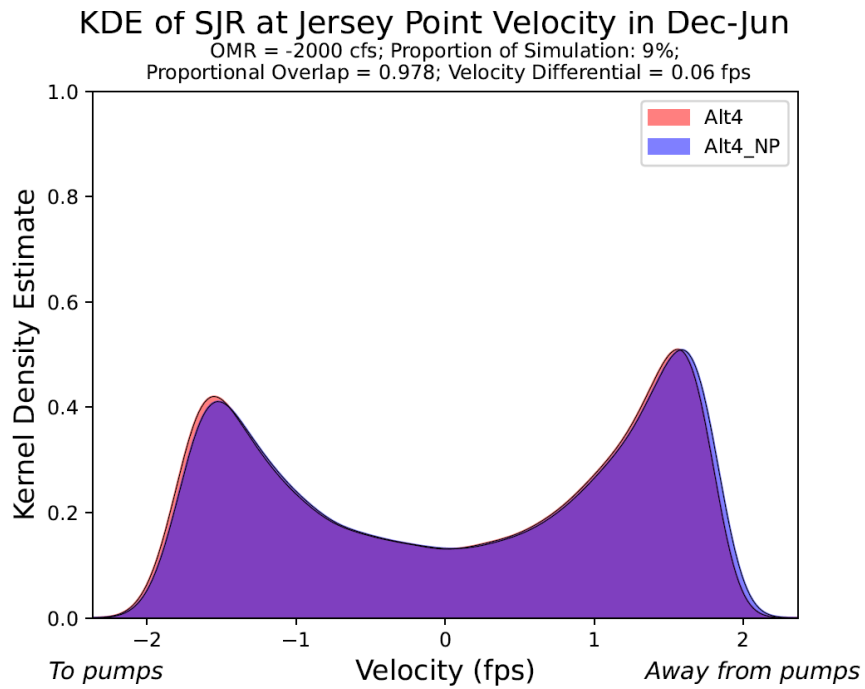


Figure I.3-96. Gaussian KDE of Velocity at San Joaquin River at Jersey Point in December through June with OMR of -2,000 cfs. Results apply to the Alt4 alternative.

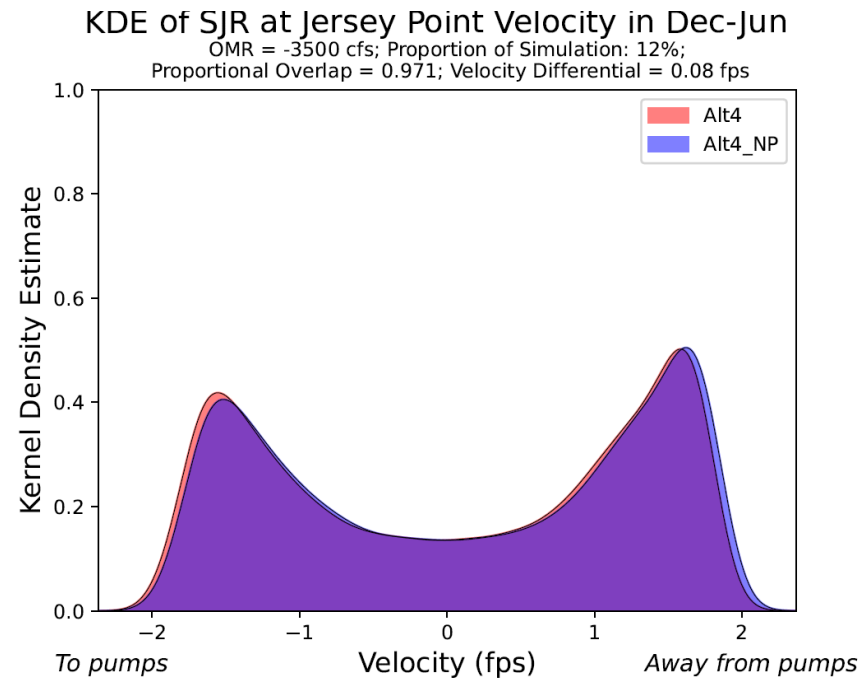


Figure I.3-97. Gaussian KDE of Velocity at San Joaquin River at Jersey Point in December through June with OMR of -3,500 cfs. Results apply to the Alt4 alternative.

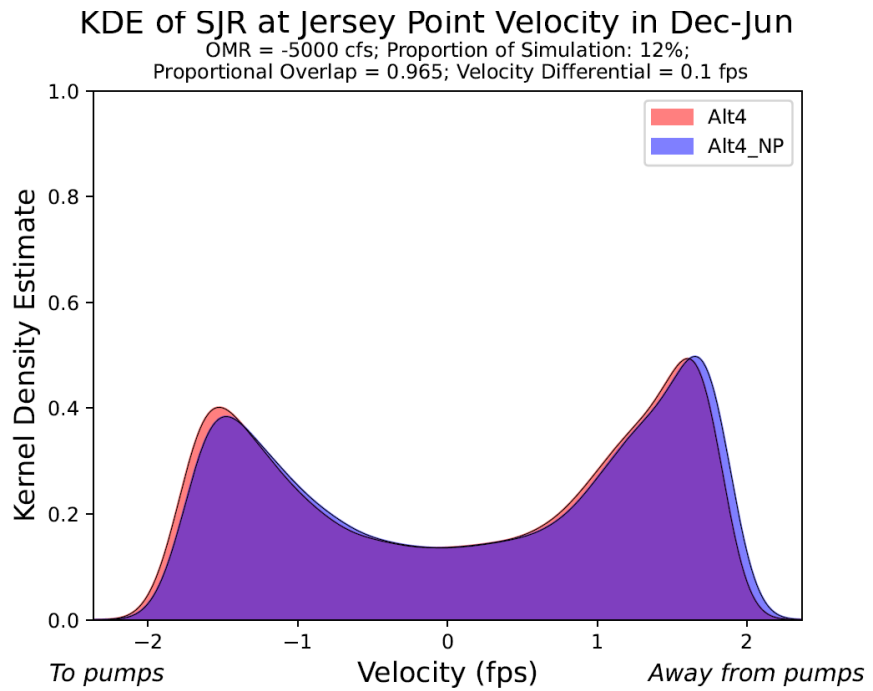


Figure I.3-98. Gaussian KDE of Velocity at San Joaquin River at Jersey Point in December through June with OMR of -5,000 cfs. Results apply to the Alt4 alternative.

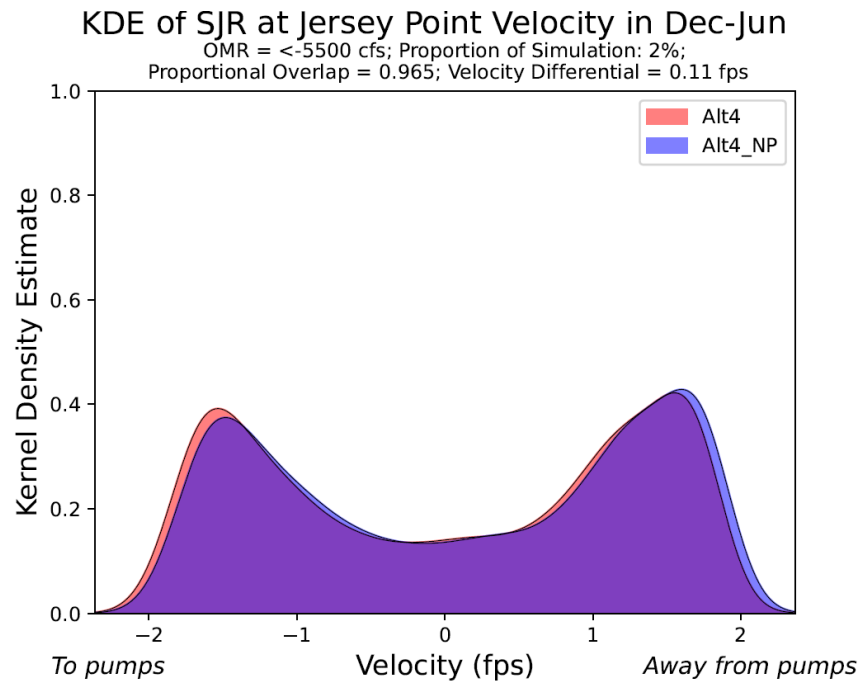


Figure I.3-99. Gaussian KDE of Velocity at San Joaquin River at Jersey Point in December through June with OMR < -5,500 cfs. Results apply to the Alt4 alternative.

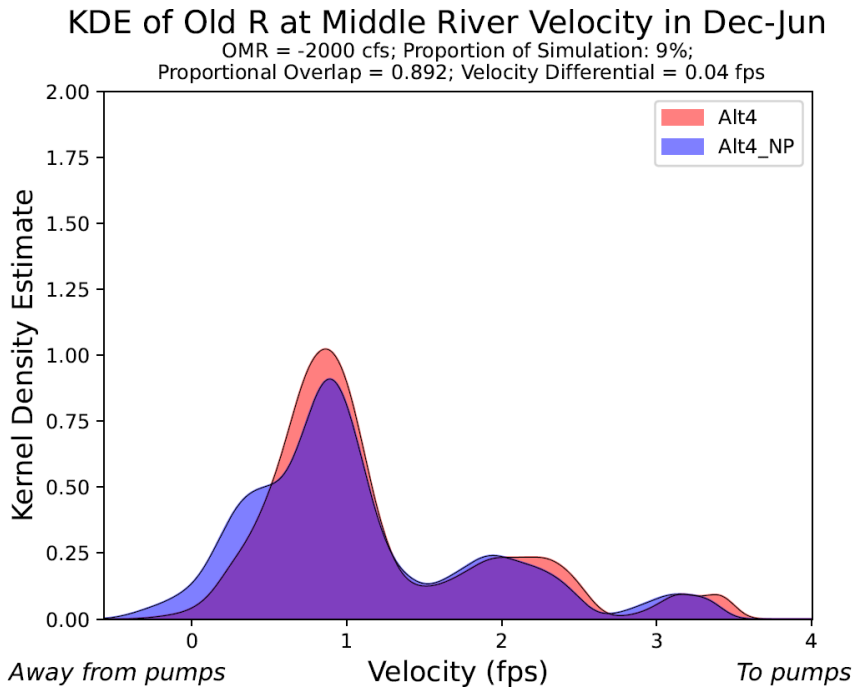


Figure I.3-100. Gaussian KDE of Velocity at Old River at Middle River in December through June with OMR of -2,000 cfs. Results apply to the Alt4 alternative.

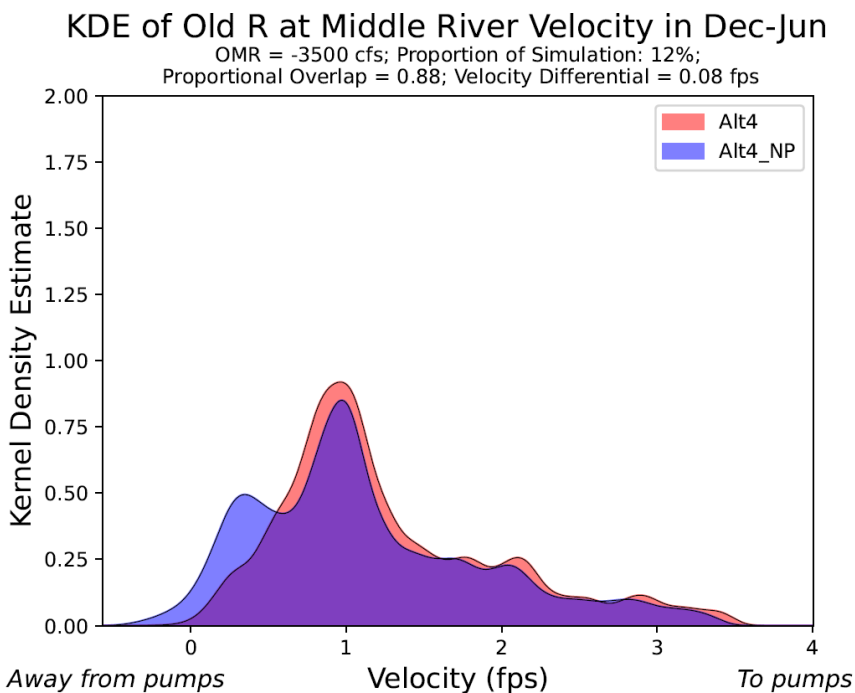


Figure I.3-101. Gaussian KDE of Velocity at Old River at Middle River in December through June with OMR of -3,500 cfs. Results apply to the Alt4 alternative.

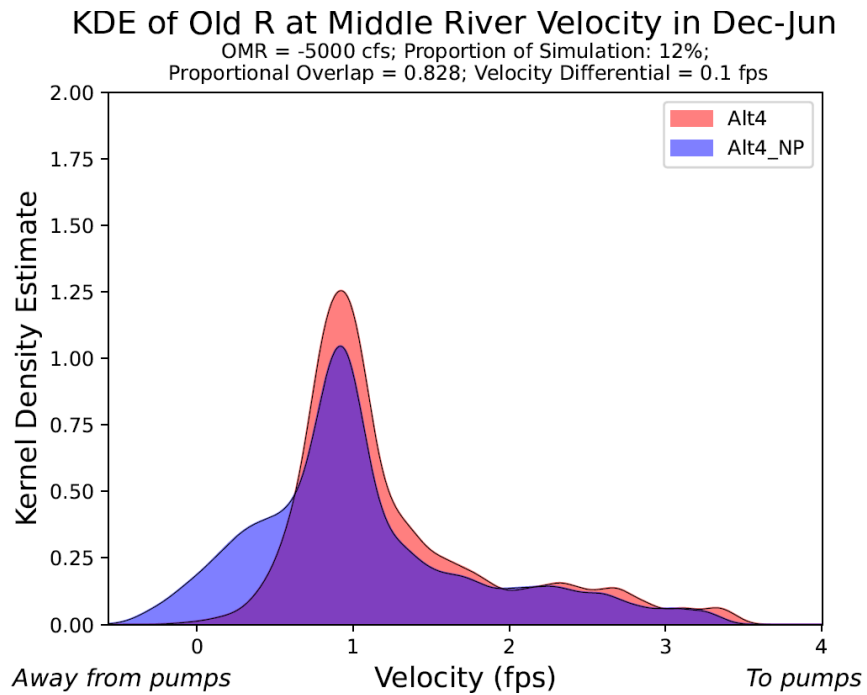


Figure I.3-102. Gaussian KDE of Velocity at Old River at Middle River in December through June with OMR of -5,000 cfs. Results apply to the Alt4 alternative.

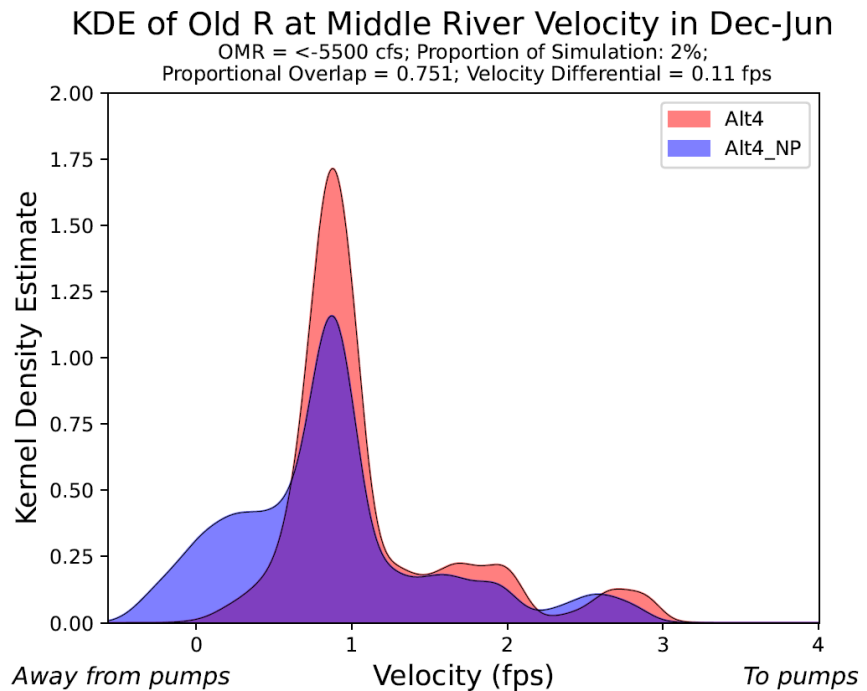


Figure I.3-103. Gaussian KDE of Velocity at Old River at Middle River in December through June with OMR < -5,500 cfs. Results apply to the Alt4 alternative.

Table I.3-7. Proportional overlap values for Turner Cut, SJR at Jersey Point, and Old R at Middle River at different OMR bins across alternatives.

Node	OMR bin	NAA	Alt1	Alt2 woTUCP woVA	Alt2 woTUCP DeltaVA	Alt2 woTUCP AllVA	Alt2 wTUCP woVA	Alt3	Alt4
Turner Cut	-2000	0.91	0.901	0.899	0.903	0.903	0.898	0.924	0.897
Turner Cut	-3500	0.853	0.858	0.851	0.86	0.861	0.851	0.876	0.852
Turner Cut	-5000	0.844	0.837	0.824	0.822	0.821	0.823	0.812	0.828
Turner Cut	<-5500	0.809	0.75	0.806	0.808	0.809	0.807	0.785	0.814
SJR at Jersey Point	-2000	0.981	0.979	0.979	0.979	0.98	0.979	0.984	0.978
SJR at Jersey Point	-3500	0.969	0.973	0.97	0.972	0.972	0.97	0.974	0.971
SJR at Jersey Point	-5000	0.969	0.969	0.966	0.965	0.965	0.966	0.962	0.965
SJR at Jersey Point	<-5500	0.964	0.953	0.964	0.964	0.964	0.964	0.961	0.965
Old R at Middle River	-2000	0.912	0.907	0.888	0.897	0.895	0.89	0.911	0.892
Old R at Middle River	-3500	0.857	0.915	0.878	0.866	0.865	0.877	0.846	0.88
Old R at Middle River	-5000	0.809	0.813	0.829	0.835	0.836	0.83	0.839	0.828
Old R at Middle River	<-5500	0.736	0.733	0.746	0.755	0.751	0.749	0.874	0.751

With incremental increases to pumping, proportional overlap at these three locations decreases. Changes to proportional overlap are more subtle along the San Joaquin River at Jersey Point as compared to Turner Cut and Old River at Middle River (Table I.3-7). Effects of pumping are smallest at the upstream-most location (San Joaquin River at Jersey Point). Since Turner Cut is less influenced by riverine flow, it is more susceptible to changes in pumping.

The range of velocities (presented on the x-axis) is much narrower at Turner Cut (ranging from -0.7 to 0.5 fps) compared to the other two locations (-1 to 4 fps at Old River at Middle River and -2.5 to 2.5 fps along the San Joaquin River at Jersey Point). Despite a small range in the velocity at this location, the proportional overlap value is still sensitive to pumping relative to the flow along the San Joaquin River at Jersey Point. Due to proximity, channel connectivity, and/or flow/velocity patterns, proportional overlap values change significantly with pumping at Old River at Middle River. Even though the proportional overlap value at this location is sensitive to pumping, the change in median velocity is smaller (~ 0.03 to 0.14 fps) compared to San Joaquin River flow at Jersey Point.

I.3.2.2 Gaussian KDE Proportional Overlap Contour Maps

Contour plots for each alternative are presented below. Each plot represents a different alternative, and each facet represents a different inflow group. The space within each line represents the area experiencing 25-100% alteration (0-0.75 proportional overlap) based on kernel density estimates. Missing contours indicate a lack of historical data, and thus simulation ability.

NAA 0.75 contour

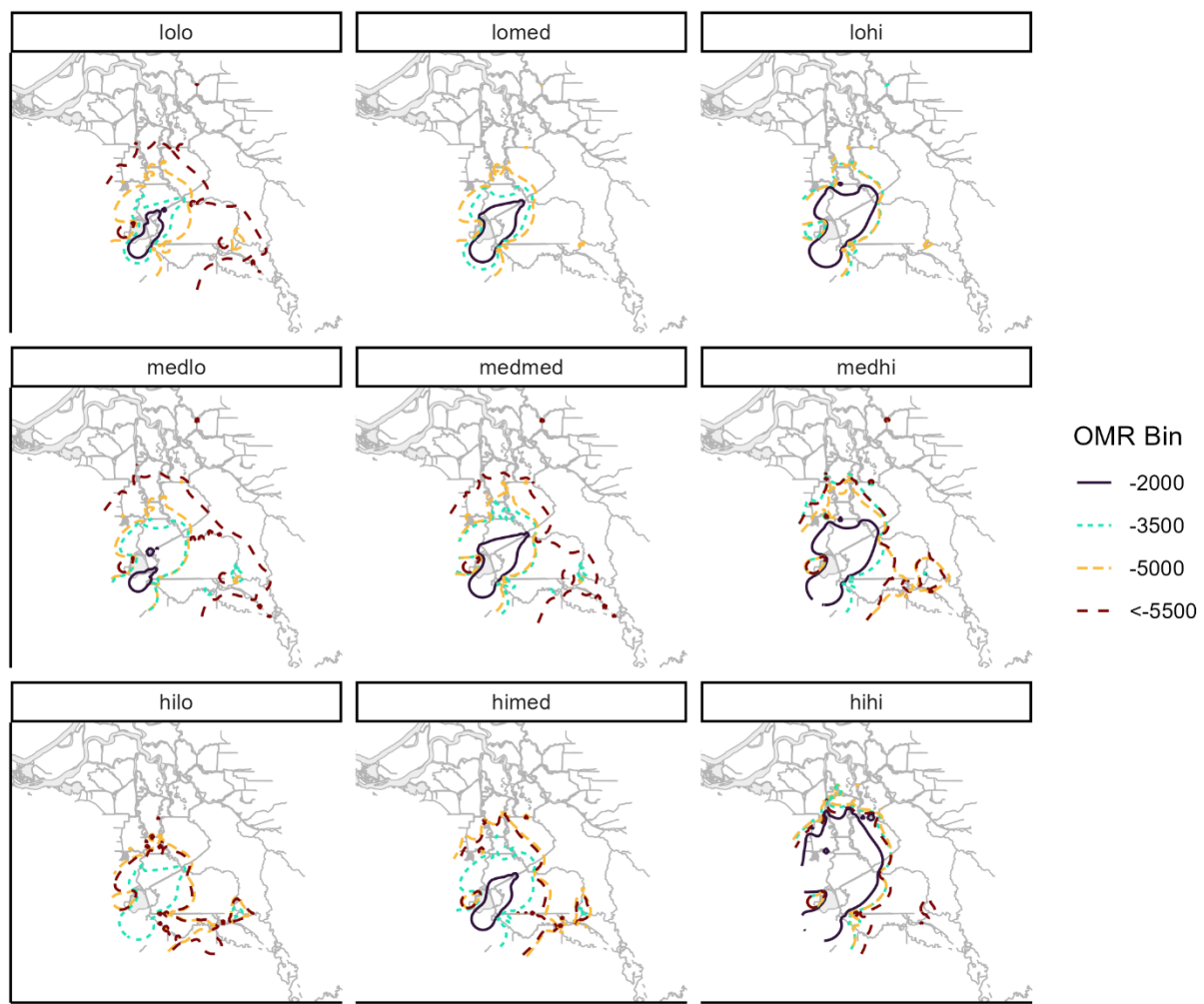


Figure I.3-104. Faceted Contour Maps Delineating Delta Export Zone of Influence Under Varying Inflows and OMR Flows. The contours identify where there is up to 75% overlap in velocity distribution with and without CVP exports. Results apply to the No Action Alternative. See Figure I.3-3 for group designations.

Alt1 0.75 contour

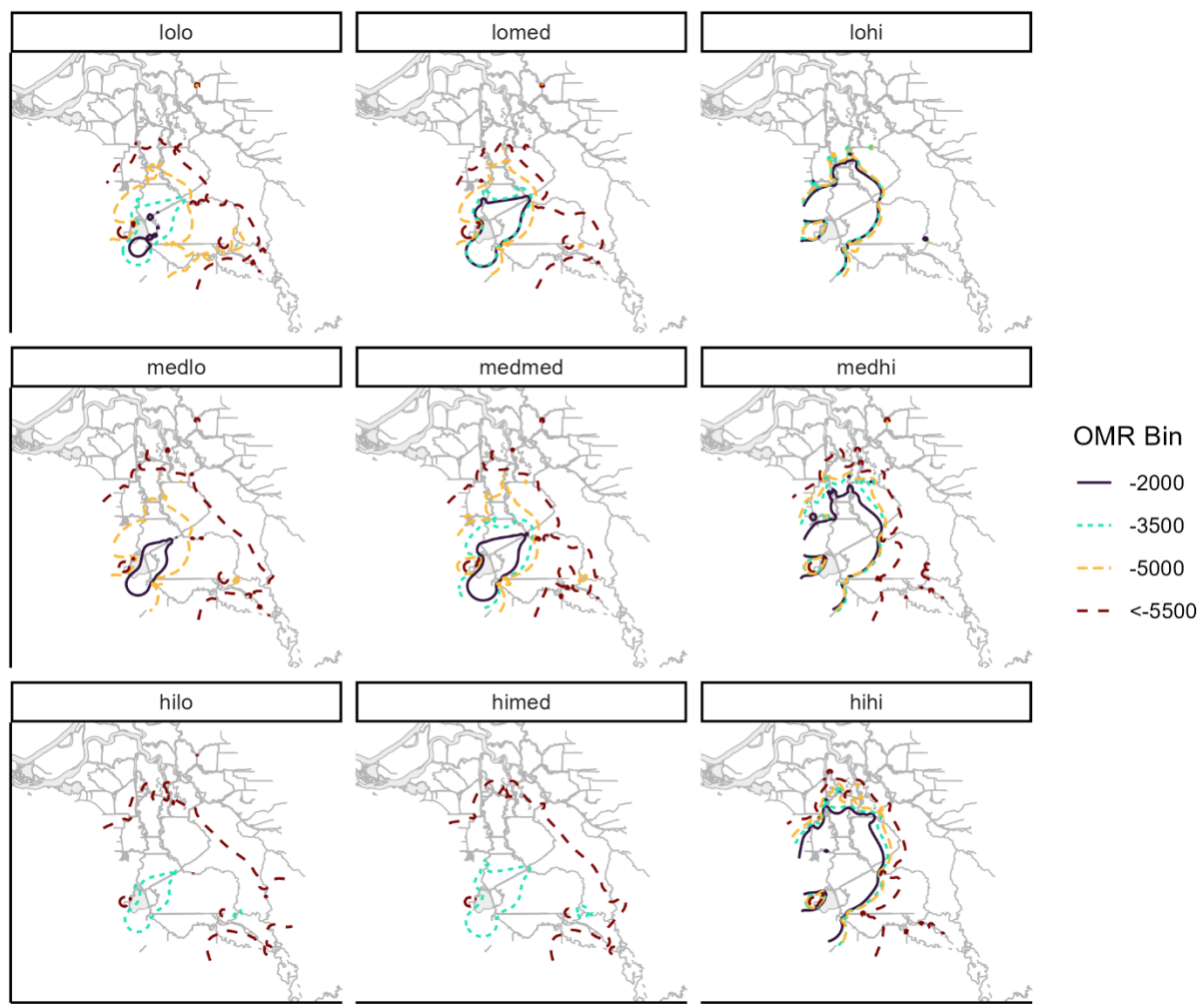


Figure I.3-105. Faceted Contour Maps Delineating Delta Export Zone of Influence Under Varying Inflows and OMR Flows. The contours identify where there is up to 75% overlap in velocity distribution with and without CVP exports. Results apply to Alternative 1. See Figure I.3-3 for group designations.

Alt2woTUCPwoVA 0.75 contour

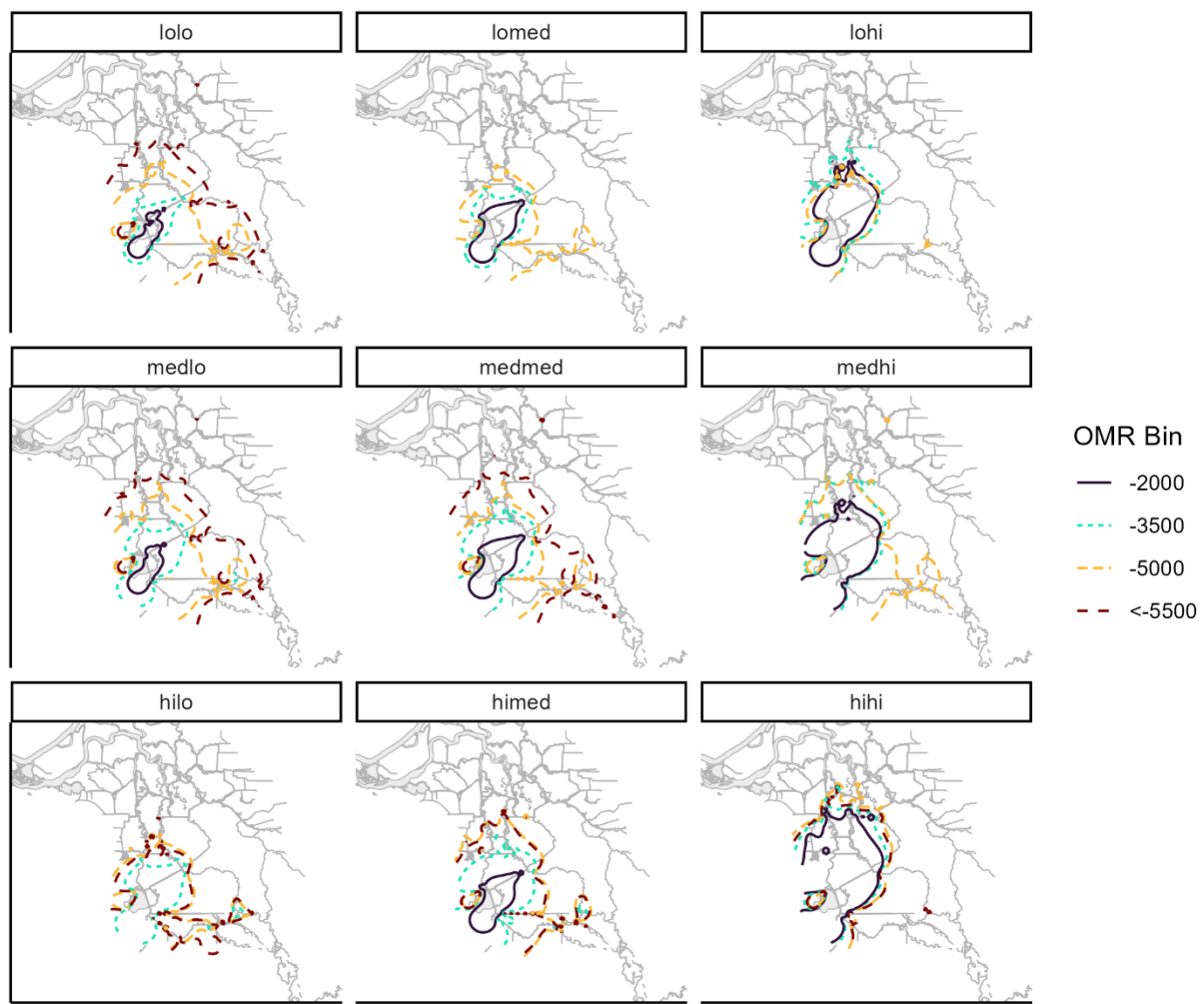


Figure I.3-106. Faceted Contour Maps Delineating Delta Export Zone of Influence Under Varying Inflows and OMR Flows. The contours identify where there is up to 75% overlap in velocity distribution with and without CVP exports. Results apply to Alt2woTUCPwoVA. See Figure I.3-3 for group designations.

Alt2woTUCPDeltaVA 0.75 contour

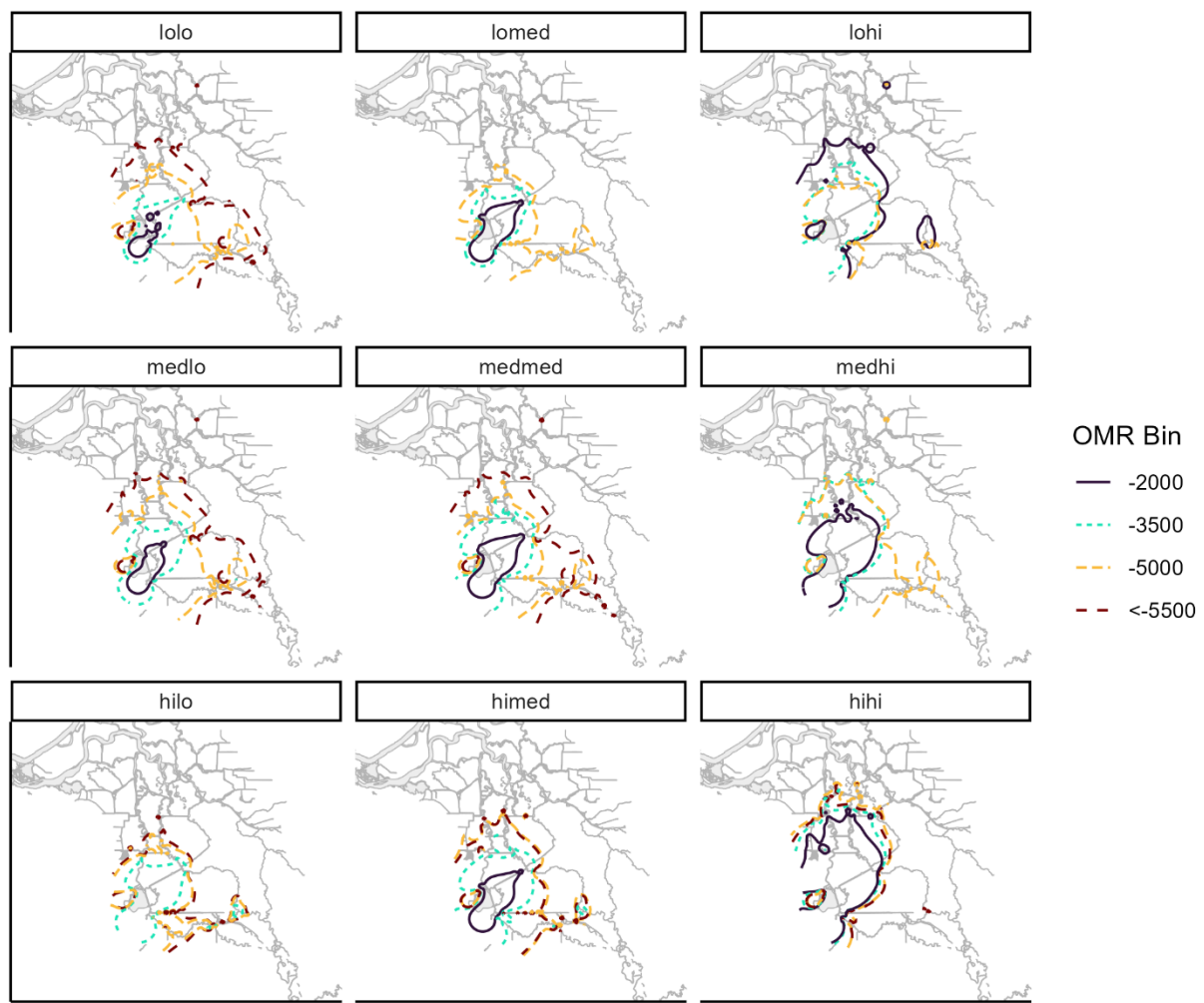


Figure I.3-107. Faceted Contour Maps Delineating Delta Export Zone of Influence Under Varying Inflows and OMR Flows. The contours identify where there is up to 75% overlap in velocity distribution with and without CVP exports. Results apply to Alt2woTUCPDeltaVA. See Figure I.3-3 for group designations.

Alt2woTUCPAIIVA 0.75 contour

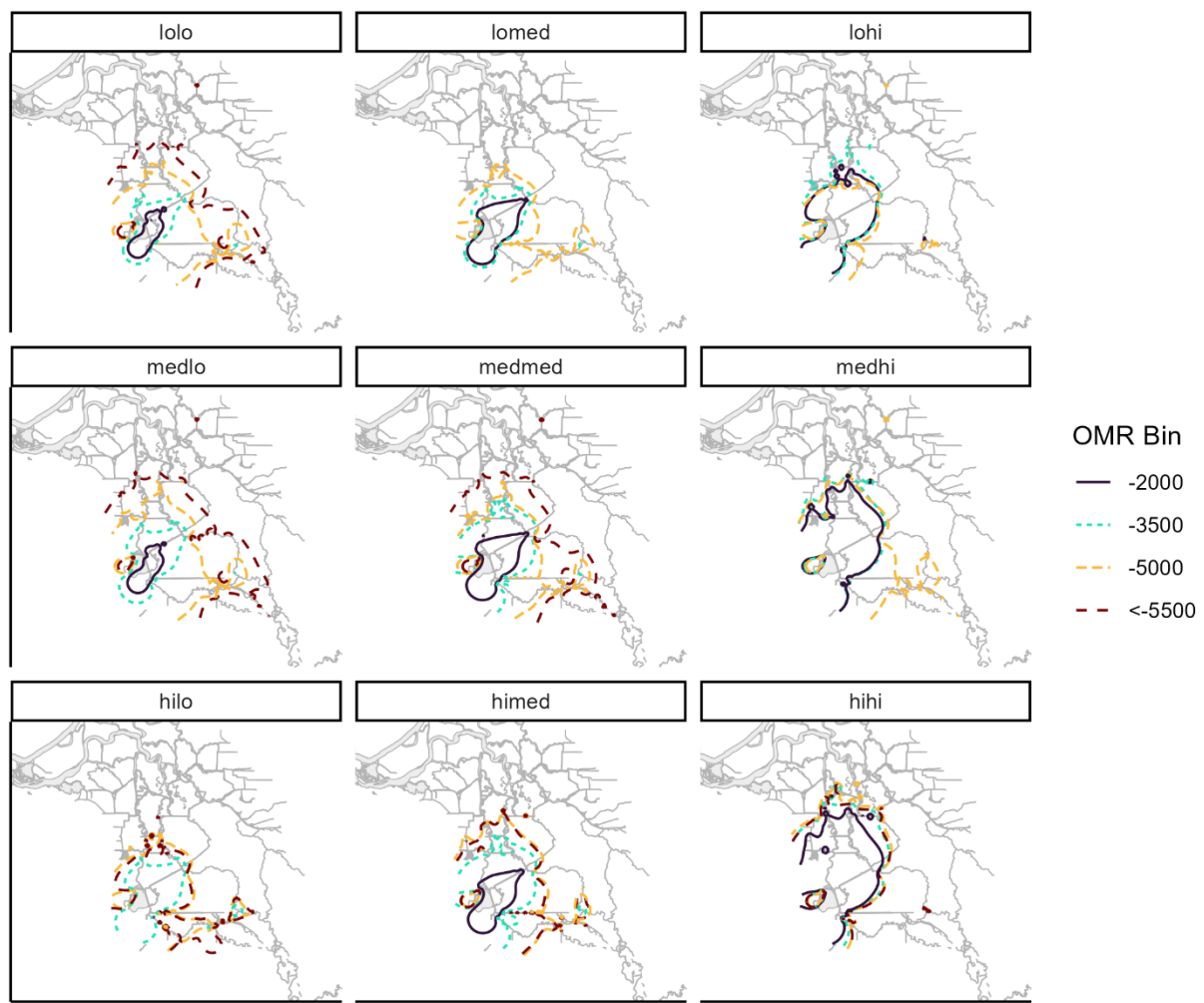


Figure I.3-108. Faceted Contour Maps Delineating Delta Export Zone of Influence Under Varying Inflows and OMR Flows. The contours identify where there is up to 75% overlap in velocity distribution with and without CVP exports. Results apply to Alt2woTUCPAIIVA. See Figure I.3-3 for group designations.

Alt2wTUCPwoVA 0.75 contour

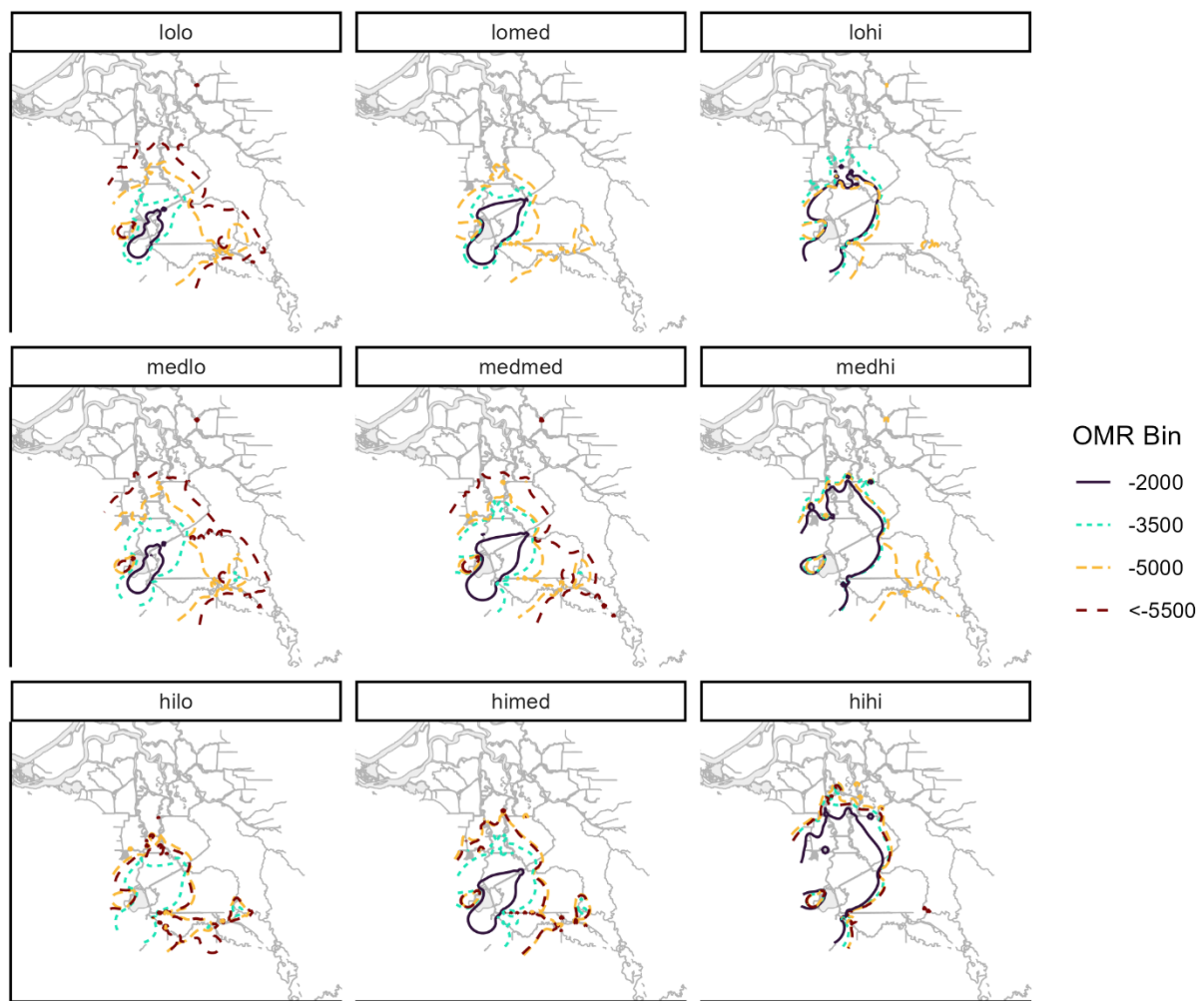


Figure I.3-109. Faceted Contour Maps Delineating Delta Export Zone of Influence Under Varying Inflows and OMR Flows. The contours identify where there is up to 75% overlap in velocity distribution with and without CVP exports. Results apply to Alt2wTUCPwoVA. See Figure I.3-3 for group designations.

Alt3 0.75 contour

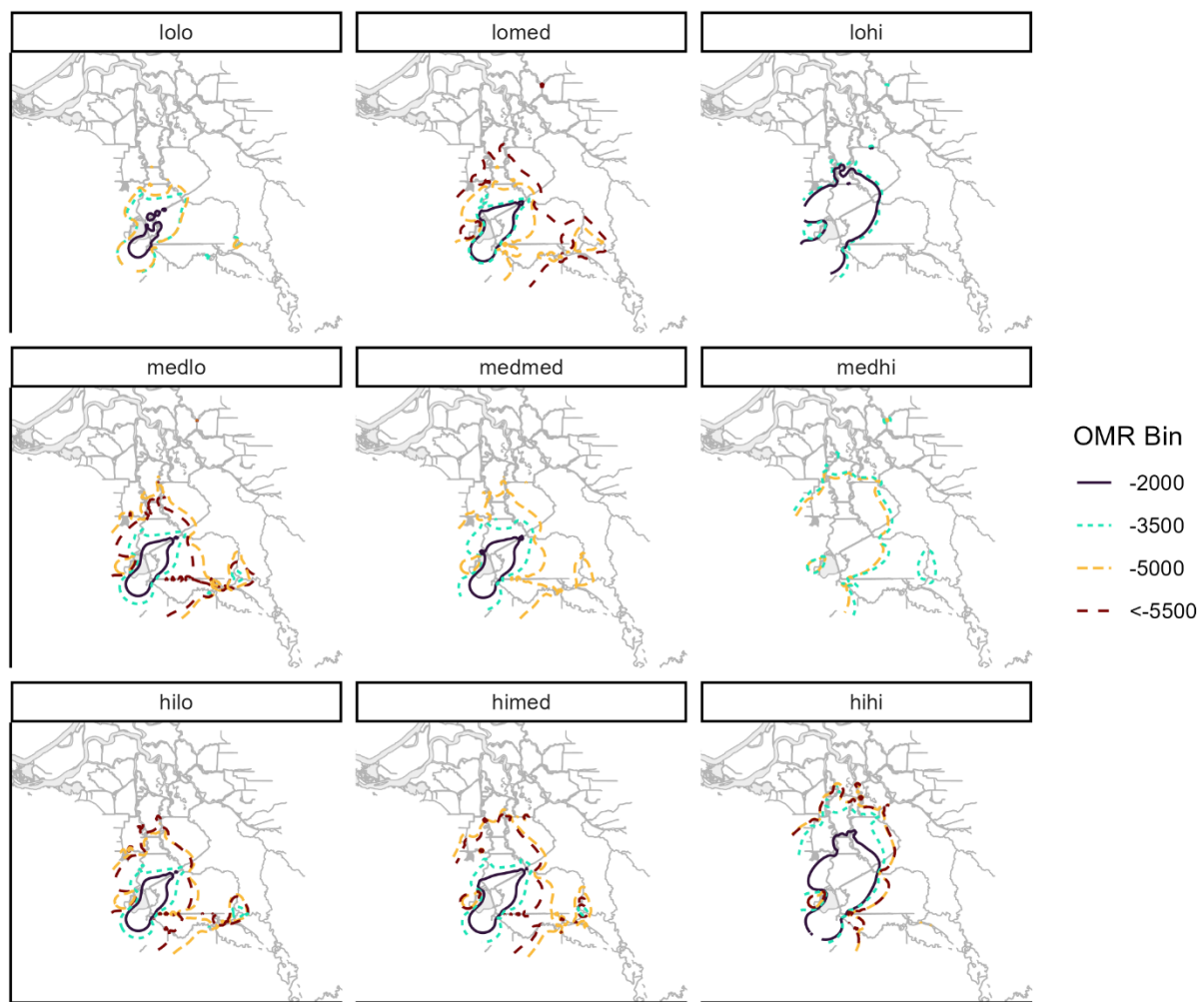


Figure I.3-110. Faceted Contour Maps Delineating Delta Export Zone of Influence Under Varying Inflows and OMR Flows. The contours identify where there is up to 75% overlap in velocity distribution with and without CVP exports. Results apply to Alt3. See Figure I.3-3 for group designations.

Alt4 0.75 contour

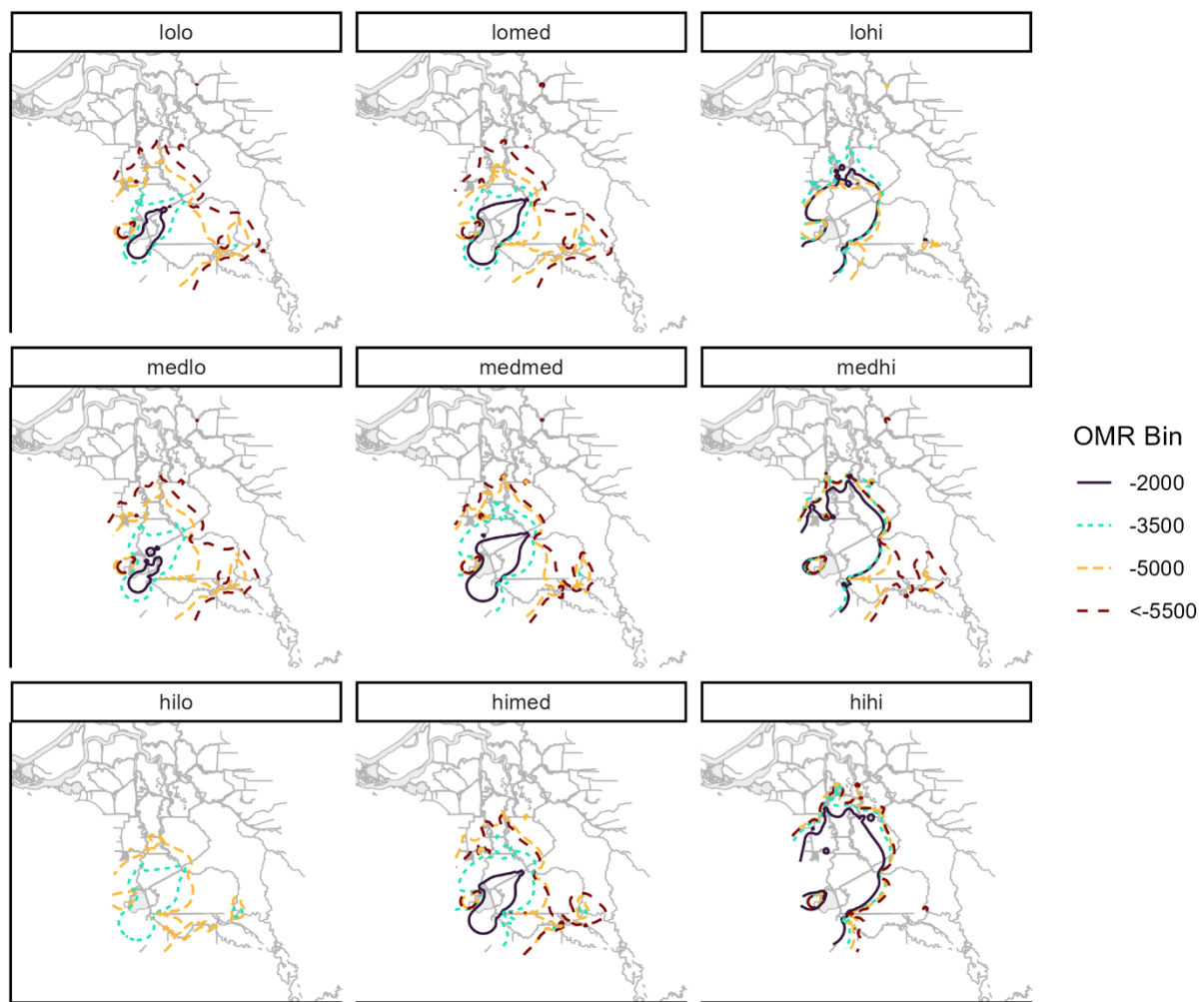


Figure I.3-111. Faceted Contour Maps Delineating Delta Export Zone of Influence Under Varying Inflows and OMR Flows. The contours identify where there is up to 75% overlap in velocity distribution with and without CVP exports. Results apply to Alt4. See Figure I.3-3 for group designations.

I.3.3 BA Key Takeaways

With incremental increases to pumping, proportional overlap at selected locations generally decreases. Changes to proportional overlap are more subtle along the San Joaquin River at Jersey Point as compared to Turner Cut and Old River at Middle River (Table I.3-7). For the three locations highlighted, proportion overlap ranges from 0.736 (NAA at less than -5500 cfs OMR at Old River at Middle River) to 0.981 (NAA at -2000 OMR at SJR at Jersey Point) (Table I.3-7). Proportion overlap across Proposed Action components ranges from 0.746 (Alt2woTUCPwoVA at less than -5500 OMR at Old River at Middle River) to 0.98 (Alt2woTUCPAIIVA at -2000 OMR SJR at Jersey Point).

Across all alternatives, most of the nodes experienced low hydrologic influence (greater than 0.75 overlap; Figure I.3-112–Figure I.3-120). The spatial extent (sum and proportion of channel length) of medium hydrologic alteration across all inflow groups and OMR bins ranges from 27,647 feet (0.7% of the DSM2 grid in NAA) to 606,560 feet (15.7% of the DSM2 grid in NAA) (Table I.3-8). Channel length altered across the Proposed Action components ranges from 45,576 feet (1.2% of the DSM2 grid in Alt2woTUCPDeltaVA) feet to 583,403 feet (15.2% of the DSM2 grid in Alt2woTUCPAIIVA) (Table I.3-8). The greatest extent of hydrologic alteration occurs in the <-5500 OMR bin, which is likely associated with greater exports.

Channel length altered and Delta Export Zone of Influence generally increase with more negative OMR (Figure I.3-104, Figure I.3-106, Figure I.3-107, Figure I.3-108, Figure I.3-121). Trends appear consistent across inflow groups containing combinations of low and medium Sacramento and San Joaquin inflow (lolo, lomed, medlo, medmed inflow groups). At high Sacramento inflow (hilo, himed, hihi inflow groups), there appears to be little difference in proportional channel length altered between -5000 and <-5500 OMR bins. In the lohi and hihi inflow groups, there also appears to be less difference in proportional channel length altered across all OMR bins.

For the -2000 and -3500 OMR bins, channel length altered generally increases with higher San Joaquin inflow (Figure I.3-104, Figure I.3-106, Figure I.3-107, Figure I.3-108, Figure I.3-122). These trends are not apparent for the -5000 and <-5500 OMR bins.

lolo

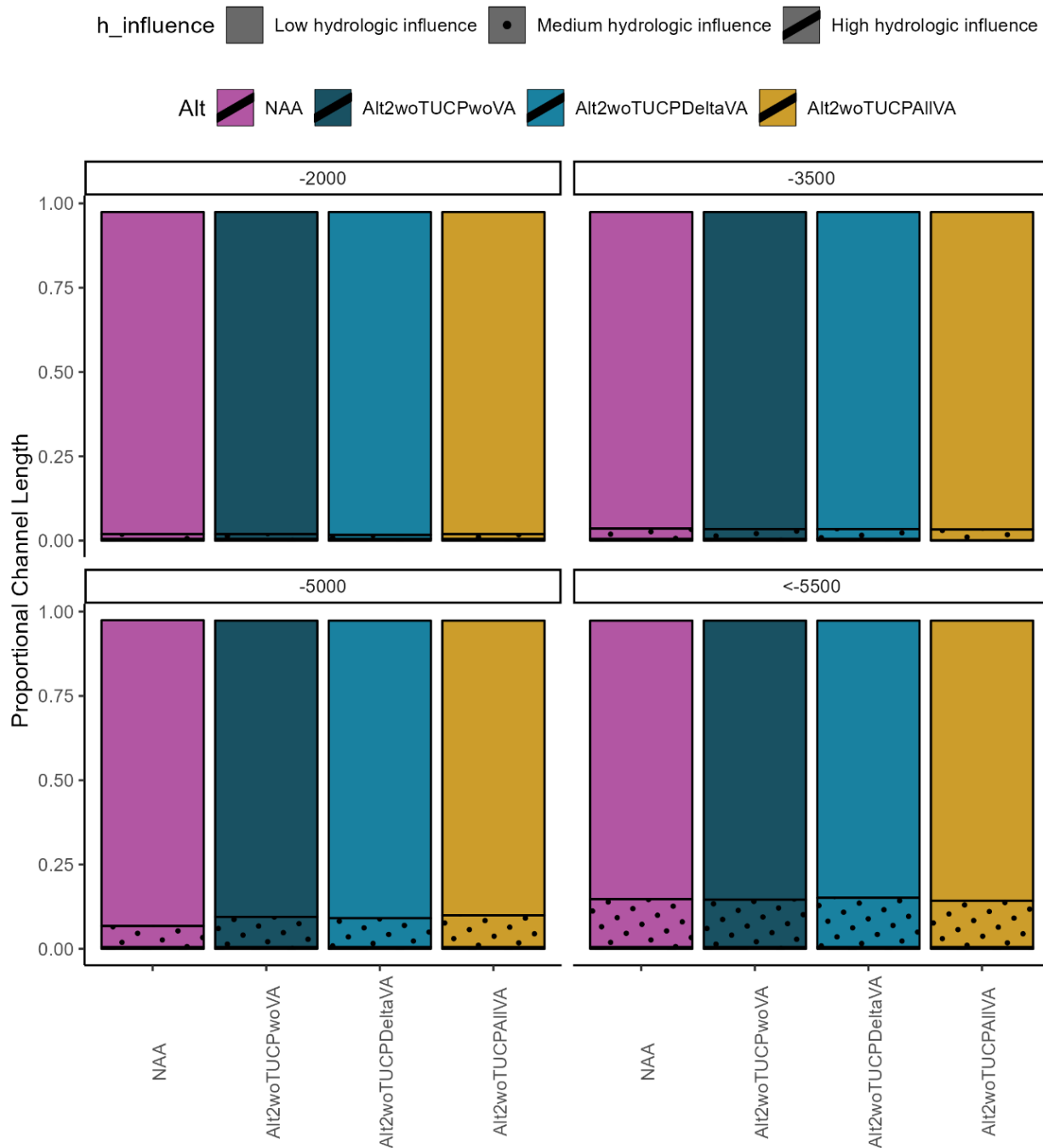


Figure I.3-112. Proportion of total channel length in the Delta (DSM2 grid) that experiences high (<25% proportional overlap), medium (25-75% proportional overlap) and low (>75% proportional overlap) hydrologic influence across PA components and across OMR bins of -2000, -3500, -5000, and less than -5500 cfs. Results apply to the lolo inflow group.

lomed

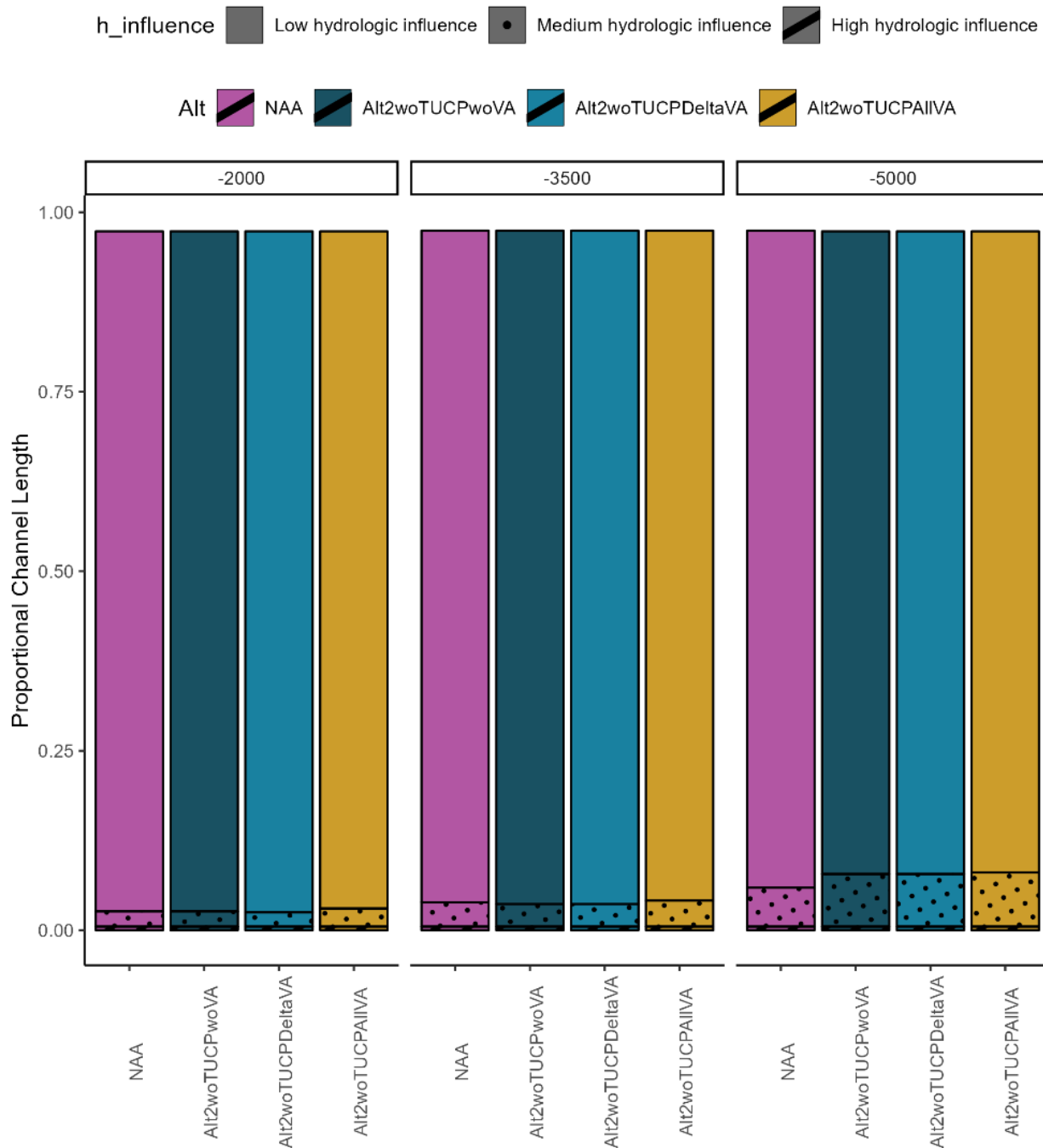


Figure I.3-113. Proportion of total channel length in the Delta (DSM2 grid) that experiences high (<25% proportional overlap), medium (25-75% proportional overlap) and low (>75% proportional overlap) hydrologic influence across PA components and across OMR bins of -2000, -3500, -5000, and less than -5500 cfs. Results apply to the lomed inflow group.

lohi

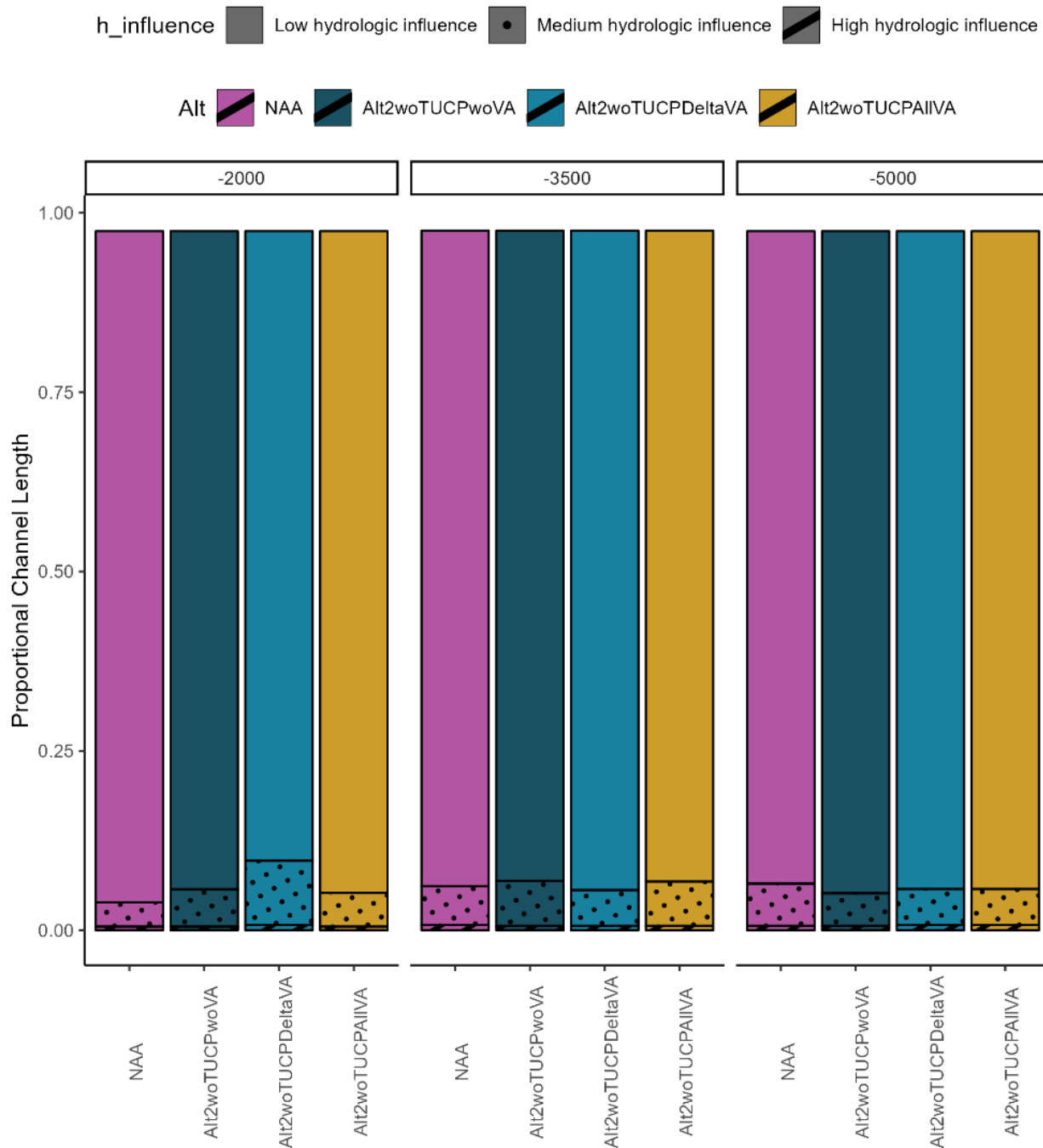


Figure I.3-114. Proportion of total channel length in the Delta (DSM2 grid) that experiences high (<25% proportional overlap), medium (25-75% proportional overlap) and low (>75% proportional overlap) hydrologic influence across PA components and across OMR bins of -2000, -3500, -5000, and less than -5500 cfs. Results apply to the lohi inflow group.

medlo

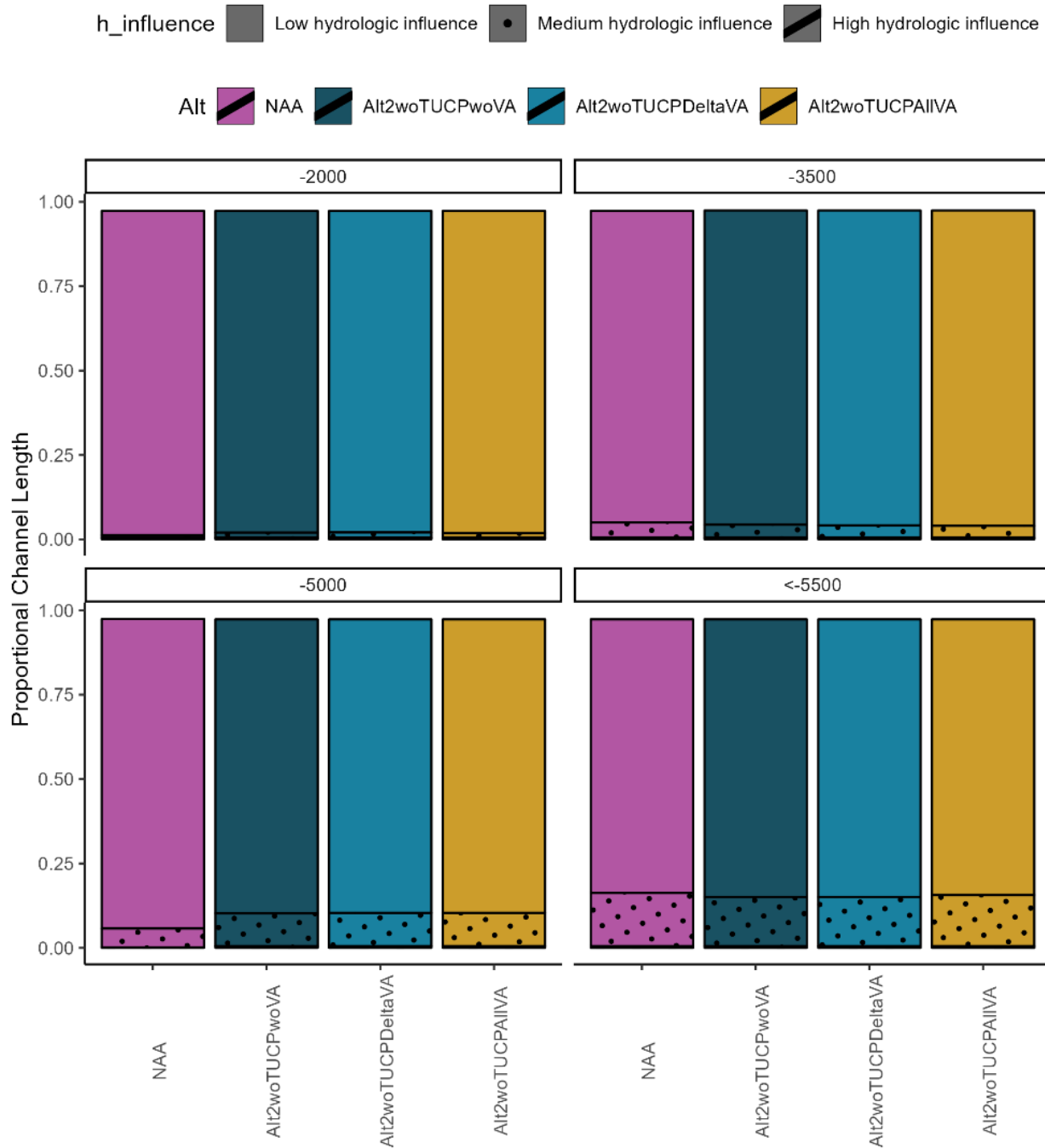


Figure I.3-115. Proportion of total channel length in the Delta (DSM2 grid) that experiences high (<25% proportional overlap), medium (25-75% proportional overlap) and low (>75% proportional overlap) hydrologic influence across PA components and across OMR bins of -2000, -3500, -5000, and less than -5500 cfs. Results apply to the medlo inflow group.

medmed

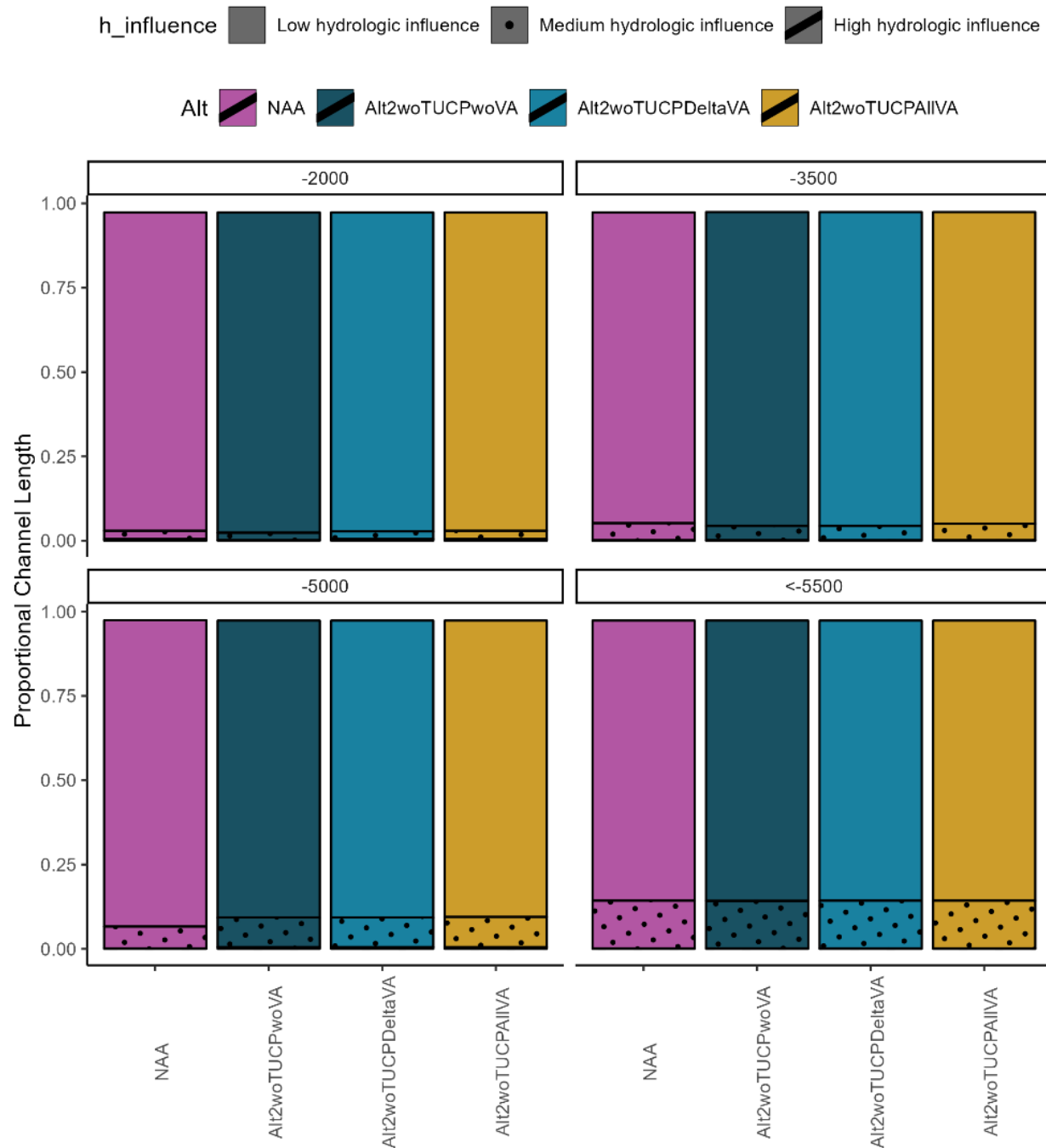


Figure I.3-116. Proportion of total channel length in the Delta (DSM2 grid) that experiences high (<25% proportional overlap), medium (25-75% proportional overlap) and low (>75% proportional overlap) hydrologic influence across PA components and across OMR bins of -2000, -3500, -5000, and less than -5500 cfs. Results apply to the medmed inflow group.

medhi

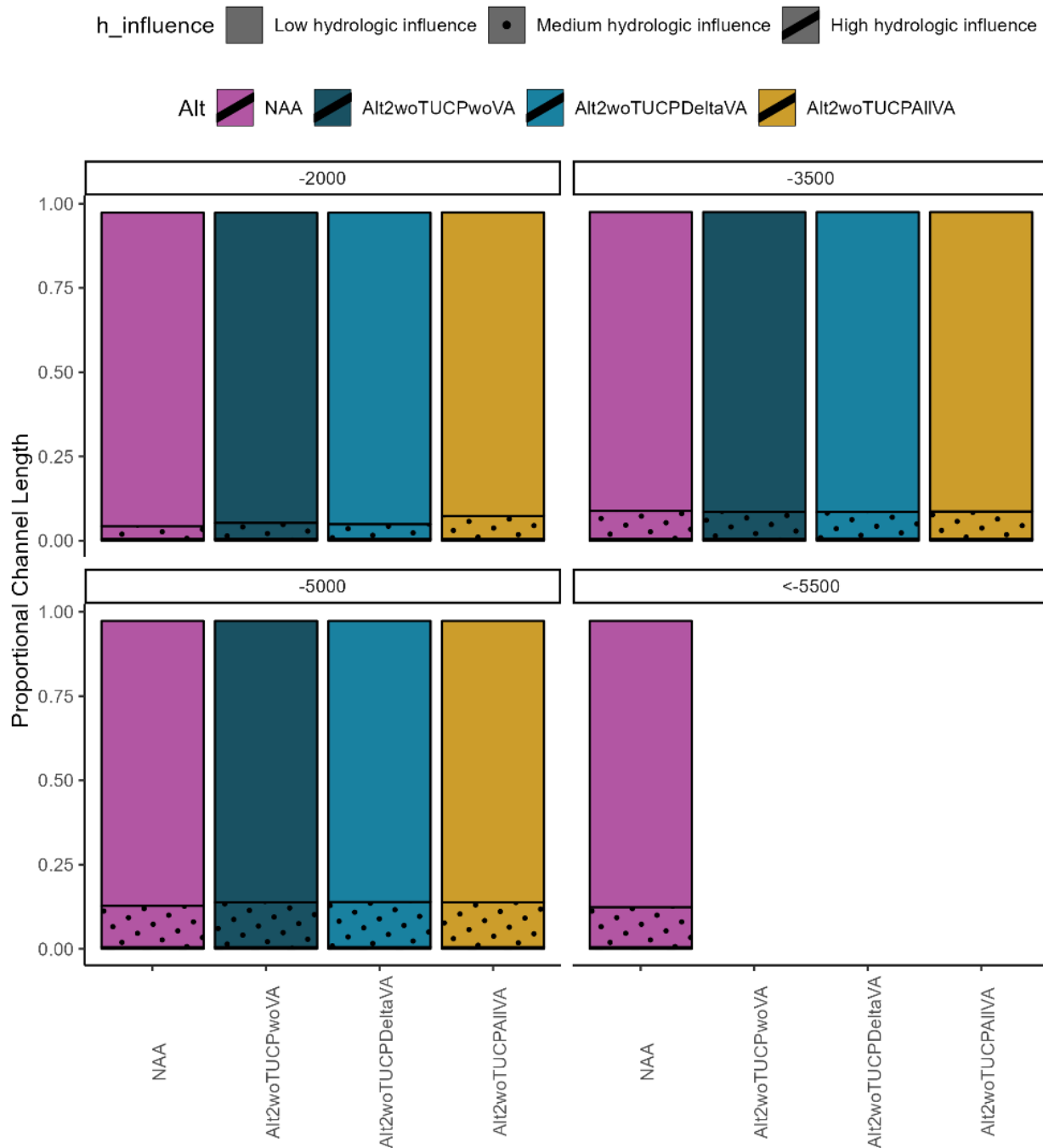


Figure I.3-117. Proportion of total channel length in the Delta (DSM2 grid) that experiences high (<25% proportional overlap), medium (25-75% proportional overlap) and low (>75% proportional overlap) hydrologic influence across PA components and across OMR bins of -2000, -3500, -5000, and less than -5500 cfs. Results apply to the medhi inflow group.

hilo

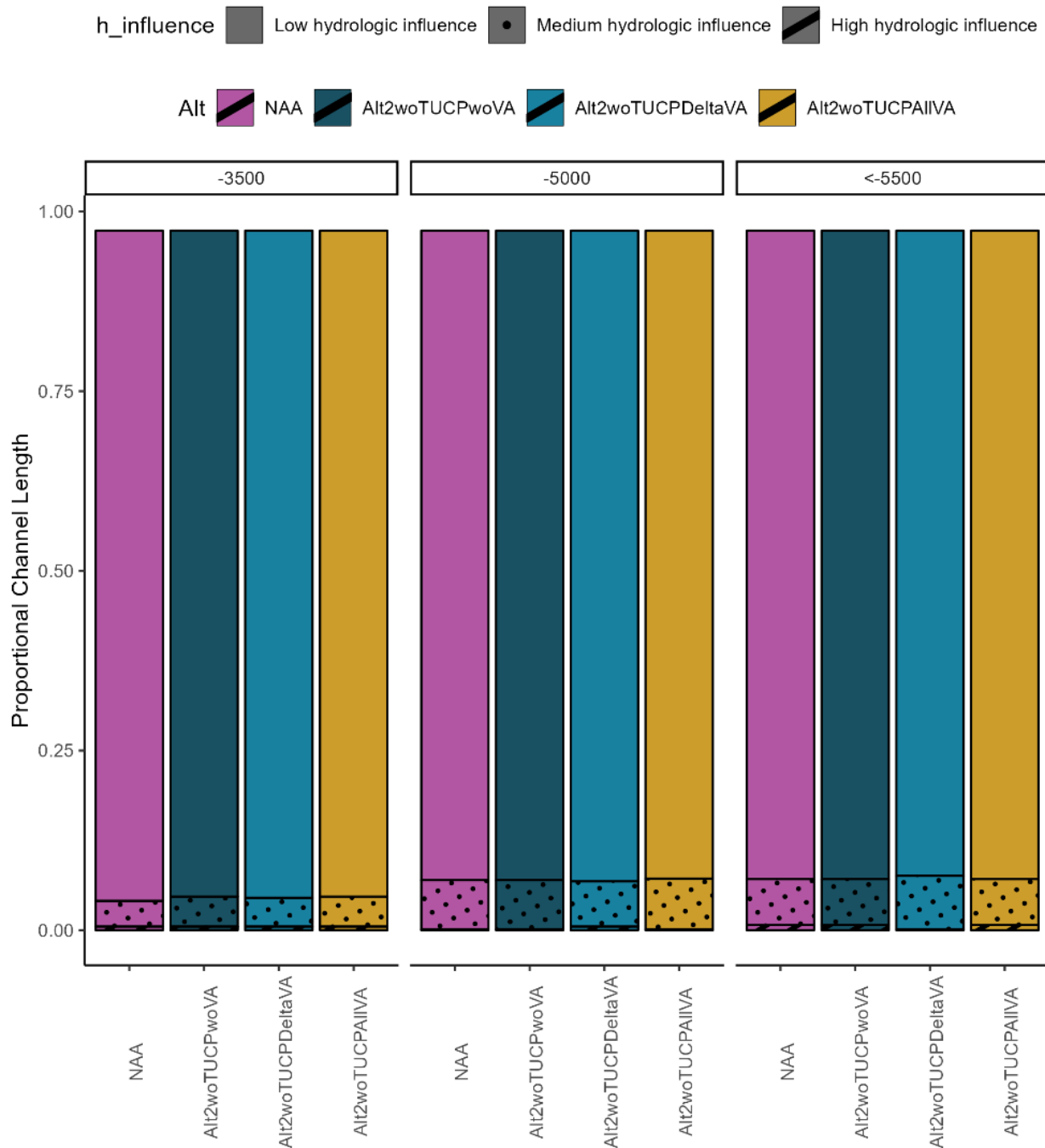


Figure I.3-118. Proportion of total channel length in the Delta (DSM2 grid) that experiences high (<25% proportional overlap), medium (25-75% proportional overlap) and low (>75% proportional overlap) hydrologic influence across PA components and across OMR bins of -2000, -3500, -5000, and less than -5500 cfs. Results apply to the hilo inflow group.

himed

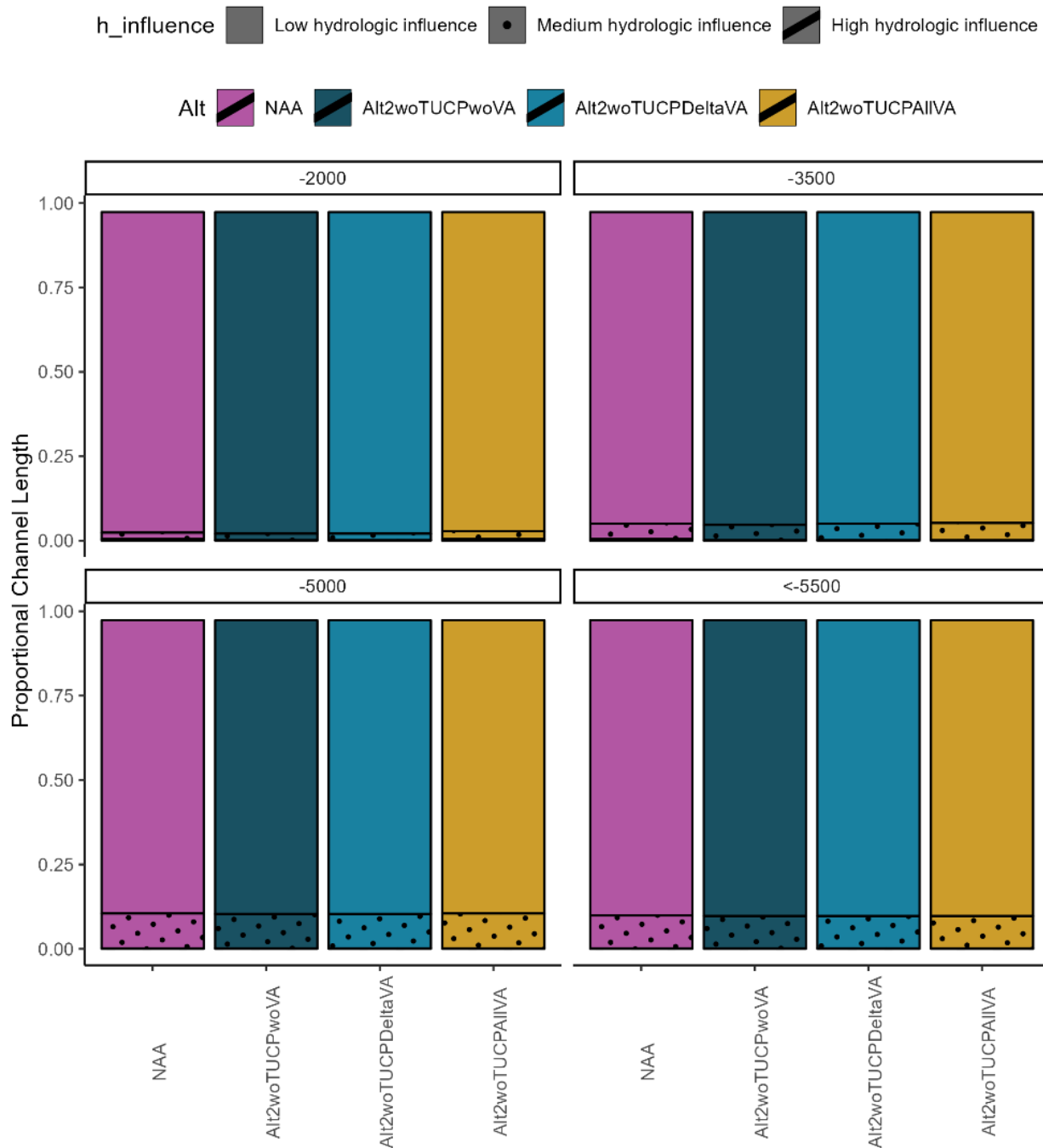


Figure I.3-119. Proportion of total channel length in the Delta (DSM2 grid) that experiences high (<25% proportional overlap), medium (25-75% proportional overlap) and low (>75% proportional overlap) hydrologic influence across PA components and across OMR bins of -2000, -3500, -5000, and less than -5500 cfs. Results apply to the himed inflow group.

hihi

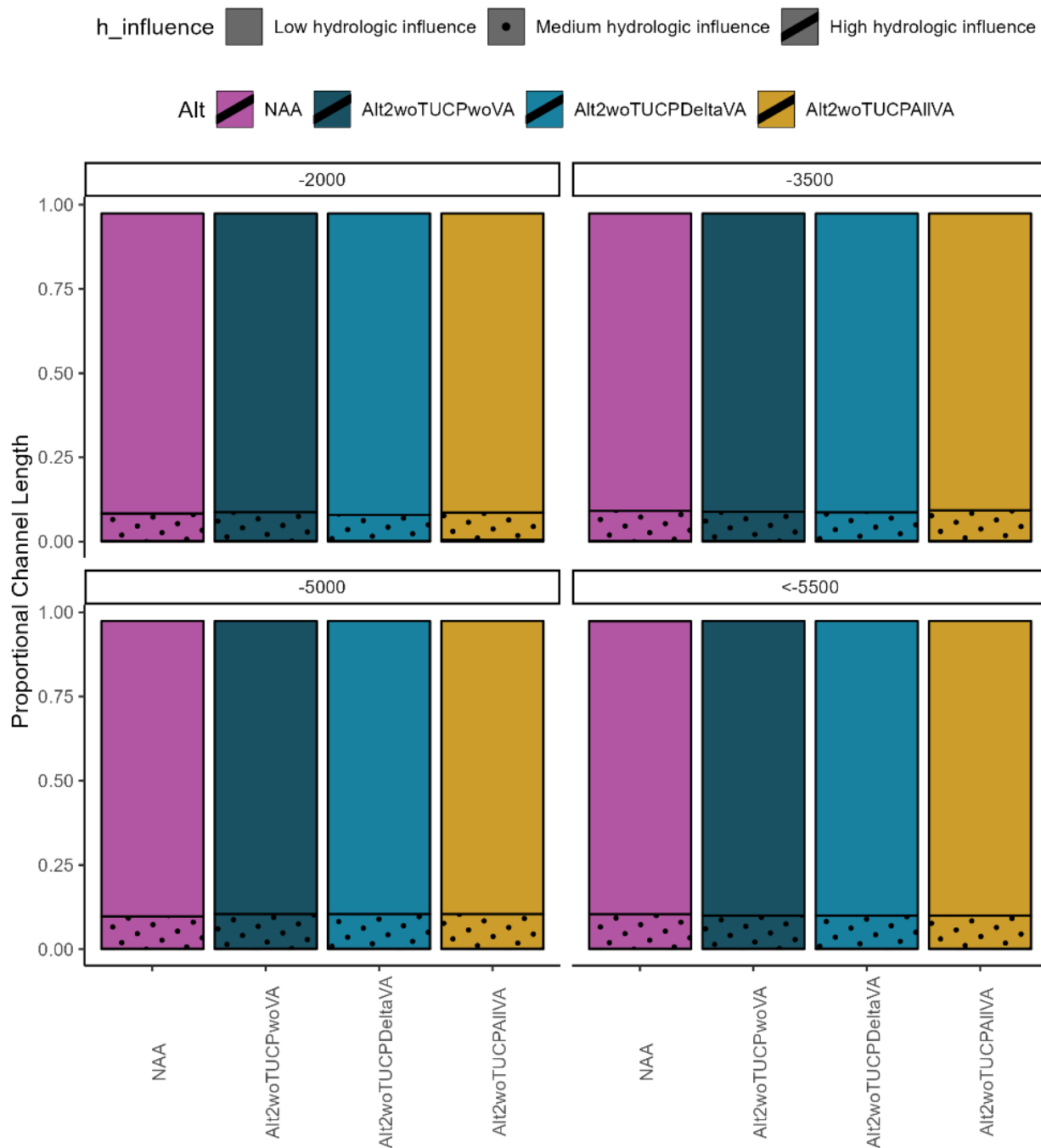


Figure I.3-120. Proportion of total channel length in the Delta (DSM2 grid) that experiences high (<25% proportional overlap), medium (25-75% proportional overlap) and low (>75% proportional overlap) hydrologic influence across PA components and across OMR bins of -2000, -3500, -5000, and less than -5500 cfs. Results apply to the hihi inflow group.

Table I.3-8. Channel length (feet) altered by pumping for No Action Alternative (NAA) and three components of the PA across inflow groups and OMR bins. Values represent total summed channel length between nodes experiencing 0.25-0.75 proportional overlap, or medium hydrologic influence. Absolute values are rounded.

Inflow group	OMR bin	NAA	Alt2woTUCP woVA	Alt2woTUCP DeltaVA	Alt2woTUCP AIIVA
lolo	-2000	54189	54189	45576	54189
lolo	-3500	117806	113044	113044	124055
lolo	-5000	240433	345257	329891	361840
lolo	<-5500	546547	542342	562344	527855
lomed	-2000	81465	81465	76711	96978
lomed	-3500	130344	120549	120549	139432
lomed	-5000	208217	281435	281435	289043
lomed	<-5500	NA	NA	NA	NA
lohi	-2000	130552	199749	344641	180584
lohi	-3500	208428	241111	191942	238045
lohi	-5000	226351	175053	193470	193470
medlo	-2000	27647	56798	59520	50971
medlo	-3500	172490	148289	138590	134670
medlo	-5000	217383	374670	377919	377919
medlo	<-5500	606560	559302	559302	583403
medmed	-2000	92454	86009	86009	92454
medmed	-3500	195201	164174	164174	188699
medmed	-5000	251330	337165	337165	345232
medmed	<-5500	546334	543002	546334	546334
medhi	-2000	143735	183314	167915	262475
medhi	-3500	319355	307325	303468	311986
medhi	-5000	470418	510174	514154	510385
medhi	<-5500	455531	NA	NA	NA
hilo	-3500	137049	160217	153086	160217
hilo	-5000	264382	264382	242315	271698
hilo	<-5500	245068	245068	287645	245068
himed	-2000	72558	76711	76711	86402
himed	-3500	175651	176405	188818	197951
himed	-5000	400448	392039	392039	400448
himed	<-5500	375420	369417	369417	369417
hihi	-2000	315738	331338	300952	311077
hihi	-3500	345153	334832	330569	352728
hihi	-5000	368941	396491	396491	396491
hihi	<-5500	395764	378812	378812	378812

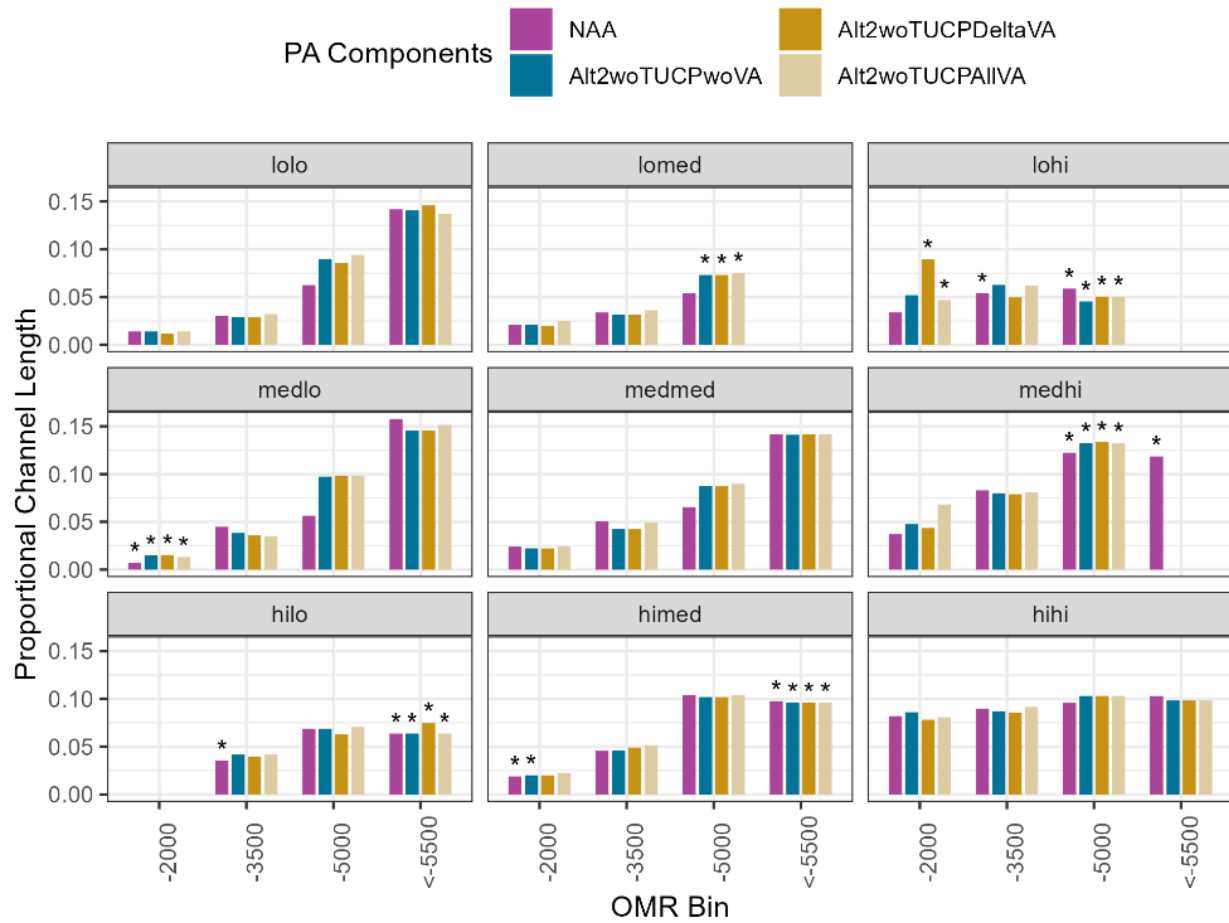


Figure I.3-121. Proportion of total channel length in the Delta (DSM2 grid) that experiences medium (25-75% proportional overlap) hydrologic influence at standardized inflow groups and across OMR bins of -2000, -3500, -5000, and less than -5500 cfs. Results are displayed across alternatives. Stars indicate combinations with five or less samples (months).

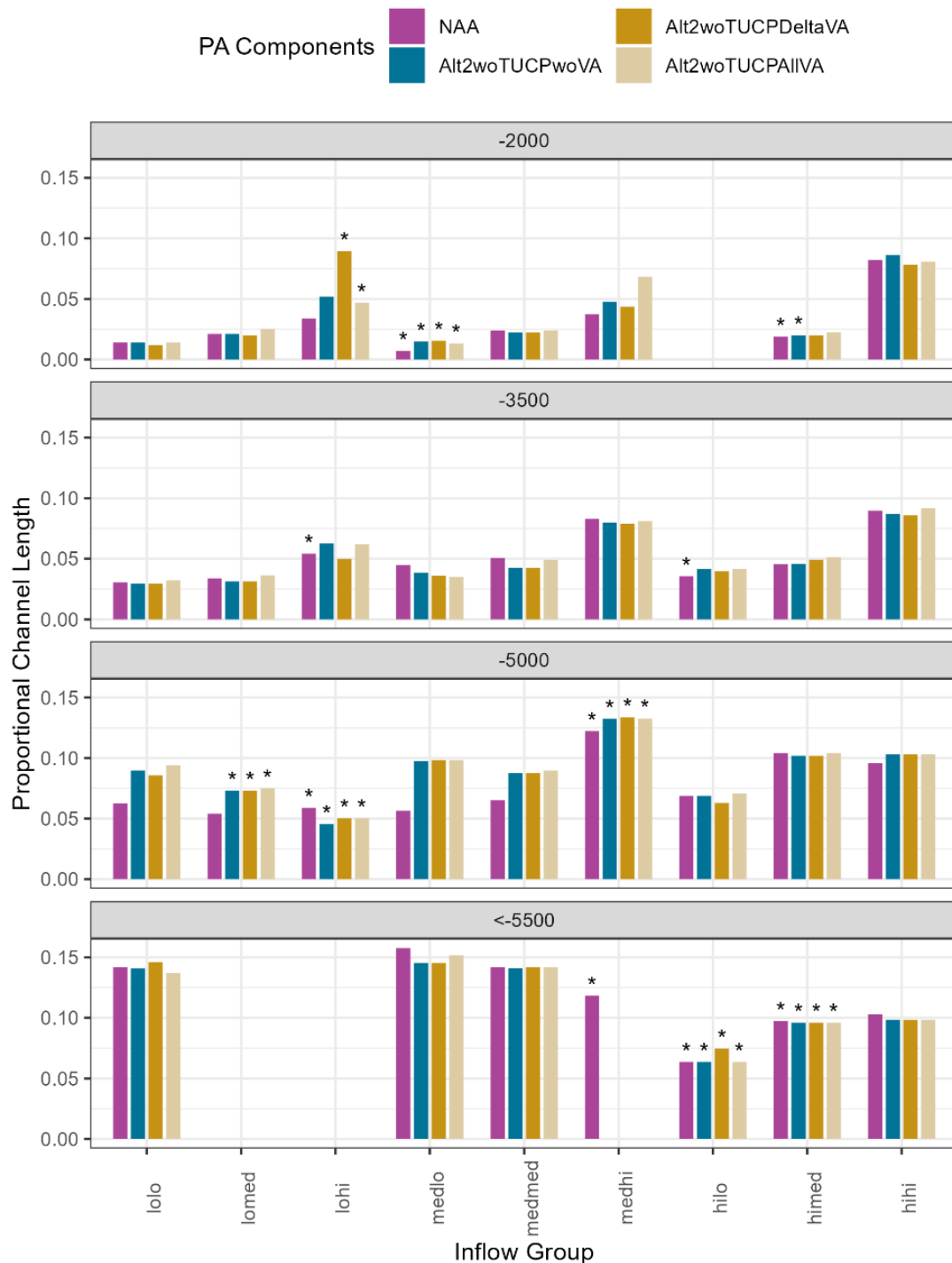


Figure I.3-122. Proportion of total channel length in the Delta (DSM2 grid) that experiences medium (25-75% proportional overlap) hydrologic influence at standardized inflow groups and across OMR bins of -2000, -3500, -5000, and less than -5500 cfs. Results are displayed across alternatives. Stars indicate combinations with five or less samples (months).

I.3.4 EIS Key Takeaways

While the sample sizes within each inflow group are relatively similar across alternative, differences between alternatives are more apparent when including OMR bin. Alt1 has a greater number of samples falling into the <-5500 OMR bin compared with other alternatives, especially in the medlo, medmed, himed, and hihi inflow groups (Table I.3-4, Figure I.3-2). The sample sizes of Alt2woTUCPDeltaVA and Alt2woTUCPAIIVA are more similarly distributed across OMR bins and inflow groups, with more months classified in the “NA” OMR bin and less classified in the -2000 or -3500 OMR bins compared with Alt2woTUCPwoVA and Alt2wTUCPwoVA in the lomed, medmed, hihi, and himed inflow groups (Table I.3-4, Figure I.3-2).

Across all alternatives, most of the nodes experience low hydrologic influence (greater than 0.75 overlap) and very few experience high hydrologic influence (less than 0.25 overlap; Figure I.3-123-Figure I.3-131).

With incrementally negative OMR, proportional overlap at selected locations generally decreases. Changes to proportional overlap are more subtle at distances further from pumping facilities (e.g. San Joaquin River at Jersey Point as compared to Turner Cut and Old River at Middle River; Table I.3-7).

The spatial extent (sum and proportion of channel length) of medium hydrologic alteration across all inflow groups and OMR bins ranges from 27,647 feet (5.2 miles and 0.7% of the DSM2 grid in NAA) to 710,057 feet (134 miles and 18.5% of the DSM2 grid in Alt1) (Table I.3-9). Across different phases of Alternative 2, summed channel length across all inflow groups and OMR bins ranges from 45,576 feet (8.6 miles and 1.18% of the DSM2 grid in Alt2woTUCPDeltaVA) to 595,220 feet (112 miles and 15.5% of the DSM2 grid in Alt2wTUCPwoVA) (Table I.3-9). For NAA, summed channel length ranges from 27,647 feet (5.2 miles and 0.7% of the DSM2 grid) to 606,560 feet (115 miles and 15.8% of the DSM2 grid) (Table I.3-9). The greatest extent of hydrologic alteration occurs in the <-5500 OMR bin, which is likely associated with greater exports.

The greatest difference in summed channel length, when compared with NAA, was observed in Alt1, which experienced 182% greater channel length altered at <-5500 OMR in the hilo inflow group (Table I.3-9). A large difference (89%) was also seen for Alt1 at the <-5500 OMR in the himed inflow group. Alt1 is the only alternative with DCC operations meeting D-1641 requirements only; all other alternatives share a different set of DCC Operations based on the 2019 BiOp. Across different phases of Alternative 2, the greatest difference in summed channel length when compared with NAA was for Alt2woTUCPDeltaVA at -2000 OMR for the lohi (164% greater channel length altered) and medlo (115% greater channel length altered) inflow groups. These results should be viewed with caution because there were very few samples simulated for these conditions. Aside from a few examples of Alt1 at high Sacramento inflow, summed channel length results vary only minorly between alternatives.

Channel length altered and delta export zone of influence generally increase with more negative OMR (Figure I.3-104-Figure I.3-111, Figure I.3-132). Trends appear consistent across inflow groups containing combinations of low and medium Sacramento and San Joaquin inflow (lolo, lomed, medlo, medmed inflow groups). At high Sacramento inflow (hilo, himed, hihi inflow groups), there appears to be little difference in proportional channel length altered between -5000 and <-5500 OMR bins. In the lohi and hihi inflow groups, there also appears to be less difference in proportional channel length altered across all OMR bins.

For the -2000 and -3500 OMR bins, channel length altered generally increases with higher San Joaquin inflow (Figure I.3-104-Figure I.3-111, Figure I.3-133). These trends are not apparent for the -5000 and <-5500 OMR bins.

Because high San Joaquin inflows are associated with more positive OMR values, at higher San Joaquin inflow, greater exports (pumping) are likely required to achieve the same OMR as at low San Joaquin inflow. As an example, in NAA at -2000 OMR, mean exports are 2,281 cfs for lolo inflow and 7,624 cfs for hihi inflow (Table I.3-3). When standardizing for Sacramento inflow, this is also apparent at -2000 OMR, with mean exports of 2,963 cfs at medlo inflow and 4,385 cfs at medhi inflow (Table I.3-3). Future work may visualize results by exports instead of OMR to better understand if exports are a more direct driver of the spatial extent of the zone of influence. It is also important to note that results do not account for the magnitude of effect and have not been examined in the context of seasonal tidal fluctuations or pumping hours (see Section I.3.1.2, *Assumptions / Uncertainty/ Caveats*). Future work may take these factors into account.

lolo

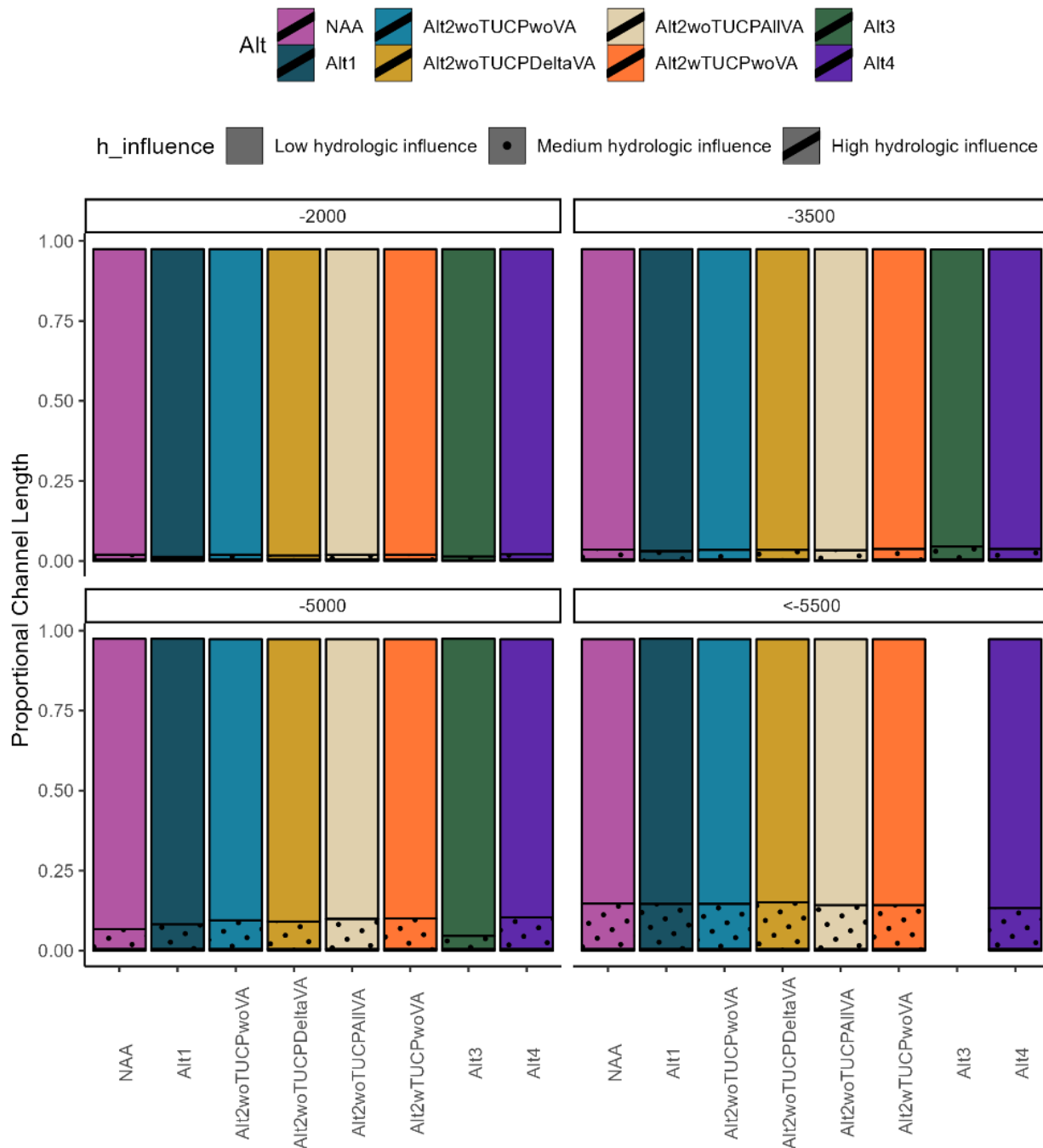


Figure I.3-123. Proportion of total channel length in the Delta (DSM2 grid) that experiences high (<25% proportional overlap), medium (25-75% proportional overlap) and low (>75% proportional overlap) hydrologic influence at standardized inflow groups and across OMR bins of -2000, -3500, -5000, and less than -5500 cfs. Results apply to the lolo inflow group.

lomed

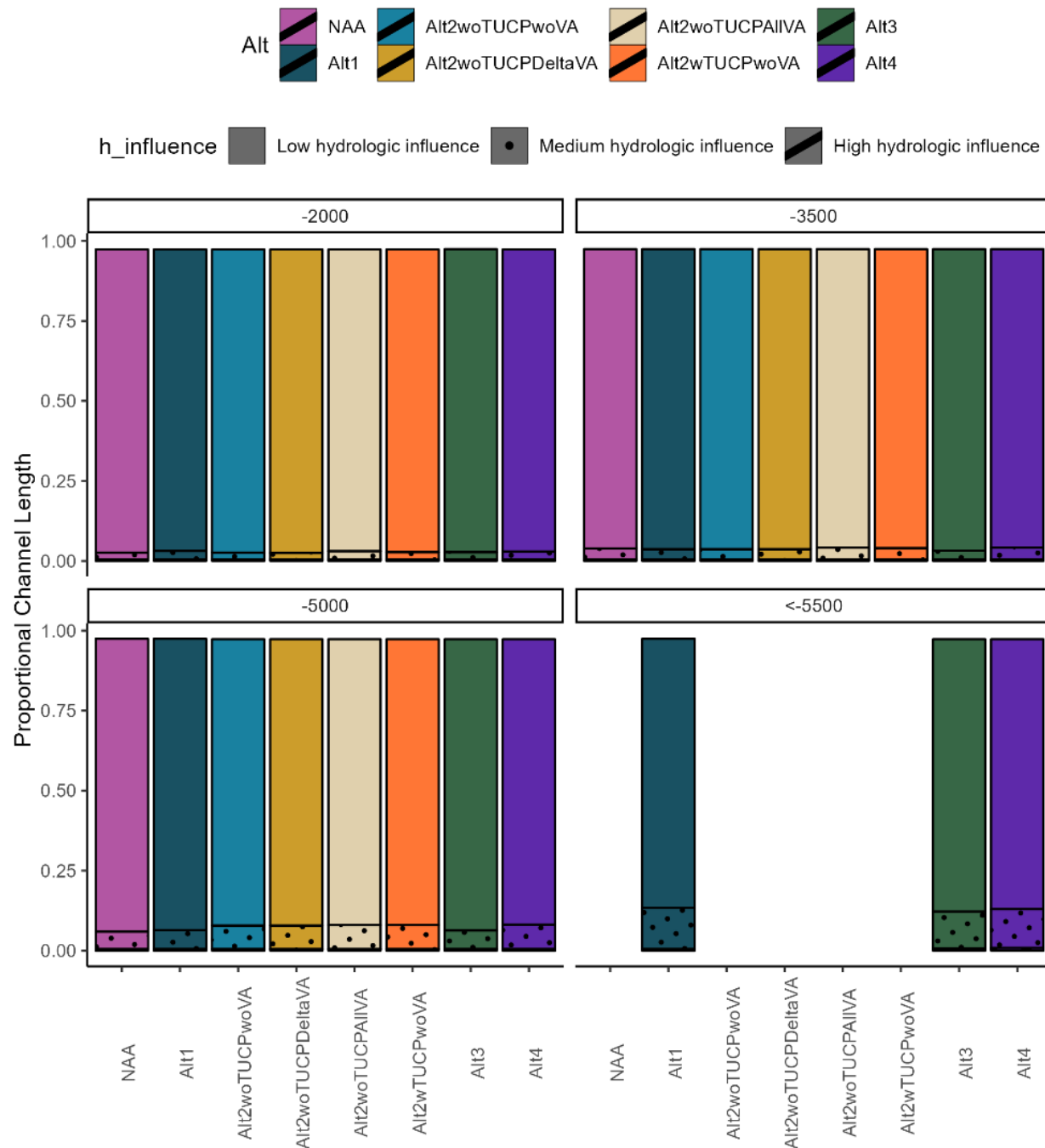


Figure I.3-124. Proportion of total channel length in the Delta (DSM2 grid) that experiences high (<25% proportional overlap), medium (25-75% proportional overlap) and low (>75% proportional overlap) hydrologic influence at standardized inflow groups and across OMR bins of -2000, -3500, -5000, and less than -5500 cfs. Results apply to lomed inflow group.

lohi

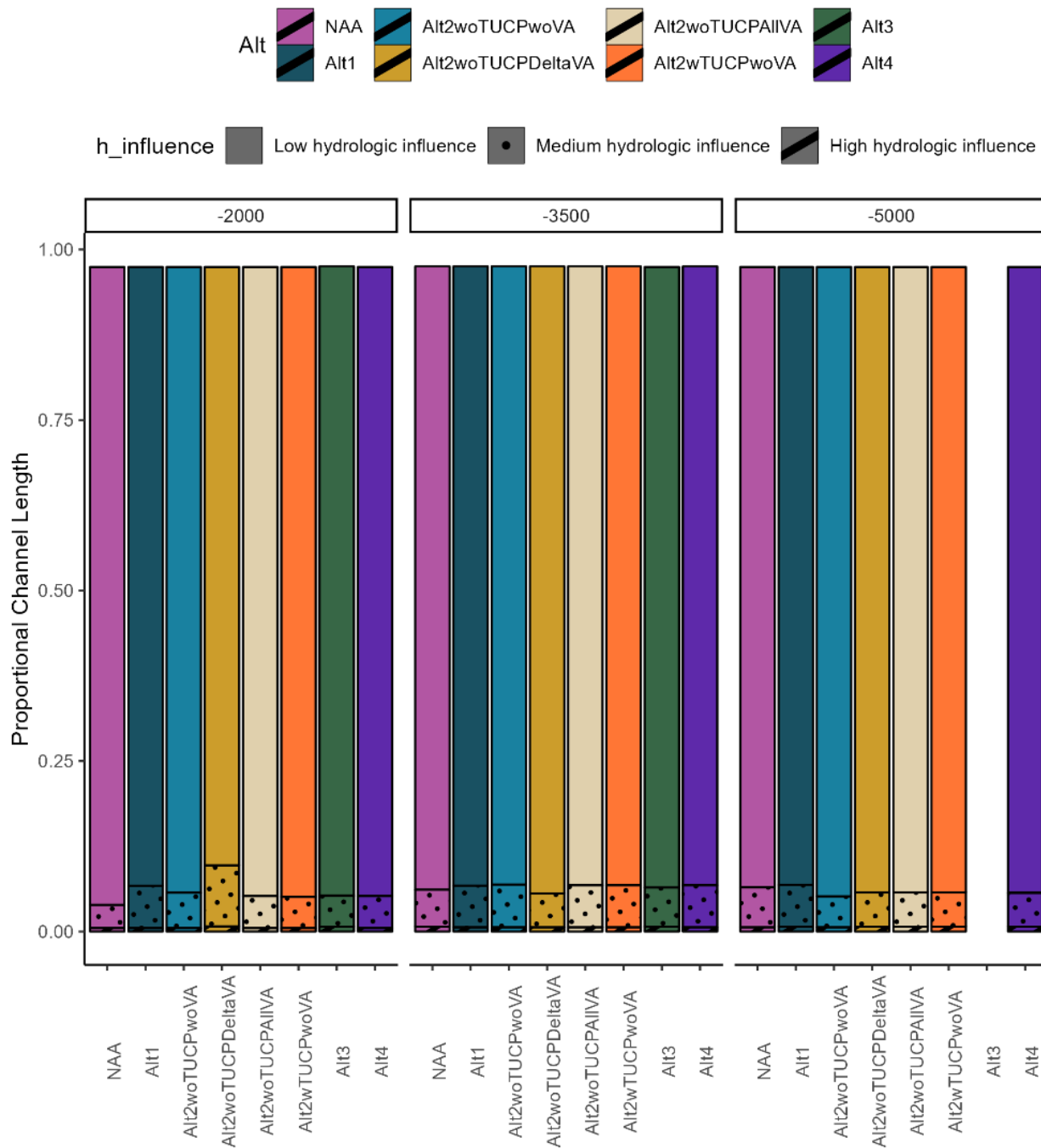


Figure I.3-125. Proportion of total channel length in the Delta (DSM2 grid) that experiences high (<25% proportional overlap), medium (25-75% proportional overlap) and low (>75% proportional overlap) hydrologic influence at standardized inflow groups and across OMR bins of -2000, -3500, -5000, and less than -5500 cfs. Results apply to lohi inflow group.

medlo

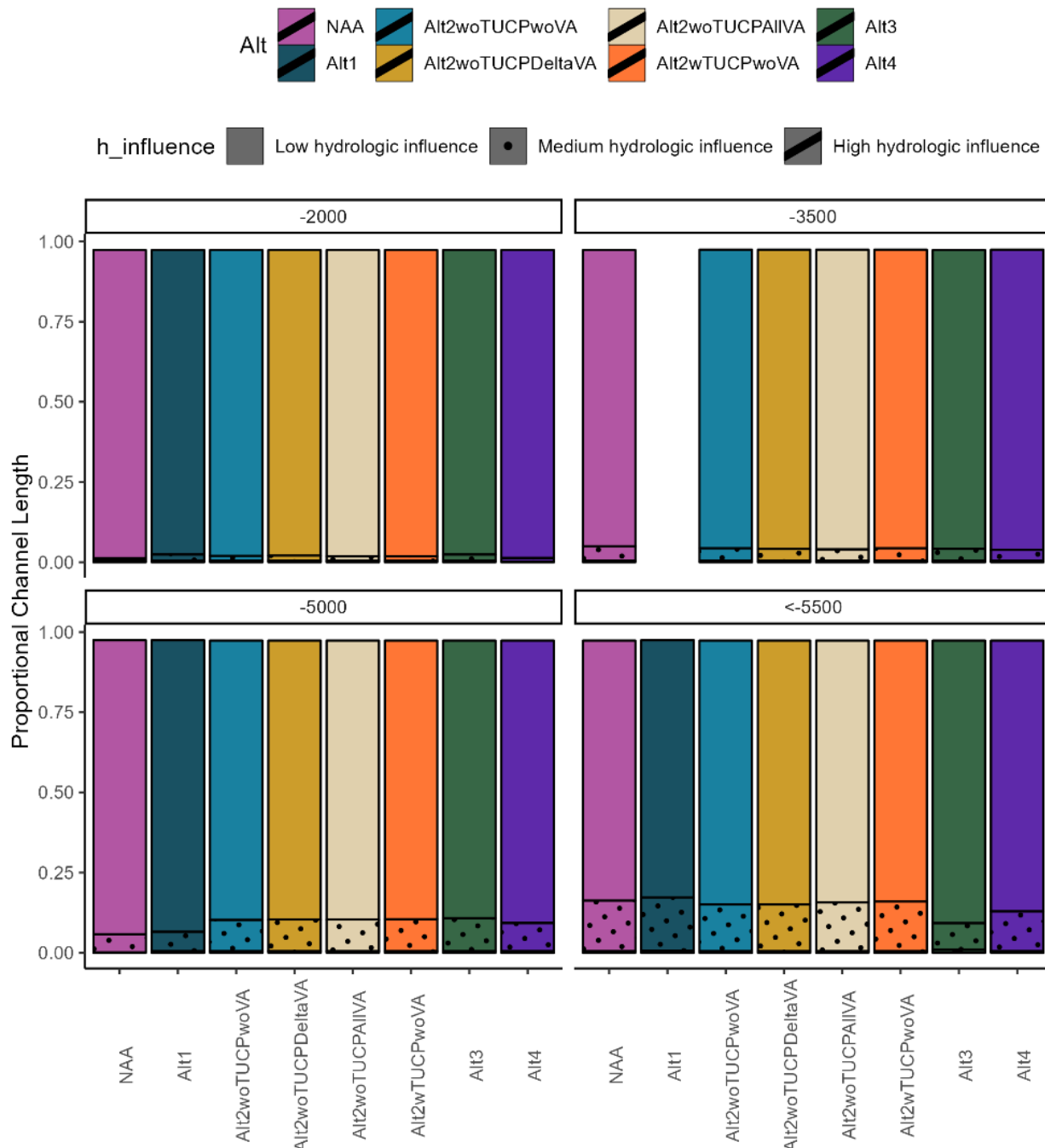


Figure I.3-126. Proportion of total channel length in the Delta (DSM2 grid) that experiences high (<25% proportional overlap), medium (25-75% proportional overlap) and low (>75% proportional overlap) hydrologic influence at standardized inflow groups and across OMR bins of -2000, -3500, -5000, and less than -5500 cfs. Results apply to medlo inflow group.

medmed

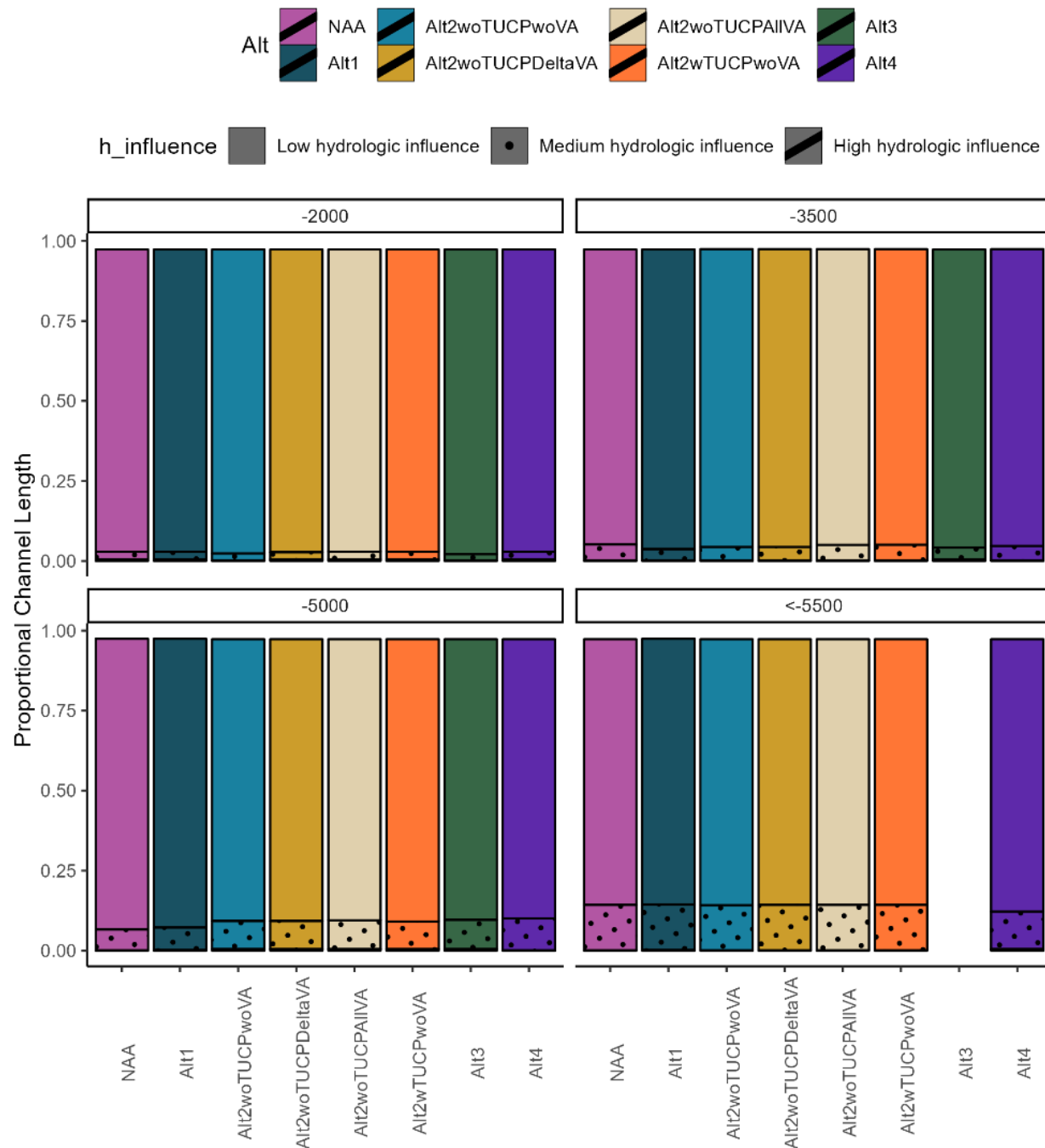


Figure I.3-127. Proportion of total channel length in the Delta (DSM2 grid) that experiences high (<25% proportional overlap), medium (25-75% proportional overlap) and low (>75% proportional overlap) hydrologic influence at standardized inflow groups and across OMR bins of -2000, -3500, -5000, and less than -5500 cfs. Results apply to medmed inflow group.

medhi

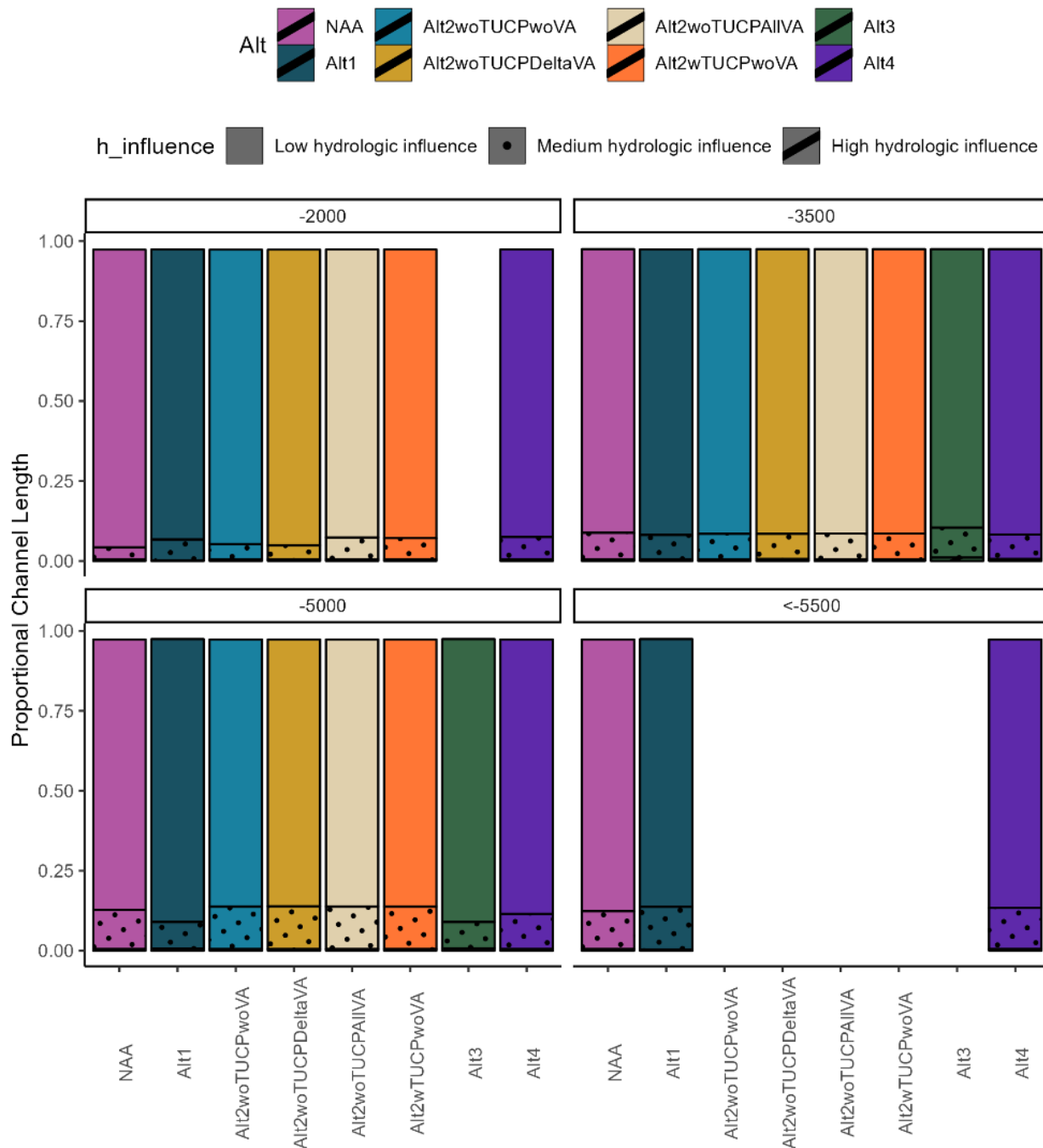


Figure I.3-128. Proportion of total channel length in the Delta (DSM2 grid) that experiences high (<25% proportional overlap), medium (25-75% proportional overlap) and low (>75% proportional overlap) hydrologic influence at standardized inflow groups and across OMR bins of -2000, -3500, -5000, and less than -5500 cfs. Results apply to medhi inflow group.

hilo

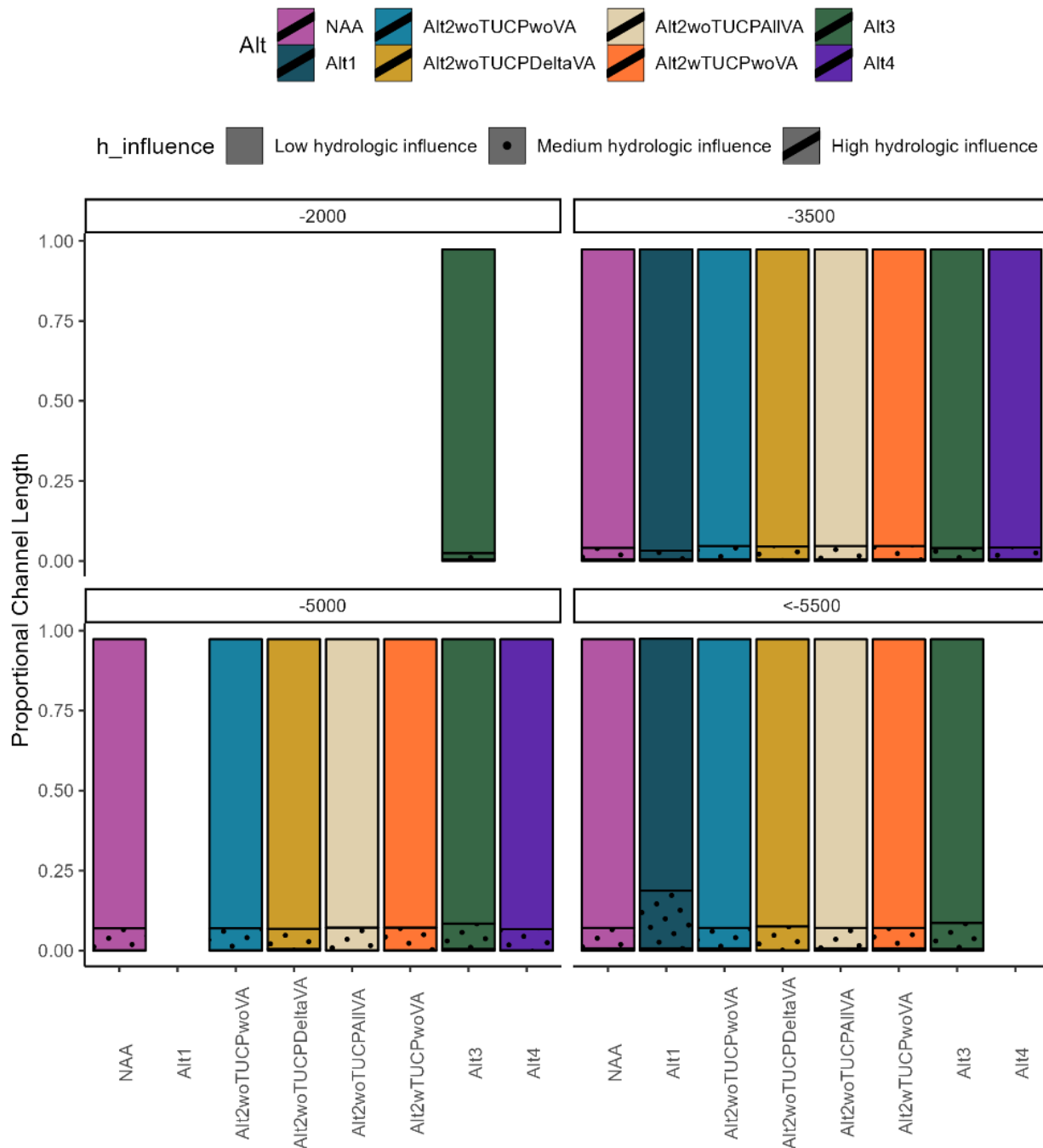


Figure I.3-129. Proportion of total channel length in the Delta (DSM2 grid) that experiences high (<25% proportional overlap), medium (25-75% proportional overlap) and low (>75% proportional overlap) hydrologic influence at standardized inflow groups and across OMR bins of -2000, -3500, -5000, and less than -5500 cfs. Results apply to hilo inflow group.

himed

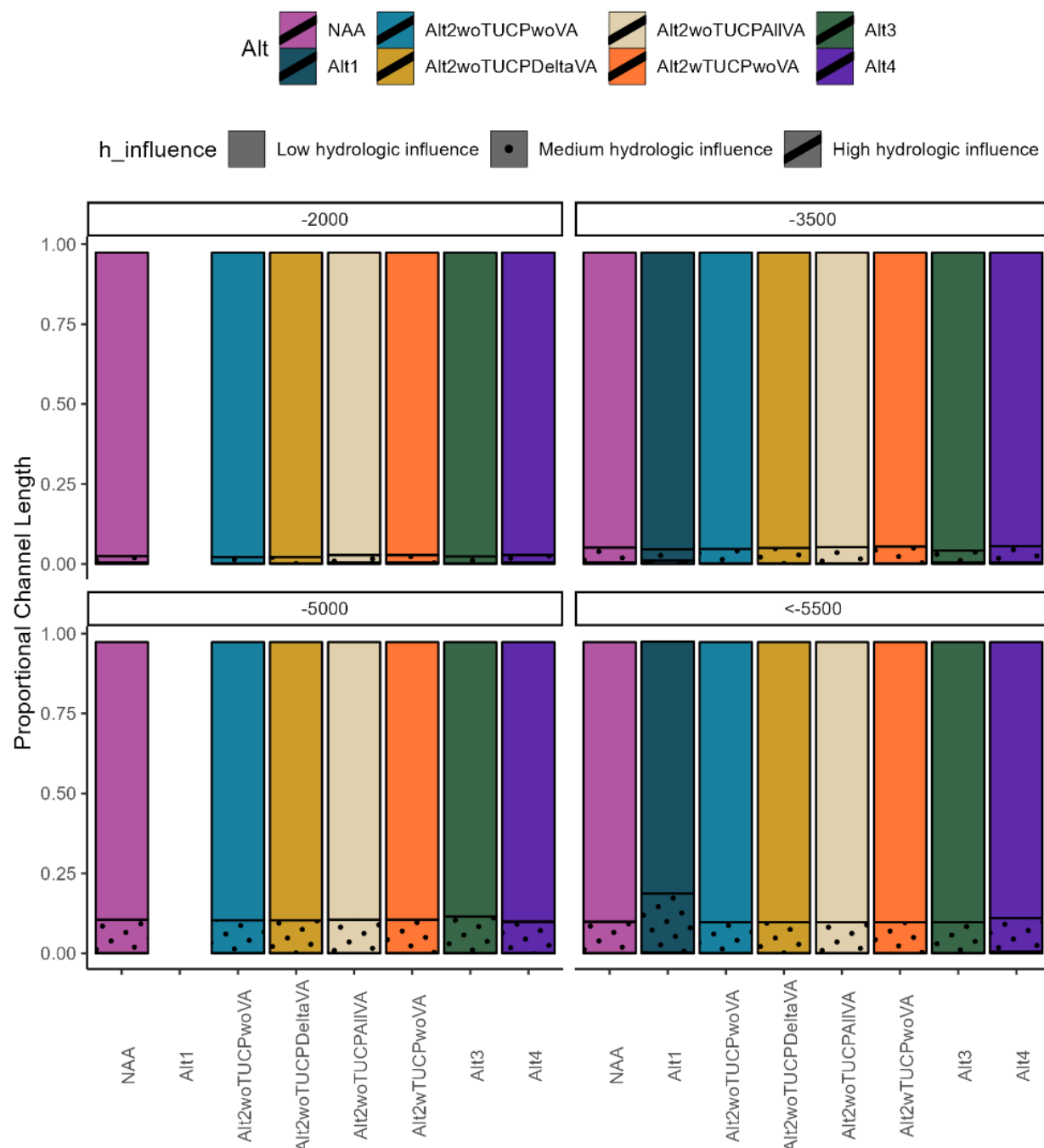


Figure I.3-130. Proportion of total channel length in the Delta (DSM2 grid) that experiences high (<25% proportional overlap), medium (25-75% proportional overlap) and low (>75% proportional overlap) hydrologic influence at standardized inflow groups and across OMR bins of -2000, -3500, -5000, and less than -5500 cfs. Results apply to himed inflow group.

hihi

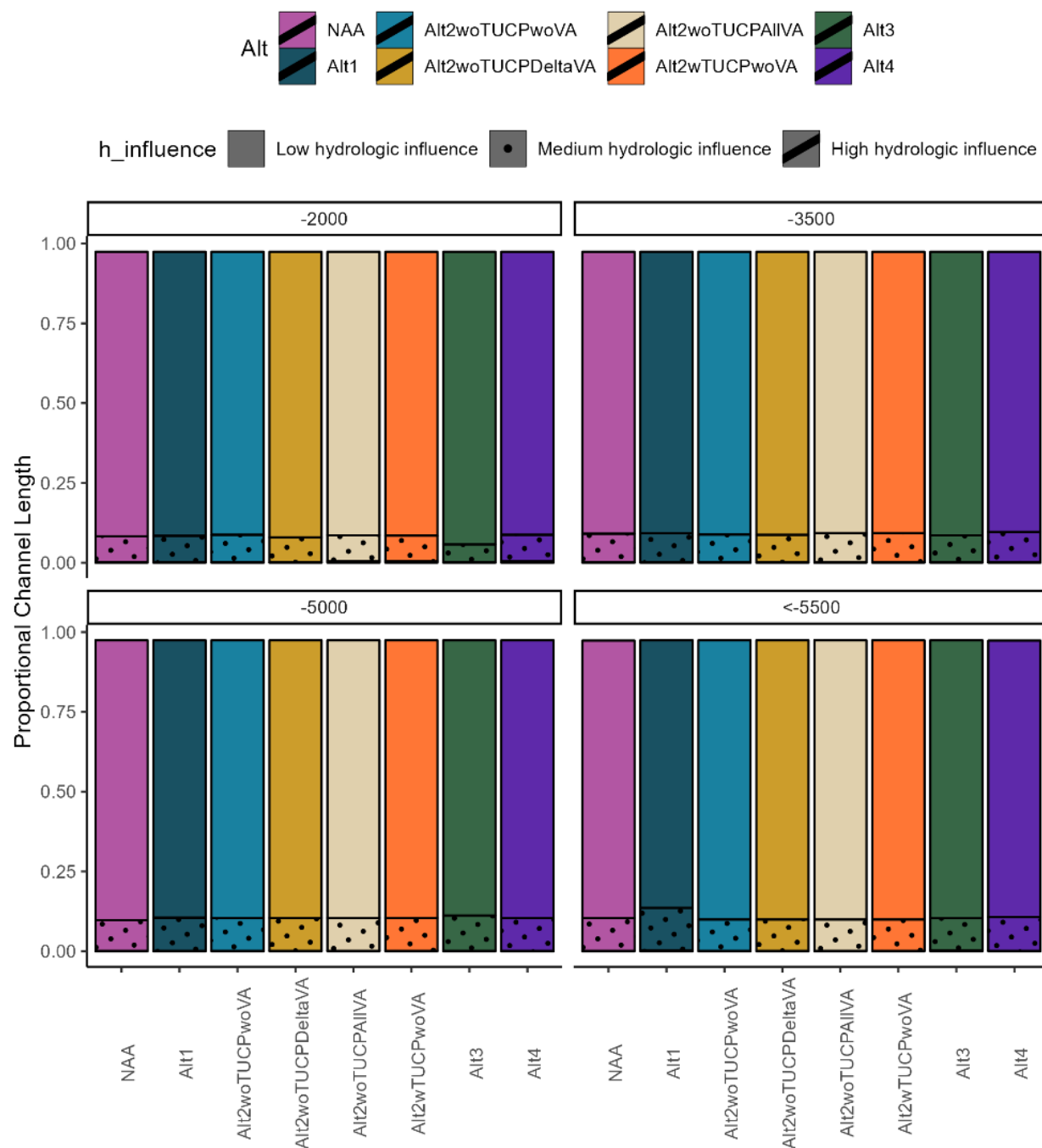


Figure I.3-131. Proportion of total channel length in the Delta (DSM2 grid) that experiences high (<25% proportional overlap), medium (25-75% proportional overlap) and low (>75% proportional overlap) hydrologic influence at standardized inflow groups and across OMR bins of -2000, -3500, -5000, and less than -5500 cfs. Results apply to hihi inflow group.

Table I.3-9. Channel length (feet) altered by pumping for No Action Alternative (NAA), Alternative 1 (Alt1), four runs of Alternative 2, and Alternative 4 (Alt4) across inflow groups and OMR bins. Values represent total summed channel length between nodes experiencing 0.25–0.75 proportional overlap, or medium hydrologic influence. Values in parentheses represent percent difference between each alternative and NAA. Absolute values are rounded.

Inflow group	OMR bin	NAA	Alt1	Alt2 woTUCP woVA	Alt2 woTUCP DeltaVA	Alt2 woTUCP AlIVA	Alt2 wTUCP woVA	Alt3	Alt4
lolo	-2000	54189 (0%)	27647 (-49%)	54189 (0%)	45576 (-16%)	54189 (0%)	48794 (-10%)	54189 (0%)	59520 (10%)
lolo	-3500	117806 (0%)	113044 (-4%)	113044 (-4%)	113044 (-4%)	124055 (5%)	153086 (30%)	124055 (5%)	124055 (5%)
lolo	-5000	240433 (0%)	297005 (24%)	345257 (44%)	329891 (37%)	361840 (50%)	157458 (-35%)	365872 (52%)	380800 (58%)
lolo	<-5500	546547 (0%)	541978 (-1%)	542342 (-1%)	562344 (3%)	527855 (-3%)	NA	527855 (-3%)	491719 (-10%)
lomed	-2000	81465 (0%)	101000 (24%)	81465 (0%)	76711 (-6%)	96978 (19%)	86009 (6%)	86009 (6%)	94255 (16%)
lomed	-3500	130344 (0%)	120549 (-8%)	120549 (-8%)	120549 (-8%)	139432 (7%)	102742 (-21%)	134670 (3%)	139432 (7%)
lomed	-5000	208217 (0%)	228476 (10%)	281435 (35%)	281435 (35%)	289043 (39%)	223757 (7%)	289043 (39%)	291861 (40%)
lomed	<-5500	NA	493876 (NA%)	NA	NA	NA	441704 (NA%)	NA	467873 (NA%)
lohi	-2000	130552 (0%)	238535 (83%)	199749 (53%)	344641 (164%)	180584 (38%)	174501 (34%)	176161 (35%)	180584 (38%)
lohi	-3500	208428 (0%)	235111 (13%)	241111 (16%)	191942 (-8%)	238045 (14%)	220352 (6%)	238045 (14%)	238045 (14%)
lohi	-5000	226351 (0%)	234862 (4%)	175053 (-23%)	193470 (-15%)	193470 (-15%)	NA	193470 (-15%)	190404 (-16%)
medlo	-2000	27647 (0%)	72558 (162%)	56798 (105%)	59520 (115%)	50971 (84%)	72558 (162%)	50971 (84%)	45576 (65%)
medlo	-3500	172490 (0%)	NA	148289 (-14%)	138590 (-20%)	134670 (-22%)	140818 (-18%)	148289 (-14%)	126424 (-27%)
medlo	-5000	217383 (0%)	231821 (7%)	374670 (72%)	377919 (74%)	377919 (74%)	394406 (81%)	381951 (76%)	337552 (55%)
medlo	<-5500	606560 (0%)	639690 (5%)	559302 (-8%)	559302 (-8%)	583403 (-4%)	321144 (-47%)	595220 (-2%)	478383 (-21%)

Inflow group	OMR bin	NAA	Alt1	Alt2 woTUCP woVA	Alt2 woTUCP DeltaVA	Alt2 woTUCP AlIVA	Alt2 wTUCP woVA		
								Alt3	Alt4
medmed	-2000	92454 (0%)	92454 (0%)	86009 (-7%)	86009 (-7%)	92454 (0%)	76711 (-17%)	92454 (0%)	92454 (0%)
medmed	-3500	195201 (0%)	138575 (-29%)	164174 (-16%)	164174 (-16%)	188699 (-3%)	139727 (-28%)	189671 (-3%)	176161 (-10%)
medmed	-5000	251330 (0%)	271281 (8%)	337165 (34%)	337165 (34%)	345232 (37%)	350767 (40%)	331544 (32%)	383716 (53%)
medmed	<-5500	546334 (0%)	546215 (0%)	543002 (-1%)	546334 (0%)	546334 (0%)	NA	546334 (0%)	449589 (-18%)
medhi	-2000	143735 (0%)	254409 (77%)	183314 (28%)	167915 (17%)	262475 (83%)	NA	254229 (77%)	268199 (87%)
medhi	-3500	319355 (0%)	294142 (-8%)	307325 (-4%)	303468 (-5%)	311986 (-2%)	359483 (13%)	311986 (-2%)	294946 (-8%)
medhi	-5000	470418 (0%)	322374 (-31%)	510174 (8%)	514154 (9%)	510385 (8%)	317894 (-32%)	510174 (8%)	422974 (-10%)
medhi	<-5500	455531 (0%)	515663 (13%)	NA	NA	NA	NA	NA	493344 (8%)
hilo	-2000	NA	NA	NA	NA	NA	72558 (NA%)	NA	NA
hilo	-3500	137049 (0%)	105506 (-23%)	160217 (17%)	153086 (12%)	160217 (17%)	135197 (-1%)	160217 (17%)	140818 (3%)
hilo	-5000	264382 (0%)	NA	264382 (0%)	242315 (-8%)	271698 (3%)	304232 (15%)	271698 (3%)	254721 (-4%)
hilo	<-5500	245068 (0%)	691451 (182%)	245068 (0%)	287645 (17%)	245068 (0%)	311950 (27%)	245068 (0%)	NA
himed	-2000	72558 (0%)	NA	76711 (6%)	76711 (6%)	86402 (19%)	86009 (19%)	86402 (19%)	86402 (19%)
himed	-3500	175651 (0%)	135964 (-23%)	176405 (0%)	188818 (7%)	197951 (13%)	139607 (-21%)	203970 (16%)	192852 (10%)
himed	-5000	400448 (0%)	NA	392039 (-2%)	392039 (-2%)	400448 (0%)	439660 (10%)	400448 (0%)	376014 (-6%)
himed	<-5500	375420 (0%)	710057 (89%)	369417 (-2%)	369417 (-2%)	369417 (-2%)	371744 (-1%)	369417 (-2%)	403479 (7%)
hihi	-2000	315738 (0%)	319078 (1%)	331338 (5%)	300952 (-5%)	311077 (-1%)	215474 (-32%)	307097 (-3%)	315738 (0%)
hihi	-3500	345153 (0%)	351039 (2%)	334832 (-3%)	330569 (-4%)	352728 (2%)	326638 (-5%)	352728 (2%)	365763 (6%)
hihi	-5000	368941 (0%)	399903 (8%)	396491 (7%)	396491 (7%)	426894 (7%)	396491 (16%)	396491 (7%)	396192 (7%)

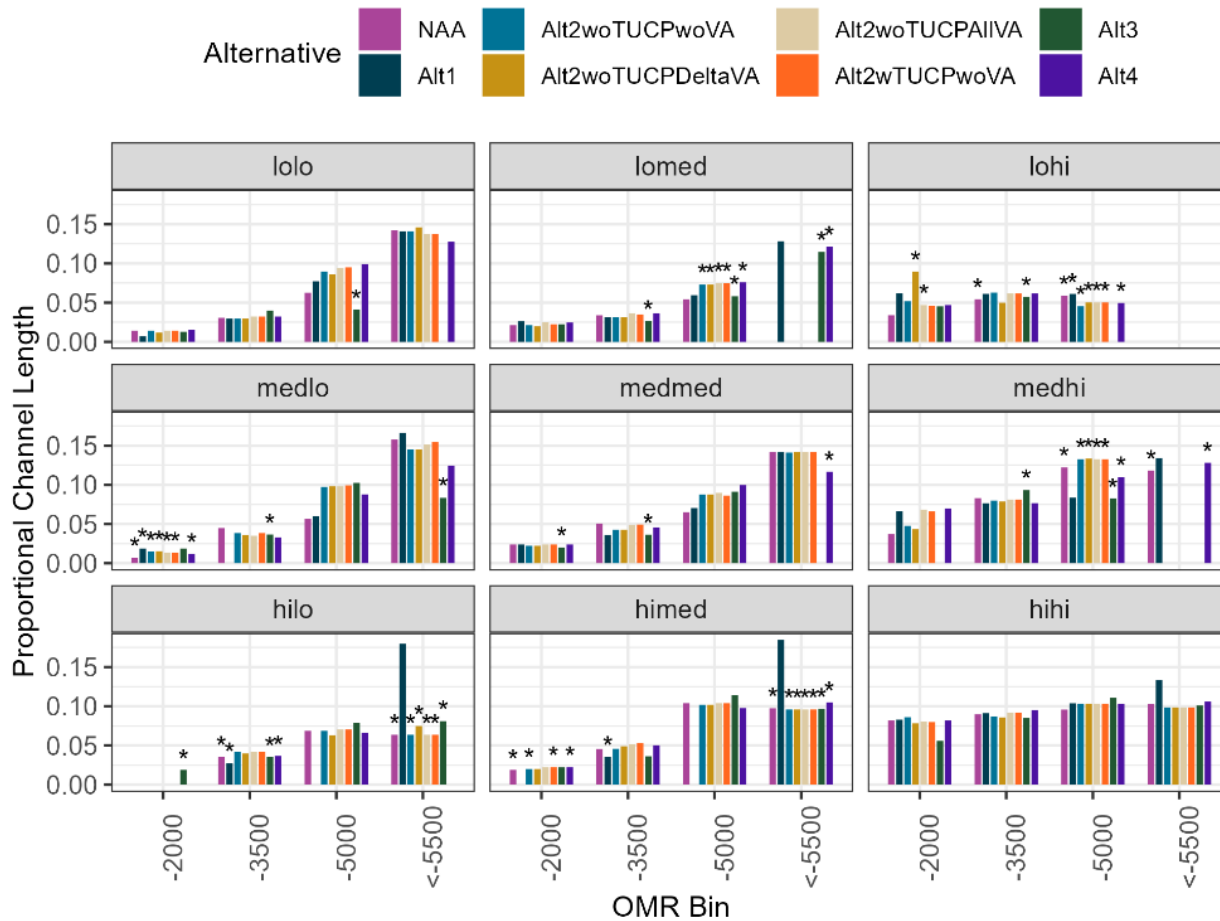


Figure I.3-132. Proportion of total channel length in the Delta (DSM2 grid) that experiences medium (25-75% proportional overlap) hydrologic influence at standardized inflow groups and across OMR flows of -2000, -3500, -5000, and less than -5500 cfs. Results are displayed across alternatives. Stars indicate combinations with five or less samples (months).

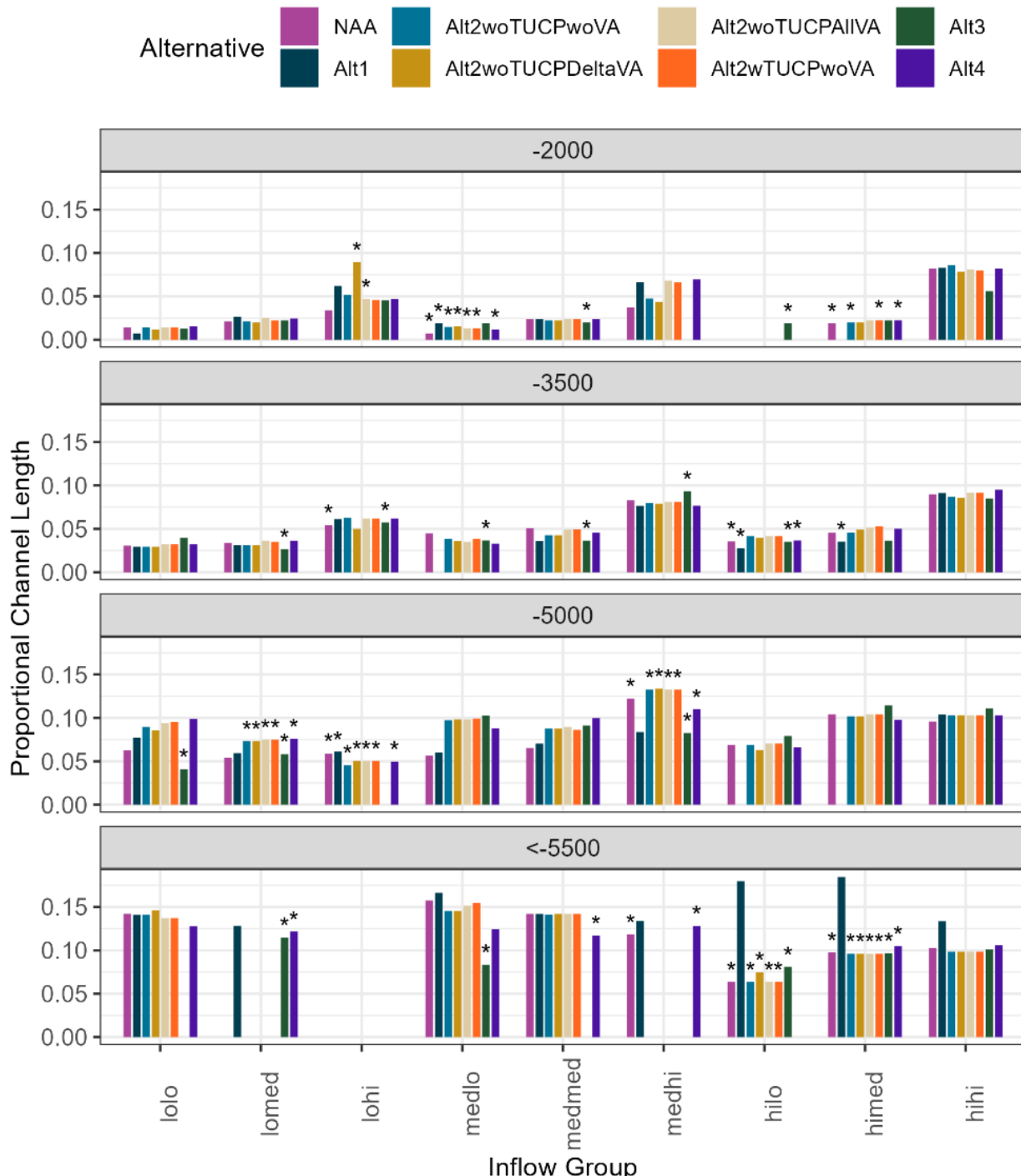


Figure I.3-133. Proportion of total channel length in the Delta (DSM2 grid) that experiences medium (25-75% proportional overlap) hydrologic influence at standardized inflow groups and across OMR flows of -2000, -3500, -5000, and less than -5500 cfs. Results are displayed across alternatives. Stars indicate combinations with five or less samples (months).